INTERSTELLAR MATTER

IN TWO STAR CLUSTERS

WILLIAM B SAMSON

PhD Thesis

University of Edinburgh

Department of Astronomy

Royal Observatory

Edinburgh

September 1971

"If I stoop

Into a dark tremendous sea of cloud,

It is but for a time;

... I shall emerge one day."

Robert Browning (1812-1889)

SUMMARY

Two very young star clusters, NGC 654 and IC 5146 are studied using three colour UBV photographic photometry to $V \approx 16^m$ and photographic polarization measures to $B \approx 15^m$, with a view to determining the distribution of interstellar matter in regions where star formation recently occurred.

NGC 654 is found to be enclosed by a shell of interstellar matter of mass $\sim$1,500 M$\odot$. The mass of all stars in the cluster is $\sim$4,000 M$\odot$. Starlight from NGC 654 is found to be polarized in a direction parallel to the galactic plane, the fainter members being more strongly polarized than the brighter ones.

IC 5146 is embedded in a dark nebula which is extremely dense near its centre. The total mass of interstellar matter in the nebula is found to be about 700 M$\odot$. Comparison of radio and optical observations show that gas and dust are not separated to any great degree by radiation from the embedded stars. A gas:dust ratio of 300:1 is found. This ratio varies with the dust grain model used. Polarization of starlight in IC 5146 is found to be very variable in both magnitude and direction, indicating the presence of complex magnetic fields within the nebula.

ACKNOWLEDGEMENTS

I would like to thank Professor H A Brück and Dr V C Reddish, who supervised this work, for their constant encouragement and for numerous stimulating discussions, and the many friends and colleagues who have helped me, in discussions and in many other ways.

It is impossible to name them all, but they include, in particular, the following:
Mr D A Cooper, Dr N M Pratt, Miss M E Sim, Miss L A Wakeman and Mr T Wallace.

I should like also to thank Miss W Gibb who has worked so hard on the typing of this thesis.

The Science Research Council provided financial support for this work.

CONTENTS

CHAPTER 1

Introduction

In our galaxy, clouds of gas and dust are distributed in a disc along with young OB and T Tau type stars which have the same distribution. Within this disc the clouds and young stars follow a pattern of spiral arms where the young stars are nearly always associated with dense clouds of interstellar matter. T Tau stars, in particular, are always found in or near dark interstellar clouds; this being especially noticeable in the Taurus region where the prototype, T Tauri is located.

OB and T Tau stars are often found in star clusters and associations where they probably form from clouds of interstellar matter. This view is supported by evidence that the chemical composition of young stars is similar to that of the interstellar matter with which they are associated.

The youngest OB aggregates are the exciting stars in compact HII regions. These stars are sometimes so heavily obscured by interstellar dust that they are invisible and can only be detected by their thermal emission at radio wavelengths.

Small, dense dark structures, globules and "elephant trunks"

can sometimes be seen silhouetted against luminous clouds of ionised hydrogen in regions of recent star formation.

Although it is clear that these structures are associated in some way with star formation, it is not known whether they are pre stellar objects or matter left over after star formation has taken place.

Certain highly luminous OB stars are anomalously obscured by circumstellar dust clouds whose presence has been verified by infrared observations. Circumstellar clouds are now recognised as being a common feature of supergiants, Wolf Rayet and T Tau stars. It is not known, however, whether these clouds have been produced by the stars themselves, or are left over from star formation.

When we observe interstellar matter near newly formed stars we are seeing a spatial relationship which may have been affected by the young stars. For example, if the dust is left over from star formation, then it is being blown away or evaporated by radiation from the young stars. If, on the other hand, it is produced by the young stars, then the amount of dust may be increasing with time.

Besides the hydrogen, helium and dust in interstellar clouds, complex molecules have been discovered and more

are being discovered all the time. These molecules are found in the dark clouds where, presumably, they form on the surfaces of grains. It is, therefore, important to know the distribution of interstellar dust to help us to understand these molecules and how they form.

The aim of this thesis is to improve our knowledge of the distribution of interstellar matters in young star clusters. The thesis is an account of observations of two such star clusters - NGC 654 and IC 5146. These two objects are the two youngest star clusters which can be observed from the latitude of Edinburgh. They were chosen from a list of 66 clusters and associations studied by Reddish (1). The observations made from the present study are photographic UBV photometry and polarimetry of the clusters.

NGC 654

Distance Estimates

Several authors have measured the distance of NGC 654. The authors, their estimates and methods are listed overleaf:

Year	Author	Distance (pc)	Method	Ref
1941	Alter	2060	pg & pv photometry	(2)
1950	Barkhatova	1250	B, V photometry	(3)
1955	Muller	1660	R, G, U photometry	(4)
1960	Pesch	2900	pe U,B,V photometry	(5)
1961	Hoag	2480	U, B, V photometry	(6)
1961	Johnson	1500	U, B, V photometry	(7)
1965	Hoag	1500	Hγ observations	(8)

Age Estimates

Age estimates for NGC 654 vary by more than an order of magnitude. Schmidt (9) found a value of log t = 6.56 from the upper termination point of the main sequence. Lindoff (10) found log t = 7.18 using a method based on the absolute magnitude of the brightest main sequence member. Reddish (1) using the absolute magnitude of the brightest member as an indicator, finds log t = 6.18. Reddish assumed a distance modulus of $10^{m}.9$ for the cluster. He says that if this were $12^{m}.3$, as some authors have found, then the age would be given by log t = 5.70.

Colour Excess

Muller (4) pointed out that NGC 654 shows unusually strong reddening, which varies across the cluster. Pesch (5) finds that the reddening varies between $0^{m}.79$ and $1^{m}.18$. Starikova (11) finds a mean colour excess of $0^{m}.92 \pm 0^{m}.128$ rms.

Reddish (1) places NGC 654 in class (b) of his four classes. This means that one or two members have anomalously high colour excesses.

IC 5146

Optical Observations

The most complete photometric study of IC 5146 is that of Walker (12). He made photoelectric and photographic UBV observations of stars in the cluster. His photoelectric observations provide a set of standard stars which have been used to calibrate observations in the present study. Walker's observations were made using the 153 cm and 254 cm telescopes at Mount Wilson Observatory. Both instruments were diaphragmed to give wider corrected fields.

Distance

By fitting a standard main sequence to the colour magnitude diagram, Walker found that the distance was about 1 kpc. He points out that this is fairly uncertain, due to the presence of pre-main sequence stars in the cluster.

Reddening

Walker finds that reddening is very variable among the member stars of IC 5146. In particular the star B D + 46° 3474, the most luminous member, is reddened by $0^{m}.6$ more

than other members in its vicinity. The stars in IC 5146 are seen against the background of a dark nebula which is, in all probability, associated with the cluster. Walker suggests that the highly reddened B D + 46^{o} 3474 lies behind the other members, inside this cloud. Reddish (1), however, suggests that the high reddening is caused by the remains of the pre-stellar cloud from which this star formed.

Age

Walker finds the age of IC 5146 to be about 3×10^{6} years, calculated from the position of the turnoff point on the main sequence. Reddish finds an age of about 4×10^{6} years from the luminosity of the brightest member.

Radial Velocity

IC 5146 is associated with a bright nebula which shines partly by reflection and partly by emission from ionised hydrogen. The radial velocity of the nebula has been determined by several authors. Miller (13), using slit spectrograph observations, finds a heliocentric radial velocity of -11.2 ± 6.0 km/sec. Williamson (14), using a Fabry-Perot interferometer, finds a value of -10.9 ± 1.0 km/sec. He finds a systematic difference of 6 - 8 km/sec between the east and west sides of the nebula. Williamson attributes this to the "braking" effect of cold gas in a

dark nebula lying to the west of IC 5146. Georgelin and Georgelin (15) find a heliocentric radial velocity of -8.3 ± 4.4 km/sec, again using Fabry-Perot techniques.

Radio Observations

The only positive radio observations of IC 5146 have been made by Riegel (16) who used the 90 m transit radio telescope at N R A O. IC 5146 was observed in the 21 cm spectral line of neutral hydrogen.

Riegel finds a heliocentric radial velocity, for the neutral hydrogen, of -13.5 km/sec which compares favourably with the optical measurements mentioned above.

The mass of neutral hydrogen found in the nebula is 670 $M_\odot$ and the mass of H_{II} found is 20 $M_\odot$. Riegel's computation of H_{II} mass is based on continuum observations of CTA 97 by Kellermann (17). It appears, however, that CTA 97 may not be associated with IC 5146 because it lies quite far from the visible nebula. In his calculations, Riegel assumes $Te = 10^4$ °K for the H_{II} region; Williamson's Fabry-Perot observations (14) indicate a temperature of less than half this. These problems will be considered further in Chapter 7.

The only other radio observation attempted on IC 5146 was

that of Churchwell et al (18) at 15.4 GH_z. No positive result was obtained.

Polarimetry

Unfortunately, none of the stars in IC 5146 or NGC 654 have had photoelectric polarization measures made of their light. It is thus impossible to check directly the photographic polarization measures made at Edinburgh for this study. There is, however, a good reason for accepting these measures as they stand. Pratt (19) used the same technique successfully in his study of H and χ Persei and found that his measurements agreed well with photoelectric ones. Since exactly the same equipment and reduction techniques have been used in this study, there is good reason to believe that these measurements are good ones.

Summary

Two young star clusters, NGC 654 and IC 5146 have been selected for this study of the distribution of interstellar matter in star clusters. Age estimates for NGC 654 vary between 1.5×10^6 years and 1.5×10^7 years. The age of IC 5146 has been estimated as 3×10^6 years and 4×10^6 years.

Both clusters show very variable reddening among their

members, indicating the presence of quantities of dust local to the clusters, possibly in the form of pre-stellar cloud remnants. IC 5146 is seen against a very dense dark nebula and there is an associated H_{II} region centred on the star B D + 46° 3474, the most luminous cluster member which can be seen. NGC 654 has no such obvious associated dust cloud or H_{II} region.

Polarization measures of starlight in IC 5146 are of particular interest because of the object's proximity, 1 kpc, and high galactic latitude, -5°.5, minimising the polarizing effect of dust lying in the galactic plane in front of IC 5146. Any polarization observed is likely to be local to the cluster. NGC 654, on the other hand, lies close to the galactic plane and is at a distance of about 2.5 kpc. Any polarization produced in the cluster is likely to be swamped by polarization due to dust in intervening spiral arms.

FIG 1: Chart of NGC 654. North is Left.

The 40/60 cm Schmidt Telescope at the
Royal Observatory Edinburgh.

THE STAR CLUSTER NGC 654

CHAPTER 2

Three Colour Photometry

Data Collection

Twelve plates were used for photographic UBV photometry of stars in NGC 654 and the surrounding area. The following table lists the plates in the order in which they were taken. Col 1 has the plate number from the catalogue kept at Edinburgh; Col 2 has the emulsion type - all plates used were Kodak ones; Col 3 lists the Schott filter type; Col 4 names the colour range - U, B or V in this case; Col 5 lists the exposure time; Col 6 lists the date of observation; Col 7 lists the local sidereal time at the start of the exposure. All plates were obtained using the 40/60 cm Edinburgh Schmidt Camera. They were developed in D19b for 6 minutes at 20°C, fixed for 20 minutes and washed for 1 hour in running water.

Plate No	Emulsion	Filter	Colour	Exp	Date	S T
707	IIaD	GG14	V	5 min	7.12.67	04.30
708	IIaD	GG14	V	5 min	7.12.67	04.45
736	IIaD	GG14	V	5 min	27.12.67	04.00
737	IIaD	GG14	V	5 min	27.12.67	04.40
732	IIaO	GG13	B	5 min	27.12.67	03.02
733	IIaO	GG13	B	5 min	27.12.67	03.15
734	IIaO	GG13	B	5 min	27.12.67	03.25

Plate No	Emulsion	Filter	Colour	Exp	Date	S T
735	IIaO	GG13	B	5 min	27.12.67	03.45
785	IIaO	UG2	U	40 min	1. 2.68	06.50
786	IIaO	UG2	U	40 min	1. 2.68	07.40
876	IaO	UG2	U	10 min	20.10.68	02.25
877	IaO	UG2	U	10 min	20.10.68	02.25

Measurement of Images

The star images on the plates listed above were measured using the semi-automatic Becker Iris Photometer (1). Operation of a foot switch produces X and Y co-ordinates and Iris reading for the star image on punched tape. The task of the operator is to find each star, referring to charts, centre it in the Iris and press the foot switch. A skilled operator can measure more than 200 images in an hour in a field with which he is familiar.

Each of the twelve plates listed above was measured at one sitting. The 45 photoelectric standard stars used for calibration were measured followed by 124 stars visible in NGC 654 and the surrounding region followed by more measurements of the 45 photoelectric standard stars. A run like this took about 1 hour to complete. In order to keep a check on iris drift, three stars - one bright, one moderately bright and one faint - were measured periodically throughout each run. No iris drift was found during the

measurement of these twelve plates. The iris photometer was kept switched on all the time during the two weeks when these plates were measured. Only the lamp was switched off between runs and this was switched on at least half-an-hour before the start of any run.

Calibration

Photoelectric standards published by Hoag et al (6) were used for the calibration of the photographic UBV photometry. There are twenty one standards in NGC 654 itself and twenty four in the nearby cluster NGC 663. The two clusters are about 1^{o} apart and differences in emulsion sensitivity, across the plate, must be taken into account. This will be discussed later in this section.

As a preliminary measurement of magnitudes a least-squares polynomial curve fit was made to the points on the photoelectric magnitude vs iris reading plot for the standard stars. A 4th degree polynomial was fitted in all cases. The magnitude of the 124 stars were then computed from the calibration polynomials. All computations were done using the ICL 4130 computer at the Royal Observatory Edinburgh. The calibrations were not examined individually at this stage and systematic errors could escape notice. The method is, however, very fast and useful for a preliminary investigation. The computer programs used are summarised below;

all but the first were written by the author:

1. NPA8: This program was written and developed by Dr N M Pratt of the Royal Observatory Edinburgh. The program translates the output from the Becker Iris photometer, which is on paper tape in EDSAC code, and outputs a table of X and Y co-ordinates and iris readings for each star measured, along with the photographic background fog level measured alongside each image.

2. WSA2: This program reads in output tapes from NPA8 along with lists of photoelectric magnitudes for the standard stars. A polynomial is fitted to the calibration points (iris, m_{pe}) and a table of magnitudes for all the stars measured is produced.

3. WSA3: This program reads in the WSA2 outputs for all the plates measured and prints out the mean U, B and V magnitudes for each star, along with their standard errors. Alternatively, a table of V, B-V and U-B magnitudes with corresponding errors is produced.

Unfortunately the polynomial calibrations produced by the computer do not behave well at the extremes of the magnitude range, owing to the small number of photoelectric

standard stars available. It was also found that systematic differences appeared between photoelectric and photographic magnitudes in certain colours. The graphs of photoelectric magnitude vs iris reading were plotted for the standards on each plate in turn. The standards in NGC 654 were plotted using a different symbol from those in NGC 663.

For IIaO plates the points from both clusters lie along the same smooth curve in the magnitude vs iris reading diagram. For IIaD and IaO plates, however, the points were found in general to lie along different curves for the different clusters. This effect is most extreme on the V plate, 707. The standards in NGC 663 have iris readings about 40 digits greater than do stars of the same magnitude in NGC 654. This effect is slightly less with the very faint stars. Three possible reasons for this come to mind:

1. The photoelectric magnitudes are discrepant.

2. The plateholder was not properly seated in the telescope; consequently the focus varies across the field.

3. The emulsion sensitivity varies across the plate.

Focus did not appear to differ.

? What is effect of mis-focus? How does it look in microscope?

Possibility no 1. is ruled out by the fact that other V plates show a reversal of the positions of the points corresponding to the two clusters on the magnitude vs iris reading diagram.

Possibility no 2. seems very unlikely - the plate was examined under a microscope and the focus did not change appreciably along any diameter.

This leaves possibility no 3., ie the emulsion sensitivity varies across the field. The background fog level readings from the iris photometer confirm this - the sky background in NGC 663 is about 10 digits higher than that in NGC 654.

It is of interest at this point to notice that the photometric work of McKuskey and Houk (20) relies on standards from one cluster to calibrate the entire LF5 field, several degrees across. Magnitudes of stars not close to the standards should not be strongly relied on, for this reason.

For final calibration, smooth curves were drawn by hand through the points on the magnitude vs iris diagrams for each plate. In cases where the NGC 663 standards differed from the NGC 654 standards the curve was drawn through the NGC 654 points, using the NGC 663 points only as guidance to the shape of the curve where NGC 654 stars were absent.

The method of calibration of iris readings from these hand-

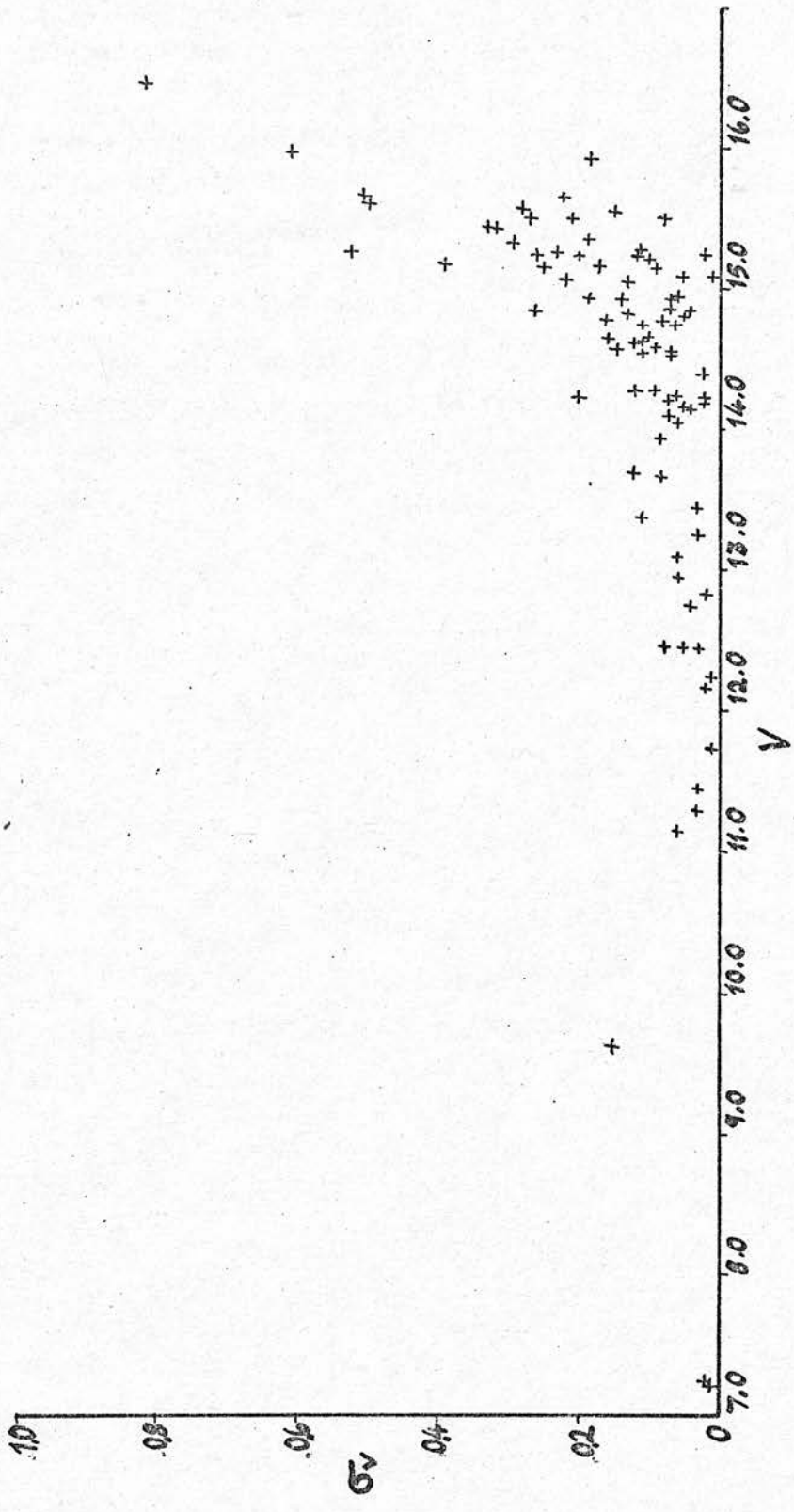

FIG 2(a): r m s Error in V Plotted vs V Magnitude.

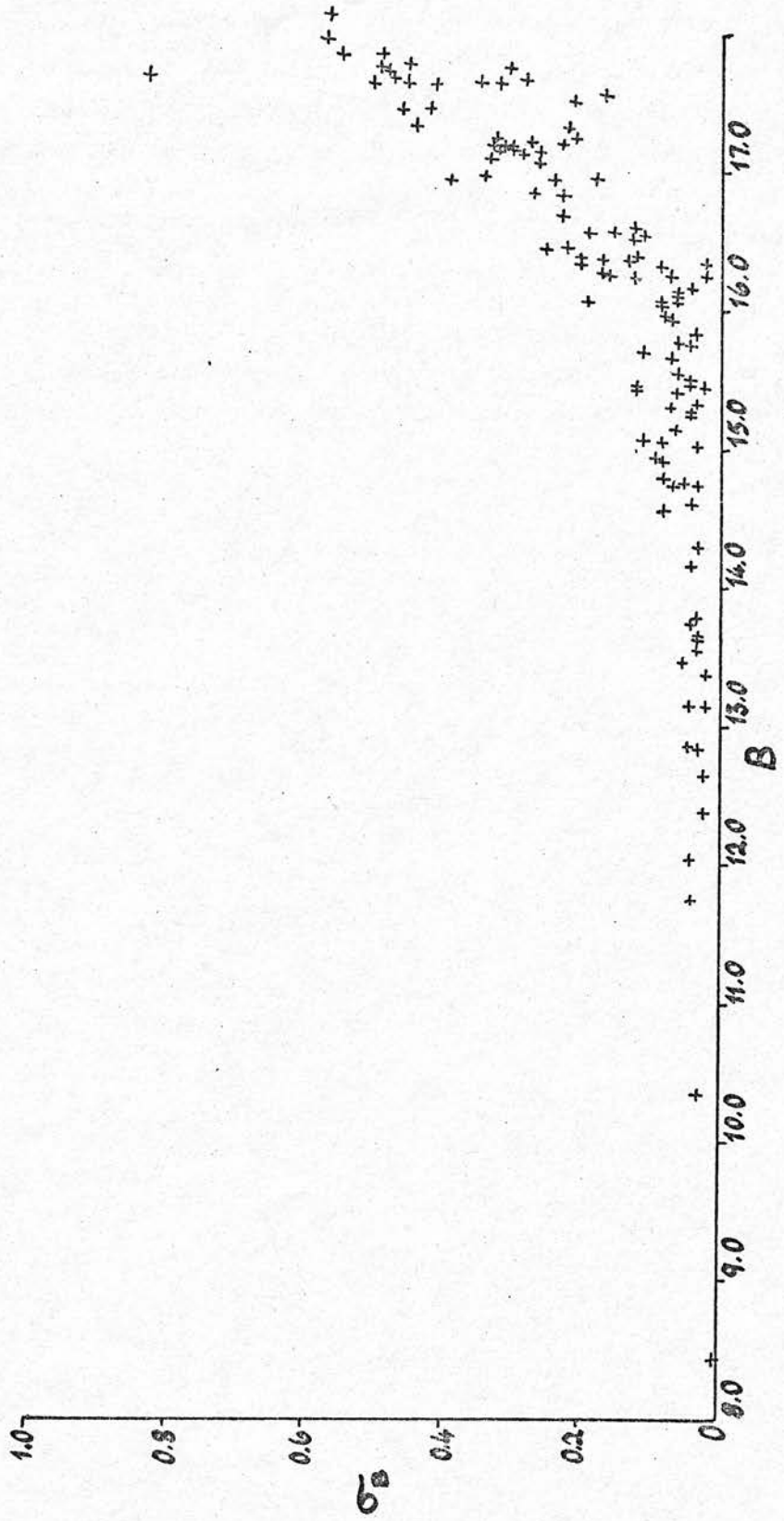

FIG 2(b) : r m s Error in B Plotted vs B Magnitude.

pp. 17, 18, 19 show
your last magnitude
virtually useless.
Why not longer exp. times?

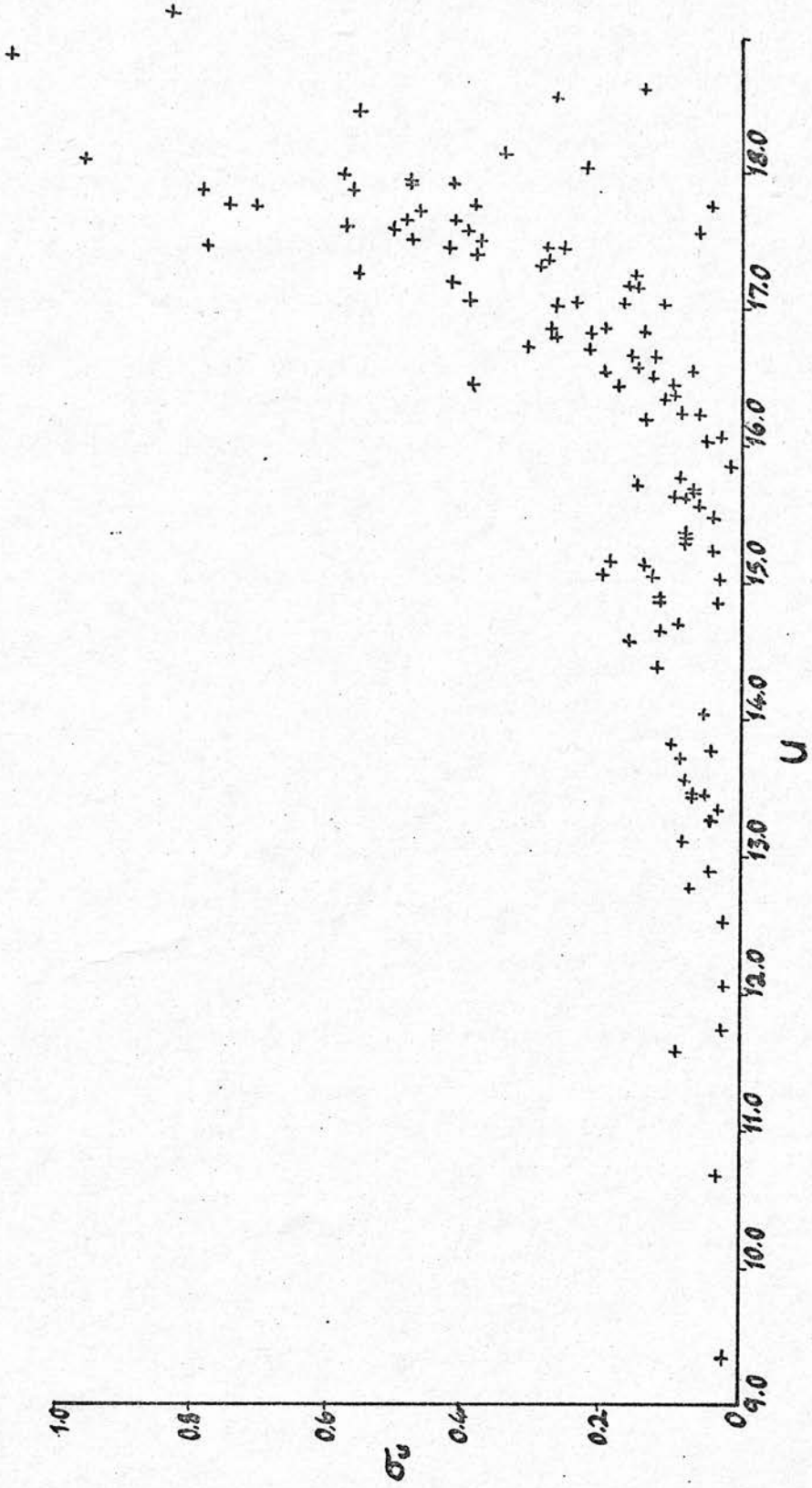

FIG 2(c): r m s Error in U Plotted vs U Magnitude.

drawn curves is as follows: a closely-spaced set of points is picked along the curve and these points are connected by straight lines to give a close approximation to the smooth curve. The points are closest together where the curvature is highest. The curve was divided according to iris reading, rather than magnitude so that the fiducial points do not always lie at the same magnitude; producing systematic errors.

The hand-drawn calibrations are applied automatically, using the computer program WSA4. This program reads in co-ordinates of the fiducial points of the calibration curve and fits straight lines between neighbouring points. The iris readings from the program stars are now read in and magnitudes are computed accordingly. The outputs from WSA4, for all the plates, are once more averaged and tabulated, using WSA3. These magnitudes are shown in Table 1.

Fig 2 shows the results of plotting V, B and U against the standard error of the mean in each. The errors rise steeply above V = $14^{m}.0$, B = $16^{m}.0$ and U = $16^{m}.0$.

Fig3 and fig 4 are graphs plotted to determine the colour equations. On fig 3, the centroid of points with B-V $< 0^{m}.775$ and the centroid of points with B-V $> 0^{m}.775$ were found. The straight line through these points gives the colour

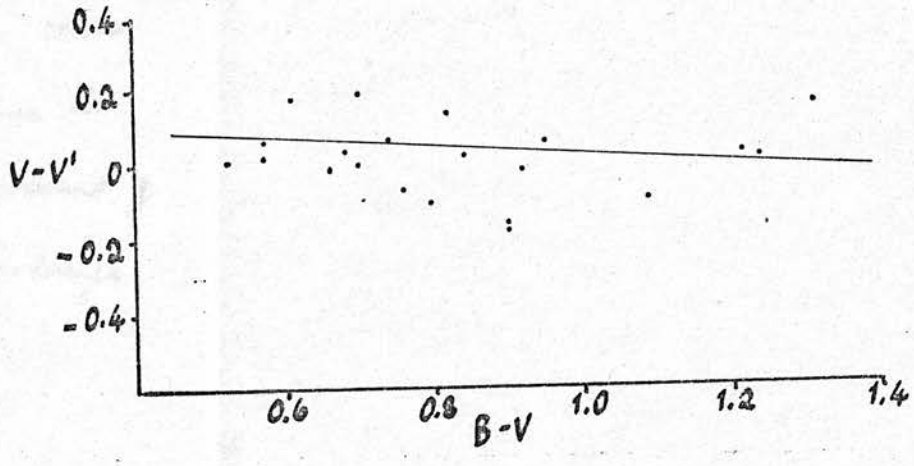

FIG 3: Photoelectric Minus Photographic V Magnitudes Plotted Against B-V to Give Colour Equation.

p 22.

Treatment of colour equation seems to take no account of photographic Purkinje effect.

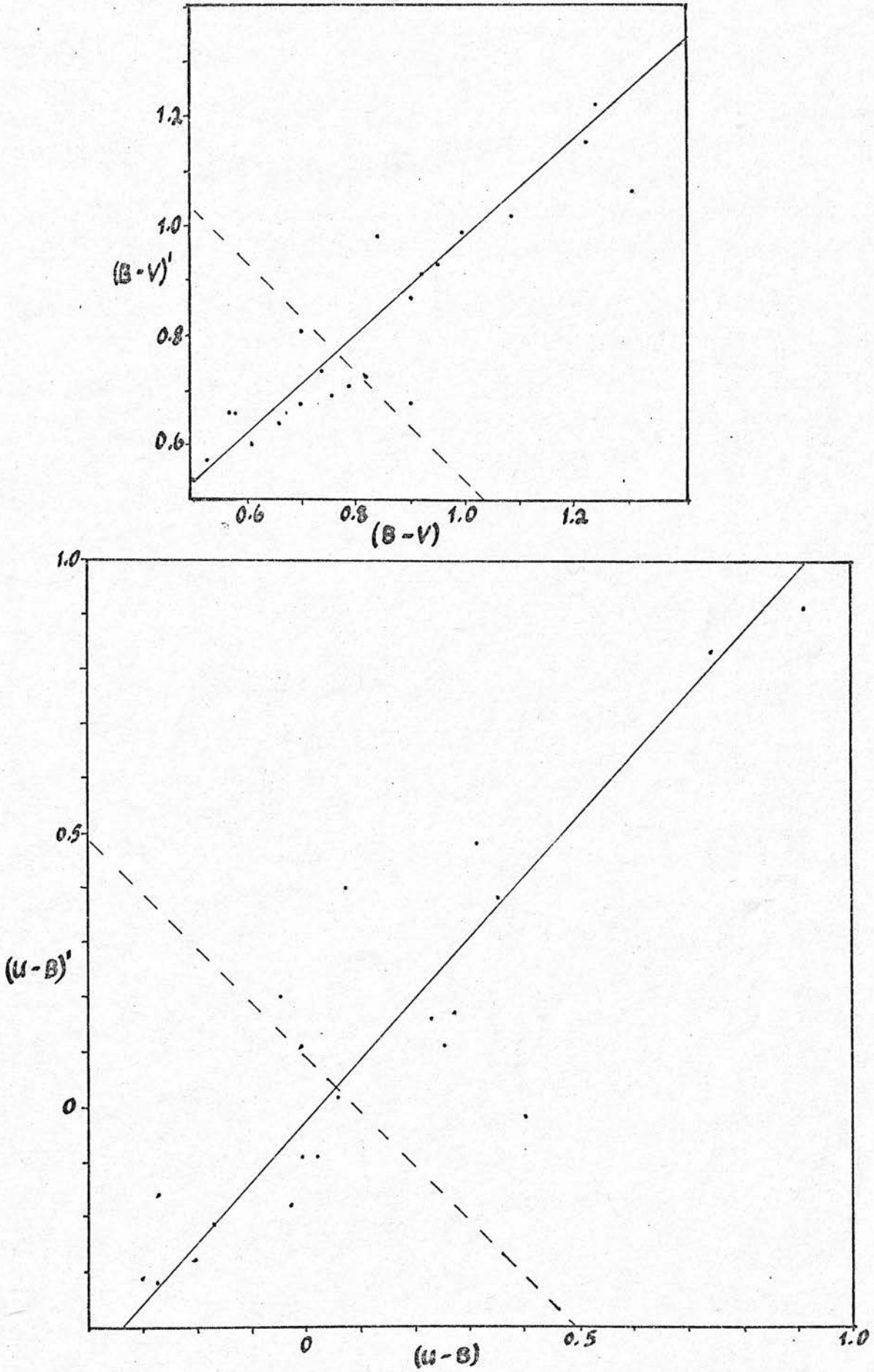

FIG 4: Photographic (B-V) and (U-B) Plotted Against Photoelectric (B-V) and (U-B) to Give Colour Equations.

TABLE 1

Star No.	V	No.of Plates	r.m.s. Error	B	No.of Plates	r.m.s. Error	U	No.of Plates	r.m.s. Error
1	7.22	4	0.01	8.46	4	0.00	9.36	4	0.02
2	15.10	1	0.00	17.31	4	0.44	19.06	1	0.00
3	0.00	0	0.00	17.64	4	0.35	17.40	2	0.39
4	15.26	1	0.00	16.60	4	0.12	16.80	4	0.27
5	14.54	4	0.11	15.49	4	0.04	15.64	4	0.10
6	14.86	4	0.26	15.79	4	0.06	16.02	4	0.05
7	14.84	4	0.13	15.72	4	0.11	15.87	4	0.20
8	12.19	4	0.02	12.85	4	0.03	12.51	4	0.02
9	15.22	4	0.12	17.10	4	0.33	17.16	4	0.17
10	15.22	4	0.20	16.86	4	0.27	17.05	4	0.24
11	15.60	3	0.50	17.22	4	0.27	18.02	2	0.23
12	15.33	2	0.29	17.63	4	0.41	18.60	2	0.14
13	15.50	2	0.08	17.47	4	0.46	18.15	2	0.35
14	14.14	4	0.04	14.80	4	0.08	14.85	4	0.03
15	11.72	4	0.01	12.38	4	0.02	12.07	4	0.02
16	14.05	4	0.06	14.75	4	0.07	14.59	4	0.16
17	14.86	2	0.04	16.24	4	0.12	16.81	4	0.22
18	14.52	4	0.07	15.31	4	0.07	15.79	4	0.09
19	14.62	4	0.11	15.01	4	0.03	15.02	4	0.03
20	14.77	4	0.08	15.45	4	0.12	15.64	4	0.08
21	15.10	1	0.00	17.19	4	0.30	17.71	4	0.47
22	14.87	1	0.00	16.28	4	0.16	17.59	2	0.51
23	11.16	3	0.06	11.76	4	0.04	11.58	4	0.09
24	13.16	1	0.00	13.76	1	0.00	13.78	3	0.04
25	15.65	2	0.15	16.52	4	0.12	17.01	4	0.27
26	0.00	0	0.00	17.16	4	0.26	17.09	2	1.74
27	14.60	4	0.09	15.16	4	0.06	15.34	4	0.08
28	15.09	4	0.22	16.12	4	0.06	16.54	4	0.20
29	15.50	2	0.21	16.38	4	0.17	17.18	4	0.16
30	15.58	3	0.28	16.39	3	0.20	17.19	4	0.42
31	15.43	4	0.33	16.25	4	0.02	16.68	4	0.12
32	15.03	4	0.13	15.96	4	0.07	16.39	4	0.10
33	15.09	2	0.01	16.38	4	0.13	16.72	4	0.31
34	15.50	4	0.27	16.38	4	0.20	16.70	4	0.22
35	13.10	4	0.06	13.73	4	0.04	13.82	4	0.10
36	16.00	1	0.00	17.53	4	0.16	18.86	2	1.07
37	12.81	4	0.02	13.56	4	0.03	13.26	4	0.04
38	14.65	4	0.16	15.26	4	0.04	15.21	4	0.04
39	16.47	2	0.82	17.69	4	0.47	17.59	3	0.58
40	15.15	3	0.25	16.16	4	0.04	17.06	4	0.40
41	13.67	4	0.08	14.30	4	0.03	14.39	4	0.12
42	14.02	4	0.07	14.77	4	0.05	14.66	4	0.12
43	0.00	0	0.00	16.37	2	0.02	17.05	3	0.17
44	13.99	4	0.08	14.74	4	0.03	14.90	4	0.12
45	12.47	4	0.08	13.16	4	0.04	13.11	4	0.08

m = 0.00 means the images could not be measured

Star No.	V	No.of Plates	r.m.s. Error	B	No.of Plates	r.m.s. Error	U	No.of Plates	r.m.s. Error
46	13.13	3	0.08	13.62	4	0.07	13.84	2	0.05
47	12.99	4	0.06	13.68	4	0.07	13.83	4	0.06
48	14.96	3	0.06	16.06	4	0.08	16.47	4	0.39
49	15.14	2	0.09	16.94	4	0.39	17.45	4	0.43
50	15.17	1	0.00	17.77	4	0.45	18.09	2	0.96
51	14.29	4	0.12	14.92	4	0.08	15.13	4	0.14
52	0.00	0	0.00	17.19	4	0.33	17.64	3	0.49
53	0.00	0	0.00	17.15	4	0.31	17.98	3	0.58
54	0.00	0	0.00	17.77	3	0.49	17.91	3	0.42
55	0.00	0	0.00	17.50	4	0.21	18.55	2	0.27
56	15.42	1	0.00	16.11	4	0.06	16.44	4	0.18
57	15.57	1	0.00	16.25	4	0.07	16.46	4	0.10
58	15.18	2	0.39	16.47	4	0.15	16.85	4	0.28
59	15.99	2	0.61	17.20	4	0.23	17.57	4	0.40
60	14.20	4	0.07	14.94	4	0.09	15.05	4	0.20
61	14.61	4	0.12	16.28	4	0.17	17.24	4	0.15
62	15.43	3	0.32	17.31	4	0.22	17.25	3	0.56
63	14.88	4	0.07	16.07	4	0.06	16.24	4	0.06
64	12.74	3	0.05	13.66	4	0.03	13.56	4	0.08
65	12.45	4	0.03	13.38	4	0.02	13.45	4	0.05
66	14.22	4	0.20	15.27	4	0.04	15.47	4	0.04
67	14.74	4	0.11	15.41	4	0.06	15.55	4	0.06
68	12.73	4	0.04	13.48	4	0.05	13.33	4	0.03
69	13.70	4	0.12	14.60	4	0.04	14.87	4	0.12
70	15.29	4	0.11	16.31	4	0.08	16.26	4	0.09
71	14.58	4	0.15	15.44	4	0.02	15.69	4	0.07
72	15.21	2	0.10	16.97	4	0.34	17.87	2	0.79
73	0.00	0	0.00	17.84	3	0.55	19.78	1	0.00
74	0.00	0	0.00	17.66	4	0.45	19.70	1	0.00
75	0.00	0	0.00	17.67	4	0.28	18.82	1	0.00
76	11.45	4	0.03	12.65	4	0.02	13.45	4	0.07
77	15.27	2	0.23	17.64	4	0.32	18.66	1	0.00
78	14.17	4	0.05	14.57	4	0.08	14.70	4	0.09
79	13.39	4	0.11	13.64	4	0.03	13.72	4	0.08
80	0.00	0	0.00	17.17	4	0.31	17.76	3	0.39
81	15.80	1	0.00	17.24	4	0.32	17.75	3	0.71
82	14.28	4	0.09	15.07	4	0.11	15.17	4	0.19
83	14.80	4	0.05	15.32	4	0.03	15.33	4	0.08
84	0.00	0	0.00	17.06	4	0.26	17.84	4	0.57
85	14.93	3	0.07	15.83	4	0.03	16.32	4	0.11
86	0.00	0	0.00	16.53	2	0.11	17.46	3	0.28
87	0.00	0	0.00	16.07	2	0.19	16.57	4	0.15
88	0.00	0	0.00	17.61	4	0.50	17.56	2	0.06
89	0.00	0	0.00	17.68	2	0.83	17.71	1	0.00
90	0.00	0	0.00	15.89	1	0.00	16.50	2	0.13

Star No.	V	No.of Plates	r.m.s. Error	B	No.of Plates	r.m.s. Error	U	No.of Plates	r.m.s. Error
91	18.10	1	0.00	16.99	4	0.18	17.47	3	0.26
92	0.00	0	0.00	15.72	1	0.00	16.07	2	0.03
93	13.44	4	0.03	14.16	4	0.04	14.02	4	0.05
94	14.80	4	0.16	15.67	4	0.07	16.20	4	0.14
95	15.91	2	0.18	17.72	4	0.48	17.75	2	0.75
96	15.17	3	0.17	16.70	4	0.23	17.31	4	0.29
97	14.77	4	0.06	15.41	4	0.12	15.30	4	0.08
98	16.70	1	0.00	17.85	3	0.49	17.50	3	0.38
99	12.46	4	0.05	13.13	4	0.02	12.90	4	0.04
100	15.37	3	0.19	16.46	4	0.22	16.82	4	0.14
101	0.00	0	0.00	18.12	4	0.56	18.89	2	0.73
102	15.25	2	0.02	16.56	4	0.15	17.50	4	0.48
103	12.25	4	0.01	12.86	4	0.04	12.97	4	0.07
104	15.24	4	0.11	16.58	4	0.19	16.87	4	0.20
105	15.31	1	0.00	17.74	4	0.31	19.18	2	0.83
106	15.10	1	0.00	17.94	4	0.57	19.14	1	0.00
107	14.54	4	0.07	15.50	4	0.04	15.69	4	0.07
108	15.23	4	0.26	16.40	4	0.12	17.02	4	0.11
109	14.83	4	0.04	16.96	4	0.24	18.42	3	0.56
110	14.68	4	0.10	15.53	4	0.06	15.72	4	0.15
111	15.66	3	0.51	17.17	4	0.32	17.94	3	0.48
112	14.90	1	0.00	17.26	4	0.21	17.66	4	0.42
113	14.94	4	0.19	15.78	4	0.04	16.55	4	0.07
114	15.76	3	0.52	16.82	4	0.23	17.48	2	0.78
115	9.62	4	0.15	10.35	4	0.03	10.68	4	0.03
116	13.24	4	0.03	13.79	4	0.03	13.45	4	0.07
117	15.65	3	0.22	17.46	4	0.42	18.02	1	0.00
118	11.30	4	0.03	12.05	4	0.04	11.74	4	0.02
119	14.82	1	0.00	16.05	4	0.08	16.66	3	0.16
120	15.09	4	0.25	15.98	4	0.08	16.32	4	0.11
121	14.92	3	0.14	17.14	4	0.29	17.75	2	0.04
122	14.40	4	0.02	15.06	4	0.08	15.05	4	0.13
123	15.38	1	0.00	17.16	4	0.32	17.36	3	0.28
124	0.00	0	0.00	17.54	4	0.46	17.92	4	0.48

TABLE 2

Star No.	V	No. of Plates	r.m.s. Error	B-V	No. of BPlates	r.m.s. Error	U-B	No. of UPlates	r.m.s. Error
1	7.18	4	0.01	1.26	4	0.02	0.83	4	0.02
2	14.92	1	0.00	2.30	4	0.44	1.61	1	0.44
3	-2.50	0	0.00	[illegible]	4	0.35	-0.20	2	0.52
4	15.21	1	0.00	1.37	4	0.12	0.20	4	0.29
5	14.55	4	0.11	0.95	4	0.11	0.16	4	0.10
6	14.87	4	0.26	0.93	4	0.26	0.23	4	0.08
7	14.86	4	0.13	0.86	4	0.17	0.16	4	0.23
8	12.24	4	0.02	0.64	4	0.03	-0.30	4	0.04
9	15.09	4	0.12	1.94	4	0.35	0.07	4	0.37
10	15.13	4	0.20	1.68	4	0.34	0.19	4	0.36
11	15.51	3	0.50	1.68	4	0.57	0.75	2	0.36
12	15.14	2	0.29	2.38	4	0.50	0.90	2	0.43
13	15.36	2	0.08	2.04	4	0.47	0.64	2	0.58
14	14.19	4	0.04	0.64	4	0.09	0.06	4	0.08
15	11.77	4	0.01	0.64	4	0.02	-0.26	4	0.02
16	14.10	4	0.06	0.68	4	0.09	-0.13	4	0.17
17	14.80	2	0.04	1.41	4	0.12	0.54	4	0.25
18	14.55	4	0.07	0.78	4	0.10	0.45	4	0.12
19	14.71	4	0.11	0.35	4	0.11	0.02	4	0.04
20	14.82	4	0.08	0.66	4	0.14	0.20	4	0.15
21	14.94	1	0.00	2.17	4	0.30	0.49	4	0.56
22	14.81	1	0.00	1.44	4	0.16	1.21	2	0.54
23	11.22	3	0.06	0.57	4	0.07	-0.14	4	0.10
24	13.22	1	0.00	0.57	1	0.00	0.04	3	0.04
25	15.67	2	0.15	0.86	4	0.19	0.47	4	0.29
26	-2.43	0	0.00	16.31	4	0.26	-0.04	2	1.75
27	14.67	4	0.09	0.53	4	0.10	0.18	4	0.10
28	15.09	4	0.22	1.03	4	0.23	0.40	4	0.21
29	15.52	2	0.21	0.87	4	0.26	0.75	4	0.23
30	15.61	3	0.28	0.80	3	0.34	0.75	4	0.46
31	15.46	4	0.33	0.81	4	0.33	0.41	4	0.13
32	15.04	4	0.13	0.93	4	0.15	0.41	4	0.12
33	15.05	2	0.01	1.31	4	0.13	0.33	4	0.34
34	15.52	4	0.27	0.87	4	0.34	0.31	4	0.30
35	13.16	4	0.06	0.60	4	0.07	0.10	4	0.10
36	15.92	1	0.00	1.57	4	0.16	1.23	2	1.09
37	12.85	4	0.02	0.73	4	0.04	-0.25	4	0.05
38	14.71	4	0.16	0.58	4	0.16	-0.03	4	0.05
39	16.44	2	0.82	1.24	4	0.95	-0.08	3	0.75
40	15.15	3	0.25	1.02	4	0.25	0.84	4	0.41
41	13.73	4	0.08	0.62	4	0.08	0.09	4	0.12
42	14.06	4	0.07	0.74	4	0.09	-0.09	4	0.13
43	-3.31	0	0.00	17.46	2	0.02	0.64	3	0.17
44	14.03	4	0.08	0.73	4	0.09	0.16	4	0.13
45	12.52	4	0.08	0.67	4	0.09	-0.04	4	0.09

Star No.	V	No. of Plates	r.m.s. Error	B-V	No. of B Plates	r.m.s. Error	U-B	No. of U Plates	r.m.s. Error
46	13.21	3	0.08	0.45	4	0.11	0.23	2	0.08
47	13.04	4	0.06	0.67	4	0.09	0.16	4	0.09
48	14.95	3	0.06	1.11	4	0.10	0.40	4	0.40
49	15.02	2	0.09	1.86	4	0.41	0.48	4	0.59
50	14.93	1	0.00	2.71	4	0.45	0.31	2	1.06
51	14.35	4	0.12	0.59	4	0.14	0.22	4	0.16
52	[illegible]	0	0.00	[illegible]	4	0.33	0.43	3	0.59
53	[illegible]	0	0.00	[illegible]	4	0.31	0.77	3	0.66
54	[illegible]	0	0.00	[illegible]	3	0.49	0.15	3	0.65
55	[illegible]	0.	0.00	[illegible]	4	0.21	0.97	2	0.34
56	15.47	1	0.00	0.67	4	0.06	0.32	4	0.19
57	15.62	1	0.00	0.66	4	0.07	0.21	4	0.12
58	15.14	2	0.39	1.31	4	0.41	0.36	4	0.32
59	15.96	2	0.61	1.24	4	0.65	0.36	4	0.46
60	14.24	4	0.07	0.71	4	0.12	0.12	4	0.22
61	14.51	4	0.12	1.71	4	0.21	0.89	4	0.23
62	15.30	3	0.32	1.95	4	0.39	-0.04	3	0.60
63	14.85	4	0.07	1.20	4	0.09	0.17	4	0.08
64	12.75	3	0.05	0.93	4	0.06	-0.07	4	0.09
65	12.46	4	0.03	0.93	4	0.03	0.08	4	0.05
66	14.21	4	0.20	1.05	4	0.20	0.19	4	0.06
67	14.79	4	0.11	0.65	4	0.12	0.15	4	0.09
68	12.77	4	0.04	0.73	4	0.06	-0.12	4	0.06
69	13.72	4	0.12	0.89	4	0.12	0.26	4	0.13
70	15.29	4	0.11	1.02	4	0.14	0.03	4	0.12
71	14.60	4	0.15	0.85	4	0.15	0.24	4	0.08
72	15.10	2	0.10	1.81	4	0.36	0.84	2	0.86
73	[illegible]	0	0.00	[illegible]	3	0.55	1.78	1	0.55
74	[illegible]	0	0.00	[illegible]	4	0.45	1.87	1	0.45
75	[illegible]	0	0.00	[illegible]	4	0.28	1.06	1	0.28
76	11.42	4	0.03	1.22	4	0.04	0.75	4	0.08
77	15.07	2	0.23	2.47	4	0.40	0.95	1	0.32
78	14.26	4	0.05	0.36	4	0.09	0.13	4	0.12
79	13.50	4	0.11	0.21	4	0.12	0.09	4	0.09
80	[illegible]	0	0.00	[illegible]	4	0.31	0.56	3	0.50
81	15.73	1	0.00	1.48	4	0.32	0.48	3	0.78
82	14.31	4	0.09	0.78	4	0.14	0.11	4	0.22
83	14.87	4	0.05	0.49	4	0.06	0.03	4	0.08
84	[illegible]	0	0.00	[illegible]	4	0.26	0.73	4	0.63
85	14.94	3	0.07	0.90	4	0.07	0.46	4	0.11
86	[illegible]	0	0.00	[illegible]	2	0.11	0.86	3	0.30
87	[illegible]	0	0.00	[illegible]	2	0.19	0.47	4	0.24
88	[illegible]	0	0.00	[illegible]	4	0.50	-0.04	2	0.50
89	[illegible]	0	0.00	[illegible]	2	0.83	0.05	1	0.83
90	[illegible]	0	0.00	[illegible]	1	0.00	0.57	2	0.13

Star No.	V	No. of Plates	r.m.s. Error	B-V	No. of B Plates	r.m.s. Error	U-B	No. of U Plates	r.m.s. Error
91	18.42	1	0.00	-1.26	4	0.18	0.46	3	0.32
92	-2.21	0	0.00	16.77	1	0.00	0.34	2	0.03
93	13.48	4	0.03	0.70	4	0.05	-0.11	4	0.07
94	14.82	4	0.16	0.87	4	0.17	0.50	4	0.16
95	15.79	2	0.18	1.86	4	0.52	0.06	2	0.89
96	15.09	3	0.17	1.57	4	0.28	0.57	4	0.37
97	14.83	4	0.06	0.62	4	0.14	-0.08	4	0.15
98	16.68	1	0.00	1.16	3	0.49	-0.30	3	0.62
99	12.51	4	0.05	0.64	4	0.06	-0.18	4	0.05
100	15.36	3	0.19	1.10	4	0.29	0.35	4	0.26
101	-2.57	0	0.00	19.34	4	0.56	0.72	2	0.92
102	15.21	2	0.02	1.32	4	0.15	0.87	4	0.51
103	12.31	4	0.01	0.57	4	0.04	0.13	4	0.08
104	15.19	4	0.11	1.37	4	0.22	0.28	4	0.28
105	15.10	1	0.00	2.53	4	0.31	1.33	2	0.89
106	14.83	1	0.00	2.96	4	0.57	1.11	1	0.57
107	14.55	4	0.07	0.95	4	0.08	0.19	4	0.08
108	15.20	4	0.26	1.19	4	0.29	0.57	4	0.17
109	14.66	4	0.04	2.21	4	0.25	1.34	3	0.61
110	14.70	4	0.10	0.84	4	0.12	0.19	4	0.16
111	15.58	3	0.51	1.56	4	0.61	0.72	3	0.58
112	14.70	1	0.00	2.46	4	0.21	0.38	4	0.47
113	14.97	4	0.19	0.83	4	0.19	0.72	4	0.08
114	15.75	3	0.52	1.07	4	0.57	0.62	2	0.81
115	9.66	4	0.15	0.71	4	0.15	0.32	4	0.04
116	13.31	4	0.03	0.52	4	0.04	-0.29	4	0.08
117	15.53	3	0.22	1.87	4	0.47	0.53	1	0.42
118	11.34	4	0.03	0.74	4	0.04	-0.26	4	0.04
119	14.79	1	0.00	1.25	4	0.08	0.57	3	0.17
120	15.11	4	0.25	0.88	4	0.26	0.33	4	0.13
121	14.74	3	0.14	2.31	4	0.32	0.57	2	0.29
122	14.45	4	0.02	0.65	4	0.08	0.01	4	0.15
123	15.26	1	0.00	1.84	4	0.32	0.21	3	0.42
124	-2.49	0	0.00	18.72	4	0.46	0.36	4	0.67

equation for V magnitudes -

$$V = V^1 - 0.1404(B-V) + 0.1416$$

where V is photoelectric and V^1 is photographic. Star 21 was omitted from these calculations because of the large scatter in observations of its magnitude.

On fig 4, the points on the (B-V) vs $(B-V)^1$ diagram were divided into two groups by the line

$$(B-V)^1 = 1^m.525 - (B-V)$$

where (B-V) is photoelectric and $(B-V)^1$ is photographic. Centroids of the two groups of points were found - omitting stars 8 and 21 due to large errors - and the straight line through the centroids gives the colour equation in B-V:

$$B-V = 1.071\ (B-V)^1 - 0.070.$$

Similarly, we have for U-B:

$$U-B = 0.9084\ (U-B)^1 + 0.0192.$$

A computer program, WSA7, applies these colour equations to the photographic magnitudes. The corrected magnitudes are shown in table 2.

Evaluation of UBV Results

All stars with 2 or fewer observations in any colour were discarded. 68 of the original 124 stars remain. This is because the stars to be measured were picked out on a high contrast print and a considerable proportion of the

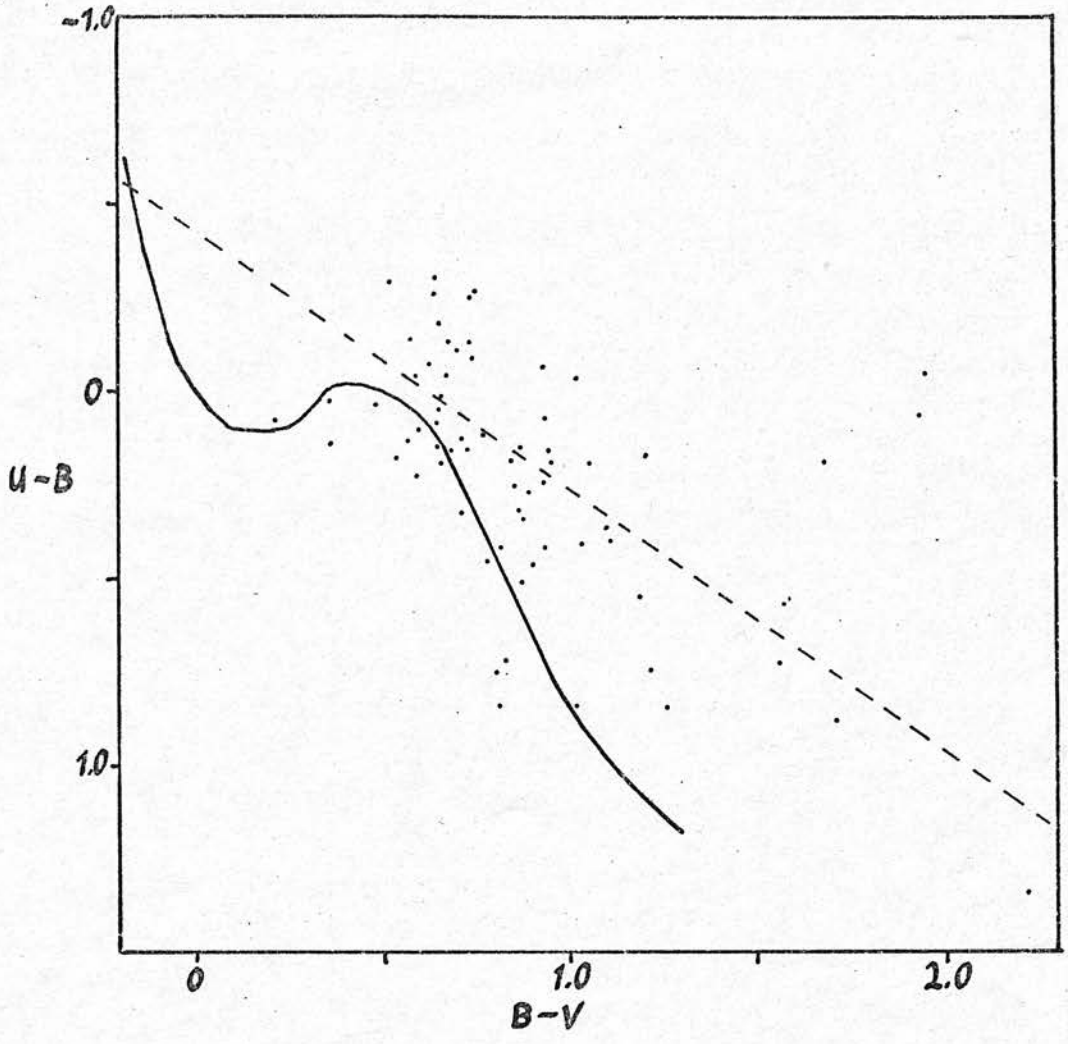

FIG 5 : U-B Plotted Against B-V for Stars in NGC 654. Solid Line Represents Zero Age Main Sequence. Dashed Line Represents Effect of Reddening.

images was of stars just on the limit of visibility.

The (U-B) vs (B-V) plot for these stars is shown in fig 5. The solid main sequence curve is from the PhD thesis of M P Fitzgerald (21). The broken line is a reddening line with gradient 0.7. All stars above this line are assumed to be OB stars. The line is drawn $0^{m}.07$ above the highest point in the "kink" of the main sequence curve; $0^{m}.07$ being the mean standard error in U-B. The reddening of any star lying below this line is ambiguous and may have two or three possible values, $(B-V)_o$ and $(U-B)_o$, the unreddened values of B-V and U-B are found by drawing a line through the point on fig 5 corresponding to the star, parallel to the standard reddening line. The points of intersection of this line with the main sequence curve give values of $(B-V)_o$ and $(U-B)_o$; assuming the star lies on the main sequence.

The unreddened values of the colours of the 68 stars were found by the above method and the results are shown in Table 4. E_{B-V}, the reddened minus the unreddened B-V magnitudes, was computed for each star and thence V_o, the unreddened value of the V magnitude. In this case we use the equation

$$V_o = V - R\, E_{B-V}, \text{ where } R = 3.$$

This number 3 is very uncertain and may well be wrong by a

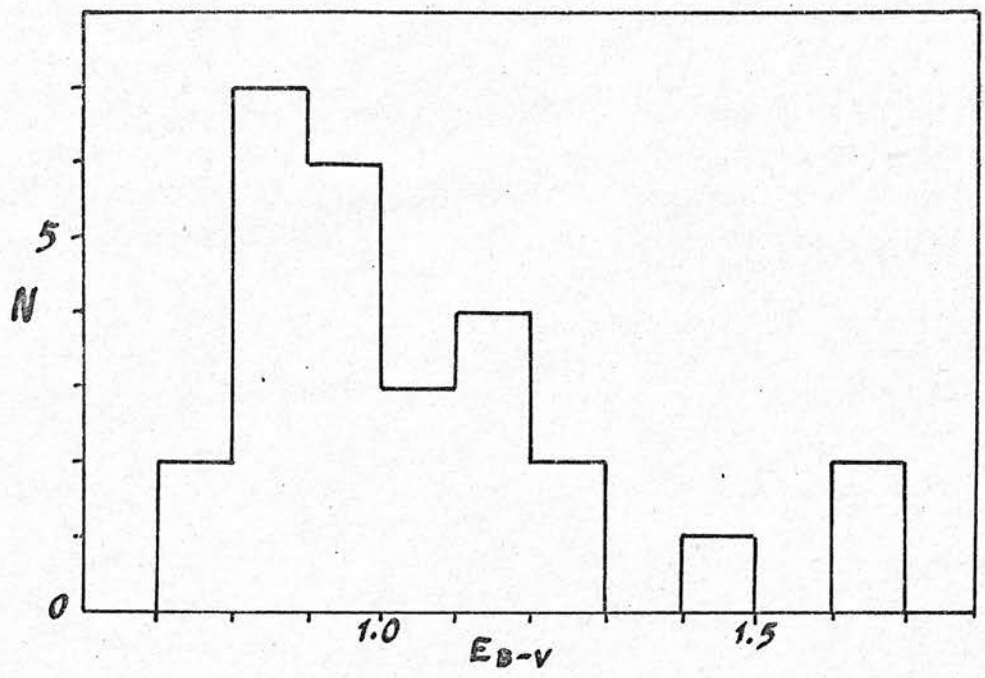

FIG 6 : Frequency Distribution of Colour Excess for Stars in NGC 654.

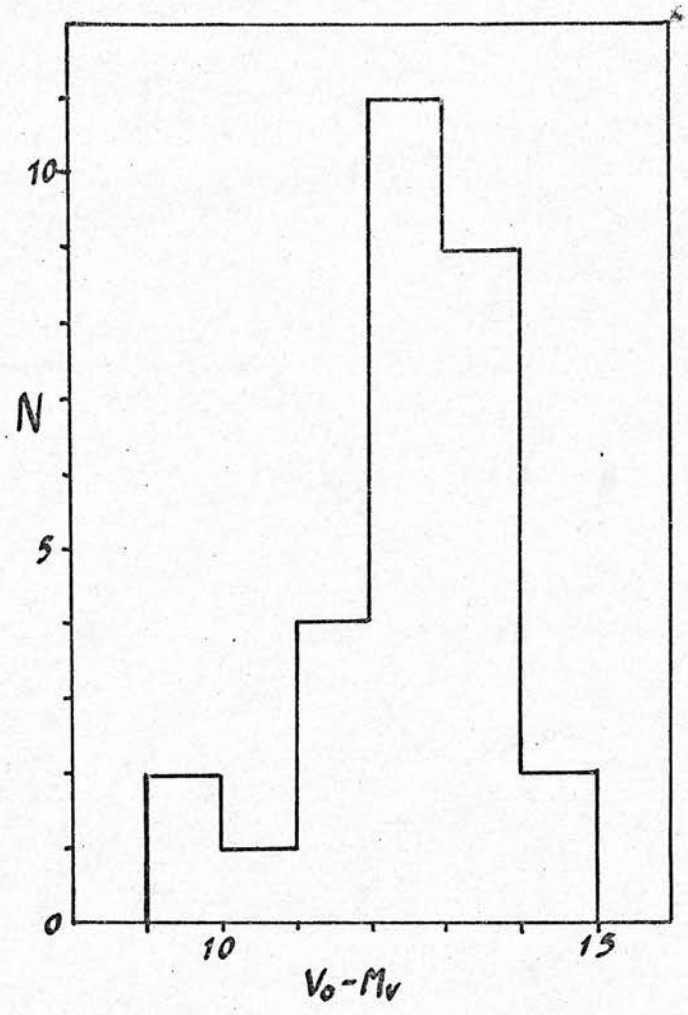

FIG 7 : Frequency Distribution of Distance Modulus for Stars in NGC 654.

factor 2.

Distance estimates from the computed values of V_o depend strongly on the value of R. The distance estimates would be less by a factor 4 if R = 6 was used.

The values of M_v given in table 4 are taken from the PhD thesis of M P Fitzgerald and correspond to values of $(B-V)_o$ for main sequence stars.

Fig 6 is a histogram of E_{B-V} for the stars with only one possible reddening, ie those stars earlier than B5 or later than K2. The early stars are, of course, far more numerous than the late ones: no late type main sequence stars could be seen at the distance of this cluster. The modal value is $E_{B-V} = 0^m.9$.

Fig 7 is a histogram of the distance modulus, $V_o - M_v$ of the stars. Once more, only stars with unambiguous reddening are shown. The modal value here is $V_o - M_v = 12^m.5$. This implies <u>distance = 3.2 kpc</u>.

If R = 6 was used in the computation instead of R = 3 we would find $V_o - M_v = 10^m.0$ giving a distance of 1.0 kpc. Until reddening processes are more fully understood, all we can say is that NGC 654 probably lies at a distance of between 1 and 4 kpc.

Stars with Ambiguous Reddening

We assume that any star with a possible value of $(B-V)_o$ corresponding to a main sequence star at the distance of the cluster is a member of the cluster. The conditions applied are

$0^m.7 < E_{B-V} < 1^m.3$

and $11^m < V_o - M_V < 14^m$.

Stars which do not fall into the above category are: 1,9, 10,19,23,27,30,51,61,63,65,70,76,78,79,83,96,97,100,103, 104,109,113,115.

1 is an F5Ia supergiant (5).

9 and 10 have large B errors.

19 has two possible main sequence interpretations.

(i) It is a nearby, unreddened A2 star.

(ii) It is a B8 star with distance modulus $13^m.6$.

We can rule out (ii) on the grounds that the $0^m.46$ reddening is much too small for a star at this distance.

23 has three possible main sequence positions:

(i) An unreddened F9 star at 250 pc.

(ii) An A2 star with $E_{B-V} = 0^m.20$ at 400 pc.

(iii) A B8 star with $E_{B-V} = 0^m.69$ at 1000 pc.

27 may be interpreted in two ways:

(i) An F0 star with $E_{B-V} = 0^m.21$ at 2000 pc.

(ii) A B9 star with $E_{B-V} = 0^m.62$ at 4000 pc.

From the reddening and distance (i) looks more likely.

30 has large U,B and V errors.

51 presents two possibilities:

(i) An F0 star with $E_{B-V} = 0^m.27$ at 1600 pc.

(ii) A B8 star with $E_{B-V} = 0^m.68$ at 3200 pc.

(ii) would imply that this is a cluster member with rather smaller reddening than usual.

61 has three possible positions:

(i) A G9 star with $E_{B-V} = 0^m.95$ at 250 pc.

(ii) An F3 star with $E_{B-V} = 1^m.31$ at 350 pc.

(iii) A B7 star with $E_{B-V} = 1^m.84$ at 1000 pc.

The high reddening of this star makes sense because the star density is very low in this region, implying a zone of obscuring matter between us and the stars there. The observations of 61 imply that this zone is closer than 1000 pc. Nearby, 63 has $E_{B-V} = 1^m.44$ and distance equal to that of NGC 654. The reddening for (iii) is probably excessive. This leaves possibilities (i) and (ii).

63 is probably a cluster member, excessively reddened by a nearby dust cloud as mentioned above.

65 is apparently a B3 star at 1500 pc. $E_{B-V} = 1^m.14$ is

large but this may be due to the dust cloud mentioned above.

70 is a B1 star with $E_{B-V} = 1^m.28$ at 9000 pc apparently. Large errors in the magnitudes probably account for this.

76 has three possible interpretations:

(i) A K0 star with $E_{B-V} = 0^m.40$ at 70 pc.

(ii) An A8 star with $E_{B-V} = 0^m.95$ at 200 pc.

(iii) A B9 star with $E_{B-V} = 1^m.28$ at 320 pc.

All the alternatives give excessive reddening for the corresponding distance; perhaps this star is associated with the above mentioned dust cloud.

78 offers two possibilities:

(i) An A3 star with $E_{B-V} = 0^m.07$ at 2500 pc.

(ii) A B9 star with $E_{B-V} = 0^m.44$ at 4000 pc.

Clearly for these two possibilities, the reddenings are excessively small for the distances involved. The star may be subluminous in some way or perhaps it is a binary. No definite conclusion can be drawn.

79 has two possible interpretations:

(i) An A7 star with no reddening at 1500 pc.

(ii) A B9.5 with $E_{B-V} = 0^m.25$ at 4000 pc.

Neither of these is likely for a main sequence star.

83 presents two possibilities:

(i) An F3 with $E_{B-V} = 0^m.08$ at 1500 pc.

(ii) A B7 with $E_{B-V} = 0^m.62$ at 6000 pc.

Again neither interpretation is likely.

96 is apparently a B3 star with $E_{B-V} = 1^m.77$ at 1500 pc. Errors are, however, large.

97 is apparently a B3 star with $E_{B-V} = 1^m.82$ at 6000 pc. It is just possible that this is a member of NGC 654.

103 has two possible interpretations:

(i) An F2 star with $E_{B-V} = 0^m.20$ at 600 pc.

(ii) A B7 star with $E_{B-V} = 0^m.69$ at 1500 pc.

These are equally likely.

104 is a B2 star with $E_{B-V} = 1^m.61$ at 3200 pc. It is possible that this is a cluster member with fairly high obscuration nearby, however the errors are rather large.

109 has large U errors.

113 is an unreddened K0 star at 600 pc.

115 offers three interpretations:

(i) An unreddened G6 star at 80 pc.

(ii) An F0 star with $E_{B-V} = 0^{m}.39$ at 150 pc.

(iii) A B8 star with $E_{B-V} = 0^{m}.80$ at 320 pc.

From the reddening, the first possibility seems most likely. Another possibility is that this is a B5Ib supergiant and a cluster member.

CHAPTER 3

Polarization of Starlight in NGC 654

Introduction

Pratt (19) has described the use of a new photographic method of measuring the polarization of starlight. This method has been used in this study of NGC 654 exactly as Pratt has described it in his paper.

The polaroid filter shown in fig 8 was designed by Dr V C Reddish. The dashed lines show the preferred direction of transmission of the polaroid. The filter is positioned just in front of the plate inside the Schmidt telescope. Three exposures are made, the filter being rotated through 120° and the telescope slightly displaced in right ascention between exposures. This results in three images for each star. If the star is seen through the central part of the filter, the three images are seen through three different orientations of the polaroid. If the star is seen through one of the three outer segments, the orientation of the polaroid does not change from exposure to exposure.

The Observing Conditions Control Curve

The three images of a star seen through an outer segment of the polaroid filter differ only because of variations

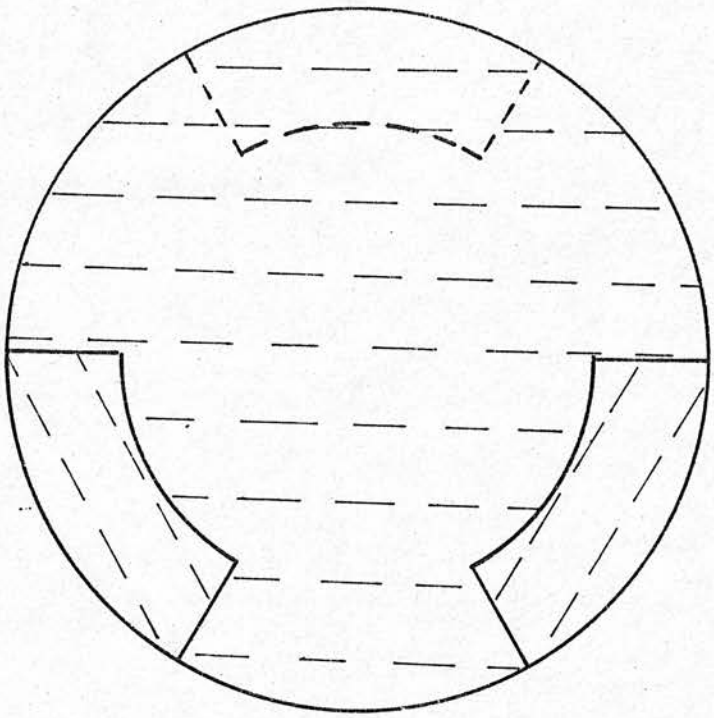

FIG 8 : Diagram of Polaroid Filter Used for Polarization Measures. Dashed Lines Show the Preferred Direction of Transmission of the Polaroid.

Plates for Polarization Measurements

in NGC 654

Plate	Emulsion	Exposure	Date	Siderial Time
880	IIaO	3 x 5 min	20.10.68	04^h12^m
924	IIaO	3 x 5 min	22. 1.69	02^h50^m
925	IIaO	3 x 5 min	22. 1.69	03^h50^m
941	IIaO	3 x 5 min	8. 2.69	03^h55^m
942	IIaO	3 x 5 min	8. 2.69	04^h32^m

in exposure time, seeing, transparency, etc. No polarization effect is present. The differences in brightness between the images of stars in these outer segments are used to give a correction to measurements of the programme stars to compensate for changes in observing conditions between exposures.

Theory

Let dm_1, dm_2 and dm_3 be the magnitude differences of the first, second and third images of a star respectively from their mean magnitude. Then the amount of polarization in magnitudes is given by the equation

$$p = 2.5 \log (1 + P) \; / \; (1 - P)$$

where $P = (10^{-dm_1/2.5} - 1)^2 + {}^1/_3 \, (10^{-dm_2/2.5} - 10^{-dm_3/2.5})^2$

and the position angle of the electric vector of polarization, θo, is given by

$$\tan 2\theta o = (10^{-dm_2/2.5} - 10^{-dm_3/2.5}) \; / \; (10^{-dm_1/2.5} - 1)$$

A full treatment of the theory is given in Pratt's paper.

Data Collection

Five plates were taken with the 40/60 cm Schmidt telescope at the Royal Observatory Edinburgh. All plates were on IIaO emulsion with three exposures of five minutes duration each for the three filter positions. All plates were taken when the moon was below the horizon so that polarized moonlight would not affect the results in any way.

Measurement of Images

All measurement of star images on polarization plates was done using the Computer Controlled Iris Photometer (CCIP).

The CCIP is fully described in Appendix 1. Co-ordinate data from a direct plate was processed using the computer program WSA9 to give co-ordinate data for all the images on the polarization plates. This program is more fully described in the chapter on the CCIP. The CCIP was used in the semi-automatic mode so that each run, beginning and ending with measurement of the photoelectric standard stars, could be done at a sitting lasting about two hours.

The stars on each plate were measured in four runs as follows:

(1) Standards - Program stars - Standards

(2) Standards - OCC I stars - Standards

(3) Standards - OCC II stars - Standards

(4) Standards - OCC III stars - Standards

where OCC I, II and III are the Observing Conditions Control regions where the orientation of the polaroid does not change from exposure to exposure.

The standards used to calibrate this work are the 21 stars listed by Hoag et al (6) in NGC 654 and the B values are used.

The programme, OCC I, OCC II and OCC III stars each number about 100 so that there are altogether between 400 and 500 images per run, remembering that each star has 3 images.

The output from each measurement run is on paper tape. These tapes are used in subsequent reductions of the data.

Reductions

All reductions of data from the CCIP were done automatically using the ICL 4130 computer at the Royal Observatory Edinburgh. Four computer programs were written and the reduction done in four stages.

WSPOL1 is a program which causes the raw data on paper tape from the CCIP to be read up on to magnetic tape. No further processing of the data is done at this stage.

Calibration curves - magnitude vs iris reading - are plotted by hand for the standard stars on each plate. The reasons for plotting calibration curves by hand are gone into fully in the chapter on UBV photometry. The co-ordinates of a series of closely spaced points on each curve are punched on paper tape for each plate. The program WSPOL2 causes these co-ordinates to be read into the computer and the iris readings are read down from magnetic tape and calibrated to give magnitudes for all the star images. These magnitudes are

then stored on another magnetic tape.

WSPOL3 causes the magnitudes to be read down from magnetic tape and averaged over the various plates. All spurious magnitudes are rejected by a procedure called the 1.5 rms cycle developed and fully described by Pratt [19]. Briefly all magnitude differences which differ by more than 1.5 times the rms deviation from the corresponding magnitude differences on other plates are rejected from the final computations. This procedure is repeated until all spurious measurements are removed. The spurious measurements are normally due to overlapping star images - these overlaps being different on different plates because of differences in the spacing of the 3 exposures. The magnitudes of the programme stars are corrected using the mean magnitude differences in the OCC regions. These corrections are magnitude dependent. Finally the magnitude differences are substituted in the formulae given in the Theory section to give strength and angle of polarization together with corresponding errors and the Stokes parameters Q and U where

$$Q = p \cos 2\theta_o \text{ and } U = p \text{ Sin } 2\theta_o.$$

Certain stars gave odd results in the output from WSPOL3. All stars were examined on each plate and obvious overlaps were picked out. Some stars had an overlap on the same image for several plates and in these cases the good

measures were sometimes rejected by the "1.5 rms cycle" in favour of the consistently bad ones. All such cases were picked out and the computations repeated on the good measures using the program WSPOL4 which was written for this purpose.

The limiting magnitude for the polarization plates is $15^{m}.00$ in B. Only stars brighter than this are listed in the table of results below. All plates were scrutinised for overlaps on the images of stars brighter than $15^{m}.00$. Stars with overlaps on four or more of the five plates are omitted. The remaining stars are as follows:

Table P1

No	Mpg	p	rms(p)	θo(deg)	Q	U	No of Plates Used
1	8.46	0.046	0.022	2	0.046	0.004	4
8	12.82	0.140	0.061	-16	0.119	-0.073	4
14	14.78	0.151	0.103	-46	-0.003	-0.151	3
15	12.36	0.139	0.051	- 7	0.136	-0.030	2
16	14.74	0.070	0.108	-81	-0.066	-0.024	4
23	11.85	0.126	0.063	- 2	0.006	-0.006	2
45	13.33	0.096	0.095	-77	-0.086	-0.042	3
64	13.74	0.112	0.021	- 8	0.109	-0.028	4
65	13.47	0.185	0.009	-51	-0.037	-0.181	3
68	13.45	0.269	0.115	43	0.010	0.269	2
69	14.76	0.196	0.027	- 5	0.194	0.032	3
99	13.15	0.173	0.068	0	0.173	0.006	2
103	12.81	0.119	0.038	10	0.111	0.044	3
115	10.44	0.095	0.037	- 9	0.091	-0.028	3
116	13.92	0.106	0.043	2	0.106	0.010	3
118	12.12	0.300	0.011	15	0.259	0.152	4

The numbering above corresponds with that used in the chapter on UBV photometry.

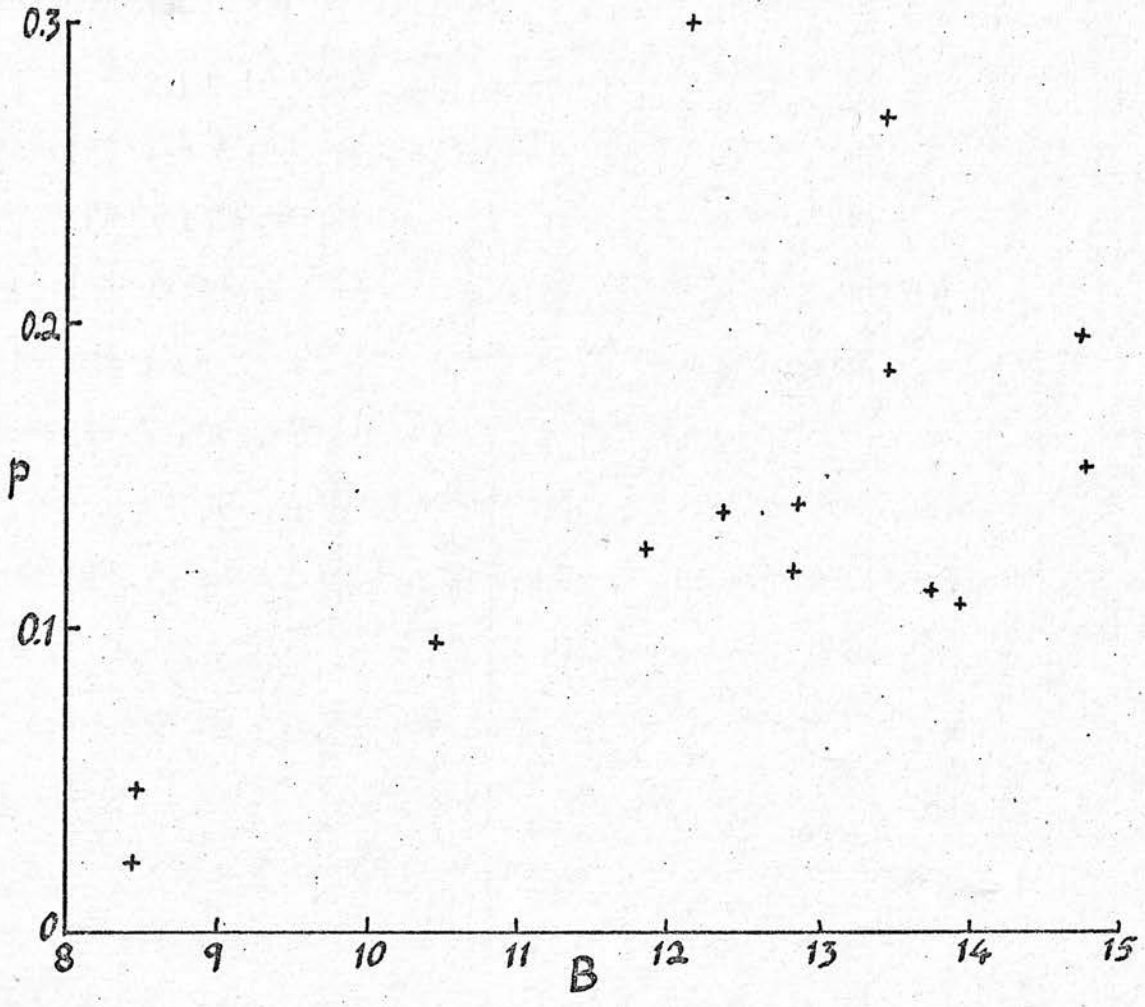

FIG 9 : Polarization Plotted Against B Magnitude for Stars in NGC 654.

The above table shows that for stars 16 and 45 the rms error in p is great enough to swamp any significance in the values of p and θo. These stars will therefore be omitted from consideration below.

Polarization and Magnitude

Fig 9 shows the polarization, p plotted vs the B magnitude for stars listed in Table P1. The two brightest stars have lower polarization than the other stars. These stars are numbers 1 and 115.

Star 115 is not a member of NGC 654 and is probably much closer to us. This means the light passes through less dust on its way to us, explaining the lower value of p.

Hall (23) has found a correlation between magnitude and polarization but attaches little significance to it because of selection effects. The correlation does, however, seem to be real and it is found too in the case of IC 5146 in this thesis. Hall mentions that radiation pressure may change the distribution of grains surrounding high luminosity stars.

Polarization and Colour Excess

Fig 10 shows polarization, p, plotted against colour excess, E_{B-V}. With the exception of star 64, the two

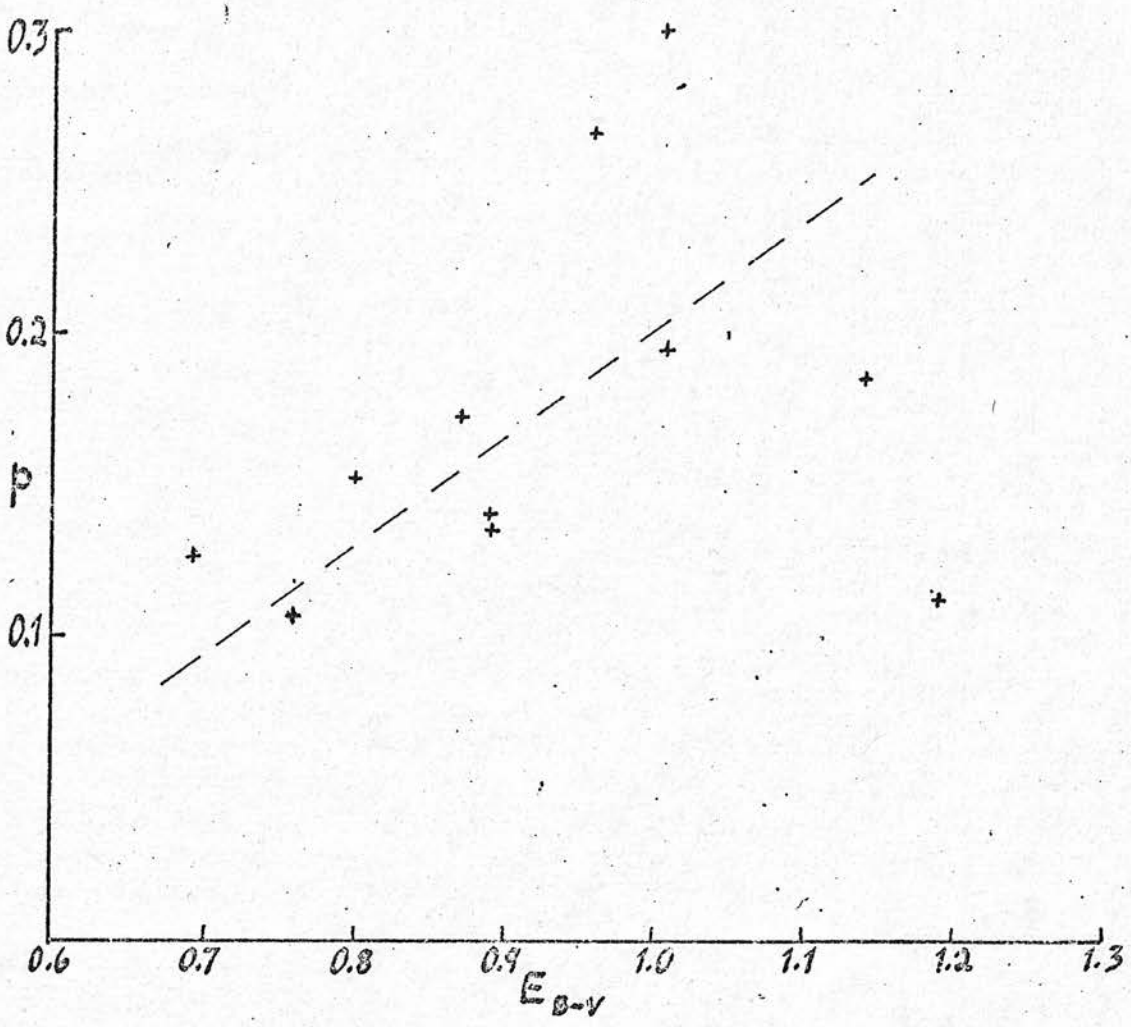

FIG 10 : Polarization Plotted Against Colour Excess for Stars in NGC 654.

quantities appear to be correlated. Stars with high polarization tend to have strong reddening too. The slope agrees with that found by Hall (22).

The Stokes Parameters, Q and U

Fig 11 shows U plotted against Q, where

$$Q = p \cos 2\theta_o \text{ and } U = p \sin 2\theta_o.$$

The mean value of Q is $0^m.103$ while that of U is $-0^m.006$. This means that the mean polarization $\bar{p}$ is about $0^m.1$ and the mean angle to the equator $\bar{\theta}_o$ is about 0^o. There are, at present, no photoelectric measurements of polarization for any of the stars studied but the measures do agree in general in both magnitude and direction with other stars in the vicinity for which photoelectric polarization measures are available. The mean polarization $\bar{p}$ is, perhaps, a little higher than usual but when one remembers that most of the stars studied here are very distant, ~3 kpc, and very blue, this result is not surprising.

Discussion

Fig 12 is a photograph of NGC 654, showing polarization vectors for the stars listed in Table P1. The lengths of these vectors are proportional to the strength of polarization p. The directions represent the direction of maximum intensity of the electric vector, θ_o.

Certain stars are conspicuous because they are different

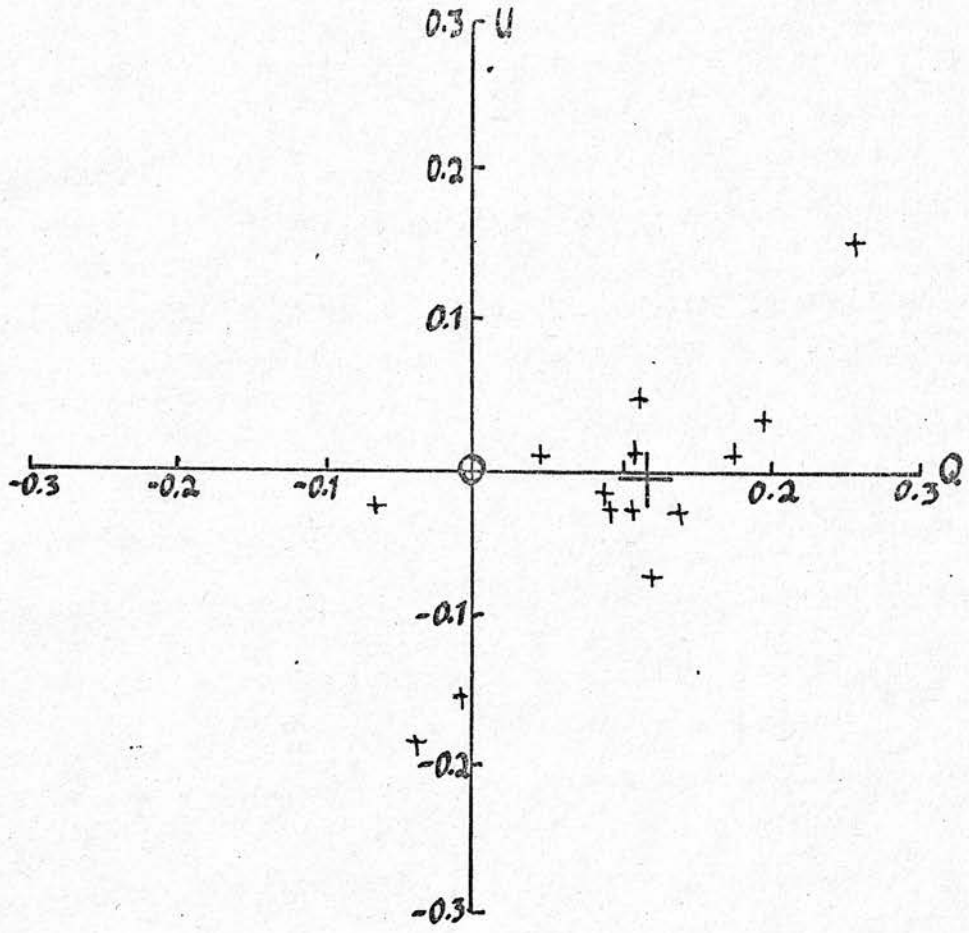

FIG 11 : The Stokes' Parameter U Plotted Against the Parameter Q for NGC 654.

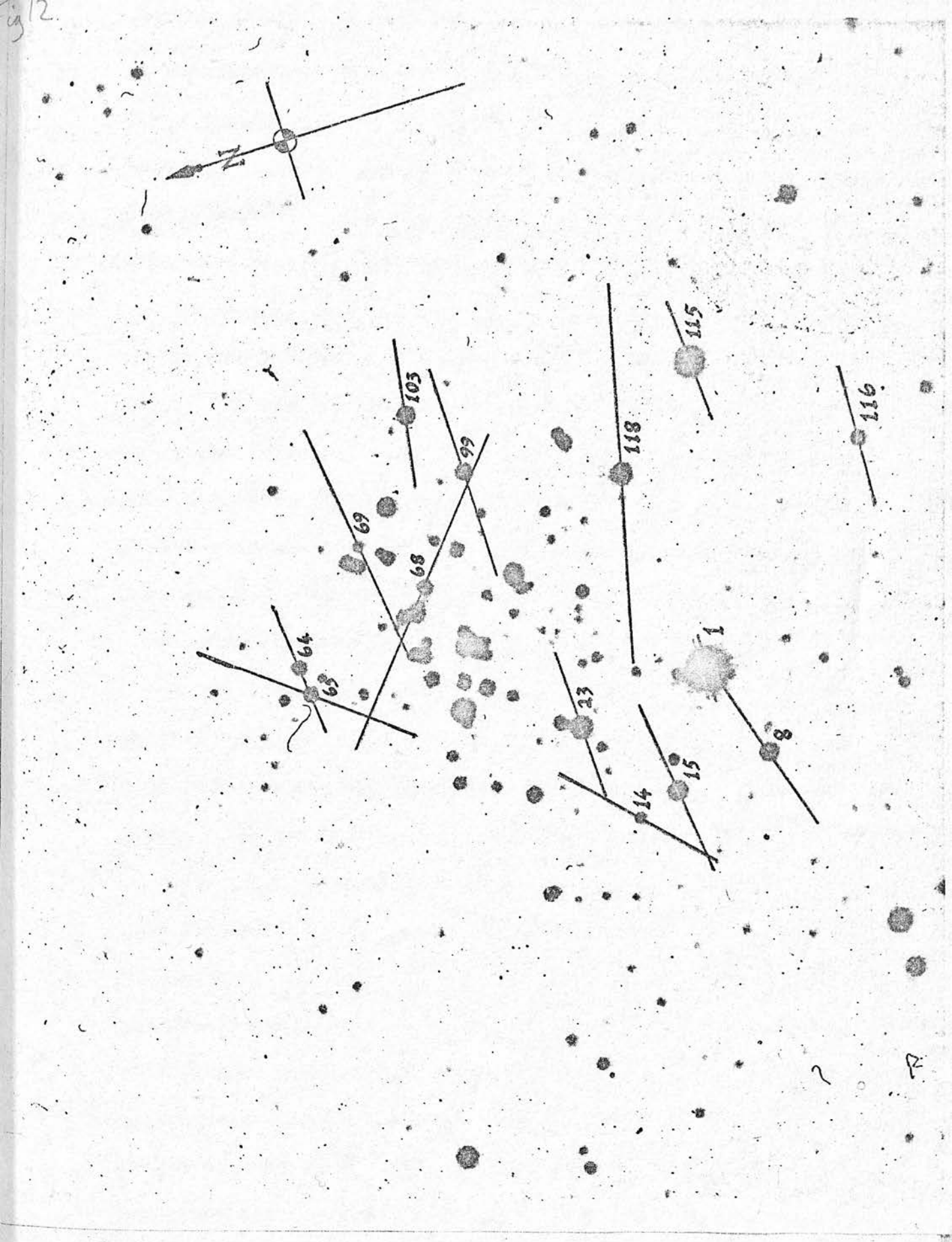

FIG 12 : Chart of NGC 654 Showing Polarization Vectors.
$0^m.1 \Rightarrow$ 2.5 cm.

in magnitude or direction of polarization, or both, from the surrounding stars: 14 is very different in terms of direction from the other stars. The rms error in p is $0^m.103$, more than half the value of p, $0^m.151$. The anomalous direction could be explained by the size of the errors.

65 is unusual in both the magnitude and direction of polarization. It has been pointed out in the chapter on UBV photometry that this star is not a member of NGC 654 but is probably a B3 star at about 1,500 pc distance, obscured to some extent by a nearby dust cloud. 68 is also unusual in magnitude and direction of polarization. This result is based on 2 measurements and errors are high.

118 has very strong polarization. This result is based on 4 out of 5 plates and they agree very wall, giving small errors. We can thus conclude that this strong polarization is real. E_{B-V} is normal, $\sim 0^m.1$ so we may have unusually good alignment of the grains in this region.

The general direction of polarization is parallel to the direction of the galactic magnetic field in our own arm and probably to that in the Perseus arm at this point. The distance modulus of 3,000 pc computed earlier suggest that the cluster is on the far side of the Perseus arm.

CHAPTER 4

The Existence of a Shell of Obscuring Matter around NGC 654

It was noticed that the colour excess, E_{B-V}, for stars in the central area of NGC 654 was apparently less than that for stars near the edge of the cluster.

Fig 13 shows the positions of cluster members. These members which are more reddened than average are shown as filled circles. Those stars with less than average reddening are represented by open circles. The circle shown on fig 13 was drawn so as to separate effectively the more reddened from the less reddened stars. The stars inside this circle are separately treated from those outside.

No of inner stars = 19.

No of outer stars = 26.

$E_{B-V} = 0^{m}.92$ for inner stars.

$E_{B-V} = 1^{m}.05$ for outer stars.

We apply Student's t-test to test the significance of the difference between these two mean colour excesses.

r m s deviation in $E_{B-V} = 0^{m}.14$ for inner stars.

r m s deviation in $E_{B-V} = 0^{m}.21$ for outer stars.

Standard error of mean = $\frac{0^{m}.14}{\sqrt{19}}$ for inner stars.

Standard error of mean = $\frac{0^{m}.21}{\sqrt{26}}$ for outer stars.

Fig 13

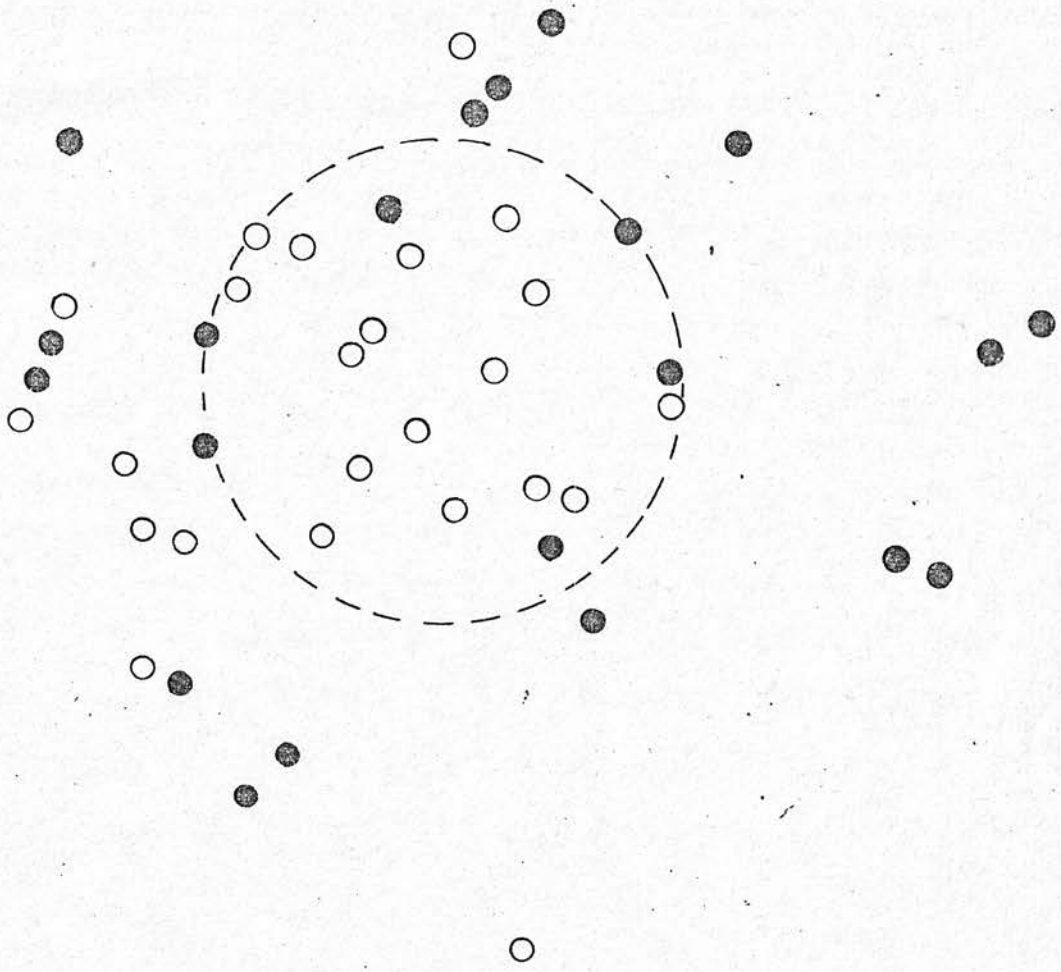

FIG 13 : The Positions of Cluster Members are Shown. Stars with greater than Average Reddening are Represented by Filled Circles. The Dashed Circle Effectively Separates the More Reddened from the Less Reddened Stars.

standard error of difference of means $= \sqrt{\left\{\frac{(0.14)^2}{19} + \frac{(0.21)^2}{26}\right\}}$

$= 0^m.05$

$t = \frac{\text{actual difference}}{\text{standard error of difference}} = \frac{0.13}{0.05} = 2.6$

Since $t > 2.58$ the difference in the means is significant at the 0.01 level of certainty.

We are thus 99 per cent certain that the inner stars are less reddened than the outer ones.

Three possible explanations of this anomaly come to mind:

(i) The inner stars are predominantly cluster members and lie closer to us than the outer stars.

(ii) A ring of obscuration lies between us and the cluster.

(iii) The cluster is embedded in a shell of dust whose inner surface coincides approximately with the circle drawn in Fig 13. This circle has a diameter of 3.6 arc mins which would be equal to 3 pc at the distance of the cluster.

(i) can be ruled out because the mean distance modulus of the inner stars is equal to that of the outer stars to four significant figures : $12^m.61$.

(ii) can be ruled out on statistical grounds; it seems most unlikely that such a ring would lie exactly between

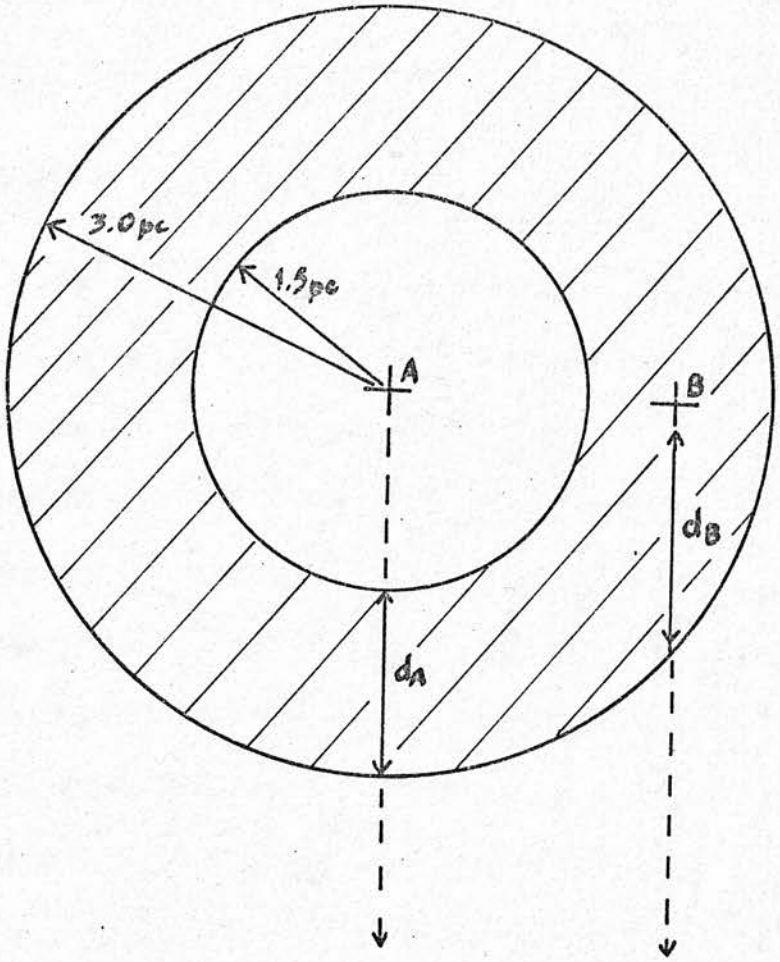

FIG 14 : A Model for a Dust Shell Surrounding NGC 654. The Hatched Region has Higher than Normal Dust Density.

us and NGC 654.

This leaves (iii).

The mass of obscuring matter around NGC 654

In order to estimate the mass of the obscuring shell around NGC 654 let us make the following assumptions (see Fig 6b):

(i) The shell is spherically symmetric.

(ii) The density of matter is uniform throughout the shell.

(iii) The inside diameter of the shell is 3.6 arc min, ie about 3 pc. It will be remembered that this is the diameter of the circle enclosing stars with less than average reddening.

(iv) The outside diameter of the shell is 6 pc; the apparent overall diameter of the cluster.

The mass calculated will depend on the outside diameter assumed and this is probably the most sensitive of the above assumptions. It seems unlikely, however, that this shell extends far beyond the outside of the cluster.

On Fig 14 we see A, a typical inner star and B, a typical outer star, d_A the path length of A's light through the shell and d_B a similar quantity for B.

$d_A \sim 1.5$ pc

$d_B \sim 2$ pc

so $d_A - d_B \sim 0.5$ pc

The mean absorption of starlight from an outer star is $0^m.4$ greater than that for an inner star.

Now $A_V = 280$ mag/g cm^{-2} of hydrogen (24) if hydrogen is present in the usual proportion, so in a cloud with extinction m we have:

$$\text{Density of hydrogen} = \frac{m}{280} \text{ g cm}^{-2}$$

For the difference of the two path lengths we have

$$\text{Density of hydrogen} = \frac{0.4}{280} \text{ g cm}^{-2}$$

$$= 1.4 \times 10^{-3} \text{ g cm}^{-2}$$

Now this is in a cylinder of length 0.5 pc = 1.5×10^{18}cms

$\therefore$ the density of hydrogen is 10^{-21} g cm^{-3}

Total volume of shell = 100 cu pc

$$= 3 \times 10^{57} \text{cm}^3$$

$\therefore$ total mass of hydrogen in shell = 3×10^{36} g

$$= \underline{\underline{1{,}500\ M\odot}}$$

Unfortunately no 21 cm H_I observations of this area are available for comparison with this estimate. Since the gas/dust ratio is about $10^{3/1}$ in the formulae quoted above the mass of dust alone ≈ 1.5 M$\odot$. This estimate can, of course, only be treated as an order of magnitude estimate. Uncertainties are due to the following factors:

(i) The shell may not be symmetrical.
(ii) The shell boundaries are uncertain.
(iii) The shell may be non-uniform.
(iv) The distance of the cluster estimated is strongly dependent on the reddening law chosen.

Total Mass of Stars in NGC 654

It is of interest at this point to compare the mass of interstellar matter computed above with the total mass of all the stars in NGC 654. This is of particular interest because, although star formation has stopped in the cluster, there has not been enough time for the remains of the pre-cluster cloud to dissipate. We may thus obtain an estimate of how much material is left at the end of star formation compared with the total mass available.

Consider the visible stars in NGC 654. The visible main sequence stars nearly all have absolute magnitudes in the range

$$-2\overset{m}{.}5 < M_V < 0.$$

We use the Salpeter initial mass function (25)

$$F(M) \propto M^{-2.35} \approx M^{-7/3};\ M_1 < M < M_2$$

Let f(M) = fraction of mass of all cluster members in stars with masses $\geq$ M

$$f(M) = \int_M^{M_2} M.F(M)\ dM \ / \ \int_{M_1}^{M_2} M.F(M)\, dM$$

$$= \int_M^{M_2} M^{-4/3}\ dM \ / \ \int_{M_1}^{M_2} M^{-4/3}\ dM$$

$$= \left[M^{-1/3}\right]_M^{M_2} \ / \ \left[M^{-1/3}\right]_{M_1}^{M_2}$$

If $M_2 >> M >> M_1$ then

$$\underline{f(M) \approx (M_1/M)^{1/3}}$$

Now the mean stellar mass

$$\overline{M} = \int_{M_1}^{M_2} M.F(M)\,dM \;/\; \int_{M_1}^{M_2} F(M)\,dM$$

$$= 4\left[M^{-1/3}\right]_{M_1}^{M_2} / \left[M^{-4/3}\right]_{M_1}^{M_2} \approx 4M_1$$

therefore $f(M) = (\overline{M}/4M)^{1/3}$

but $\overline{M} \doteq 0.1\ M\odot$ and since the faintest star we see has $M_v = 0$

then $M \doteq 4M\odot$

therefore $\underline{f(4M\odot) = 0.18}$

If $M_2 \gg M$, average mass of stars with masses greater than M is 4M

$$= 16\ M\odot$$

Now total no of stars greater than $4M\odot$ (ie $M_v \doteq 0$) is 45 from observation, therefore the total mass of stars in the cluster is

$$16 \times 45 / 0.18 = \underline{4{,}000\ M\odot}$$

We compare this with the estimate of 1,500 M⊙ for the mass of interstellar matter remaining after star formation and conclude that about 75% of the pre-cluster cloud was used up in star formation.

The Relationship between Position and Luminosity of Members of NGC 654

The existence of a shell of interstellar matter around NGC 654 suggests that star formation took place first of all in the middle of the pre-cluster cloud and the radiation pressure from these luminous young stars blew a

hole in the middle of the cloud; later star formation, therefore, would have taken place in the outer regions of the cloud.

Fig 15 shows the V_o vs E_{B-V} diagrams for outer and inner parts of the cluster respectively. The spread in both V_o and E_{B-V} is greater for stars in the outer region.

If star formation did, indeed, take place more recently in the outer region we would expect that V_o, the unreddened V magnitude, would in general be brighter for the outer stars than for the inner ones. We find the following mean values for V_o:

$$\overline{V}_o \text{ (outer)} = 11\overset{m}{.}00 \pm 1\overset{m}{.}06 \text{ r m s}$$

$$\overline{V}_o \text{ (inner)} = 11\overset{m}{.}39 \pm 0\overset{m}{.}82 \text{ r m s}$$

$$\text{r m s error of the mean (outer)} = \frac{1\overset{m}{.}06}{\sqrt{26}}$$

$$\text{r m s error of the mean (inner)} = \frac{0\overset{m}{.}82}{\sqrt{19}}$$

since there are 26 stars in the outer region and 19 stars in the inner region.

r m s error in the differences of the two mean magnitudes

$$= \sqrt{\left(\frac{(1.06)^2}{26} + \frac{(0.82)^2}{19}\right)}^{m}$$

$$= 0\overset{m}{.}28$$

Applying Student's t-test we have

$$t = \frac{\text{Actual difference}}{\text{r m s error in difference}} = \frac{0.39}{0.28} = 1.4$$

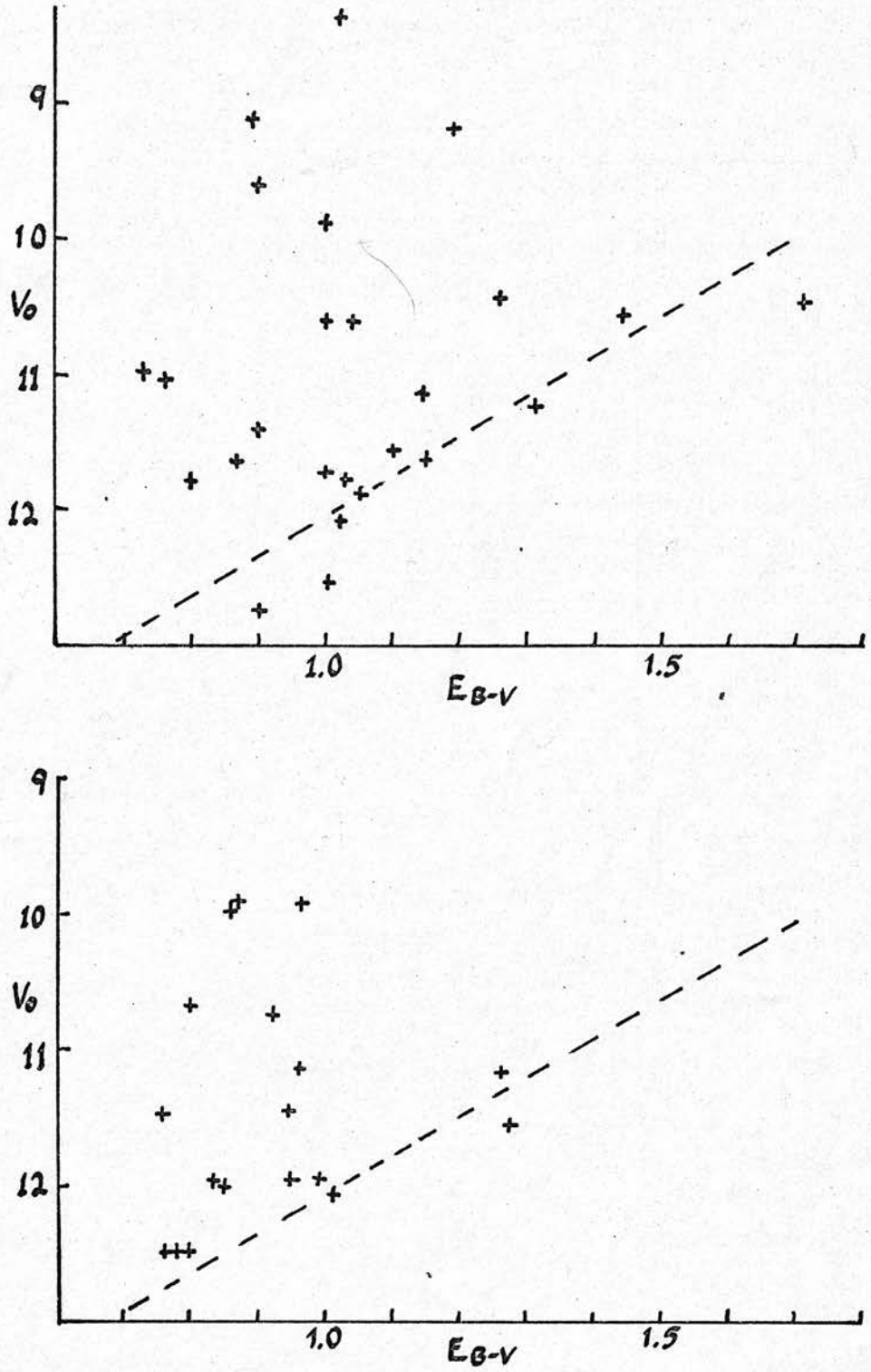

FIG 15 : V_o, the Unreddened V Magnitude, Plotted Against Colour Excess for Outer (above) and Inner (below) Parts of NGC 654.

so there is, statistically, one chance in six of the two mean luminosities being the same.

V_o has been computed using the equation

$$V_o = V - R\, E_{B-V}$$

where R is 3, R could, however, be as great as 6. In this case the values of V_o for the outer stars would be even more different from that of the inner ones. We would find an even more significant difference in luminosity between outer and inner members.

The 40/60 cm Schmidt Telescope at the
Monte Porzio Catone Outstation.

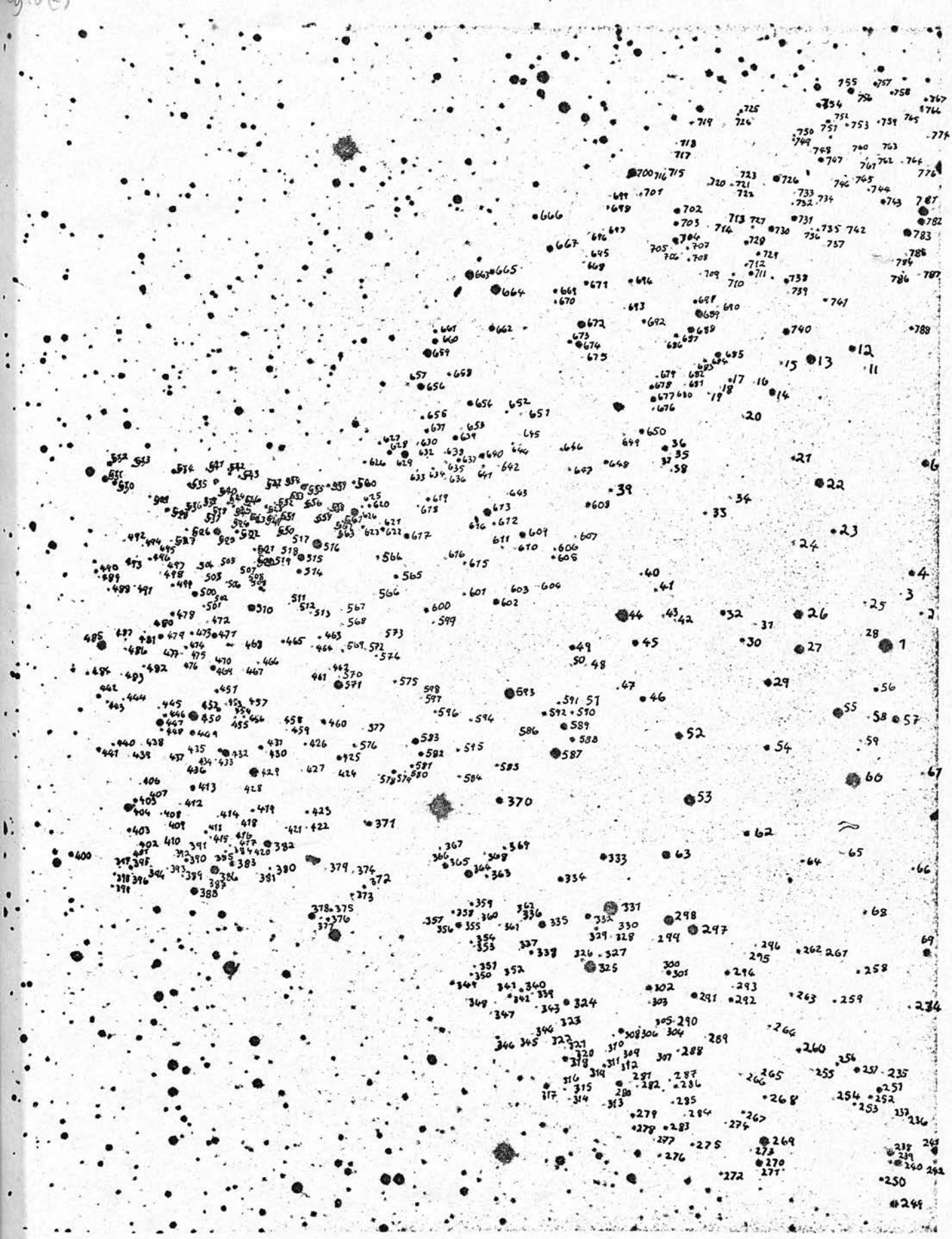

FIG 16(a) : Chart of IC 5146. Top is North.

Fig 16(b)

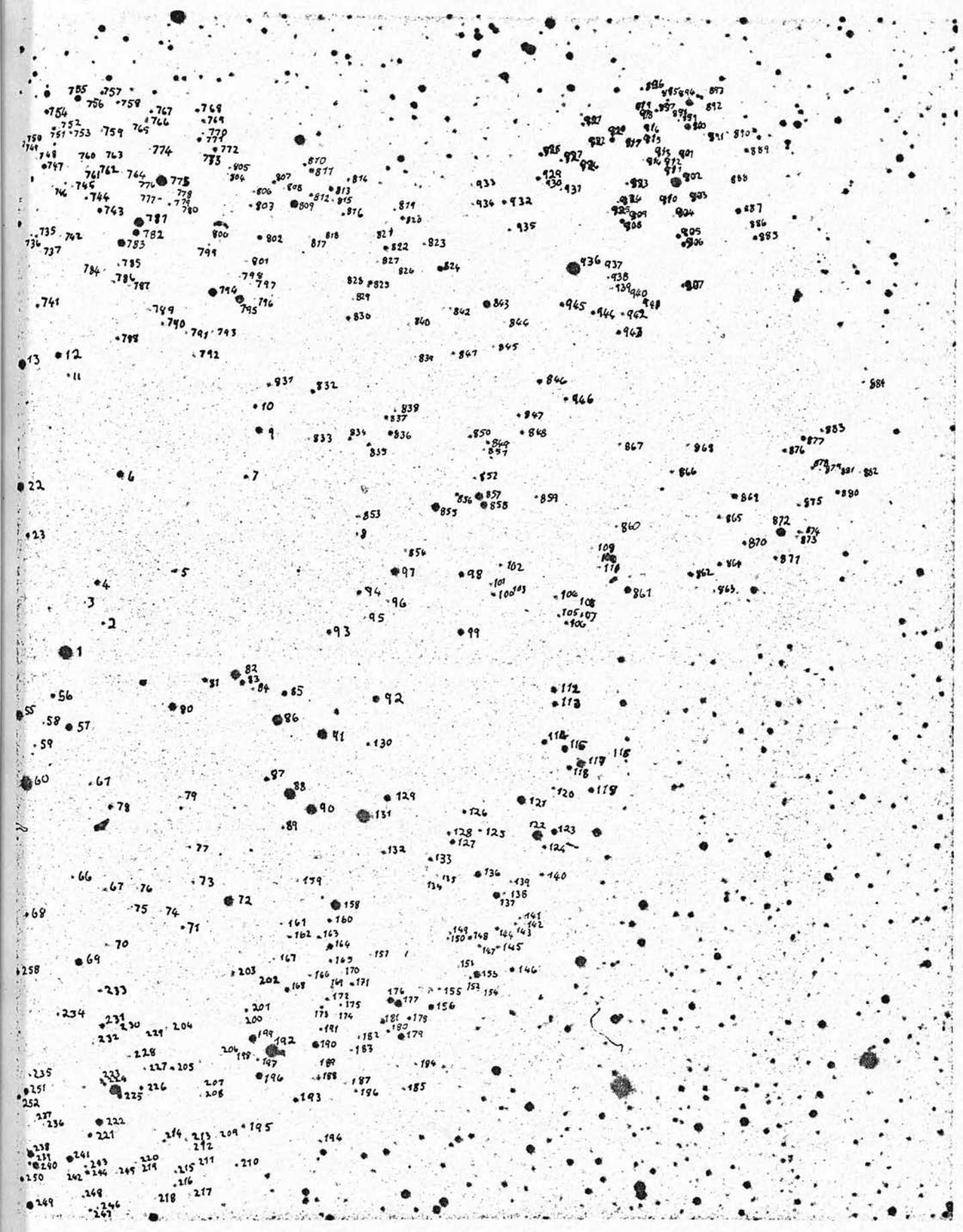

FIG 16(b) : Chart of IC 5146. Top is North.

CHAPTER 5

Three Colour Photometry

Introduction

Walker (12) has done UBV photoelectric and photographic photometry of stars in IC 5146. His photometry reaches a limiting magnitude of 17^m in the V waveband. He studied 76 stars, most of which are cluster members, lying inside the boundary of the dark nebula in which the cluster is embedded.

The present study does not concentrate on cluster members because the limiting magnitude attainable on the 40/60 cm Schmidt camera is 16^m in V and since so few members exceed this brightness, little useful work could be done on them. Instead, a much larger number of stars is studied, covering a wider field than that looked at by Walker. All stars inside a circle about 1^o in diameter, centred on BD + 46^o 3474, are measured. BD + 46^o3474 is star 1 on the figures 16(a)&(b),which show all stars measured in the present study and the numbers assigned to them. The circle centred on this star includes the whole of the dust cloud plus a ring of background stars seen around the cloud. In addition two other areas are studied, one in a dust lane leading to a complex system of dust clouds lying to the north west of

the cluster and the other in an apparently dust free area to the east of the cluster. Both of these regions adjoin the circular region in which the cluster lies.

Observations

Observations were made using the 40/60 cm Schmidt telescope at the Royal Observatory Edinburgh with the exception of plate 299 which was taken using the 40/60 cm Schmidt telescope at the observatory's outstation at Monte Porzio Catone, Italy. All plates were developed for 5 minutes in D19b, fixed for 20 minutes and washed for 1 hour in running water. The plates are listed along with various data in the table below.

Plate No	Emulsion	Filter	Colour	Exp	Date	S T
299	IIaD	GG14	V	8 min	17. 4.68	17^h58^m
692	IIaD	GG14	V	5 min	7.12.67	22^h35^m
695	IIaD	GG14	V	5 min	7.12.67	23^h20^m
725	IIaD	GG14	V	5 min	19.12.67	01^h30^m
687	IIaO	GG13	B	5 min	25.11.67	03^h10^m
699	IIaO	GG13	B	5 min	7.12.67	00^h40^m
728	IIaO	GG13	B	5 min	24.12.67	23^h40^m
729	IIaO	GG13	B	5 min	24.12.67	00^h00^m
771	IIaO	UG2	U	40 min	23. 1.68	02^h25^m
772	IIaO	UG2	U	35.5 min	23. 1.68	03^h00^m
841	IaO	UG2	U	10 min	14.10.68	22^h02^m
842	IaO	UG2	U	10 min	14.10.68	22^h19^m

Measurement

All V, B and U plates were measured using the semi automatic Becker Iris Photometer (25) at the Royal Observatory Edinburgh. XY co-ordinates and iris readings are recorded on punched paper tape when the operator presses a foot switch.

946 star images plus the background fog level alongside each image were measured on each plate. In addition, the 30 photoelectric standard stars measured by Walker (12) were measured at the start and finish of each measuring run. Each plate was measured in a working day in three sessions of three hours each. The stars were measured at a rate of just over 100 per hour but this rate increased as the field became more familiar.

In order to keep a check on iris drift, three stars - one bright, one moderately bright and one faint - were measured at thirty minute intervals throughout each run. In fact, no significant drift was found during any one run. The photometer was kept switched on during the three weeks taken to measure these plates. Only the lamp was switched off between runs and was switched on at least half-an-hour before starting a run. The alignment of the photometer optics was checked regularly.

Reduction of Measurements

The measurements were reduced using the system of computer programs described in Chapter 2 .

The errors in the B and V magnitudes were rather large, but tolerable. The errors in U magnitudes were very much larger, typically about $0^{m}.3$. This was much too large to be tolerated and some method of reducing it had to be found.

There are two reasons for the excessively large errors:

(i) The stars near the edge of the field are about $0^{o}.5$ distant from the photoelectric standard stars. This is equivalent to about 12 mm on the plate. Emulsion characteristics can change considerably over this distance. This was pointed out in Chapter 2 where the calibrations for two clusters separated by about 1^{o} were entirely different. This effect is most pronounced on IIaD and IaO emulsions but does not seem to be significant on IIaO emulsion.

(ii) The bright nebula in IC5146 has the effect of making those stars seen against it appear brighter. Although there is emission from the H_{II} in this nebula, it is predominantly a reflection nebula. The nebula thus appears brighter in the U waveband than in the B or V wavebands.

These two effects are sufficient to account for the large errors in U magnitudes. Effect (i), the non-uniformity of emulsion characteristics, cannot be corrected because of the limited number of photoelectric standard stars available. Standards covering the entire magnitude range, all over the field, would be required to allow for this effect.

Effect (ii), due to background nebulosity, is magnitude dependent and no consistent equation could be formed relating background fog level to error.

The U plates were all re-measured using the Computer Controlled Iris Photometer. This machine is described in Appendix 1. It is optically similar to a Becker Iris Photometer and will automatically find star images, centre on them and record iris readings. The machine was used in its fully automatic mode. Despite the objective method of measurement, the resulting U magnitudes were as poor as before.

Early in 1970 the GALAXY machine came into general operation in the Royal Observatory Edinburgh. GALAXY is described in Appendix 2. GALAXY measures the positions and sizes of star images on photographic plates. In the present study, the image sizes are the main items of interest. These measures of image size or "M-values" correspond to the iris readings

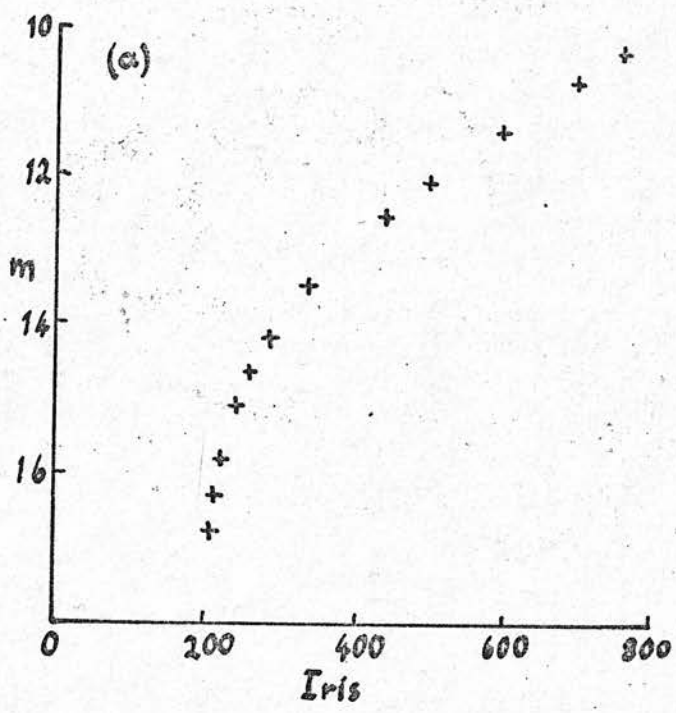

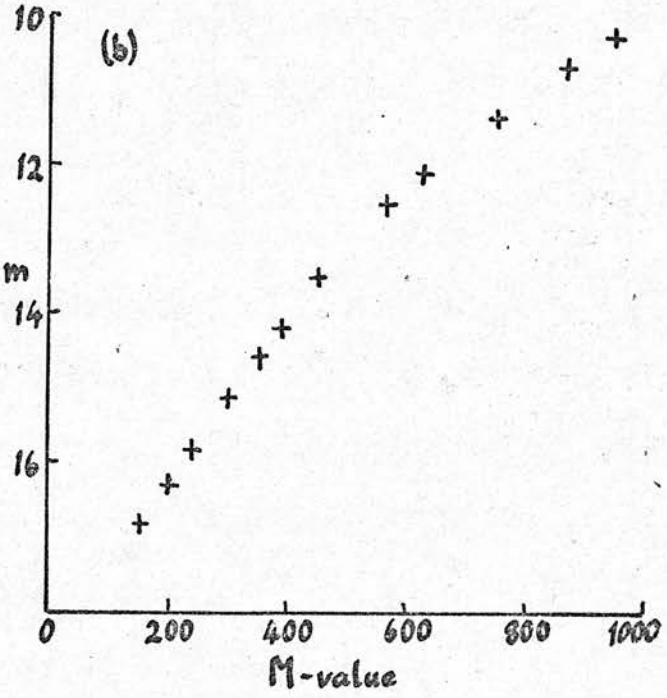

FIG 17(a) : Iris Photometer Calibration Curve.

FIG 17(b) : GALAXY Machine Calibration Curve.

of the Becker iris photometer and have a one to one relationship with stellar magnitude. M-values are obtained by matching the density profile of an image with one of 1000 model profiles.

The four U plates were re-measured on GALAXY. The effect of variable background fog level (BFL) can be allowed for more easily than can be done with iris photometer measurements. The reason for this can be seen on fig 17.17(a) shows a calibration curve for iris photometer readings with photoelectric magnitude plotted against iris reading. The curve falls away very steeply at the faint end, giving a very non-linear relationship between magnitude and iris reading. This means that the relationship between BFL and the error in measured magnitude is magnitude dependent and so it is very difficult to correct for in the absence of very large numbers of photoelectric standard stars.17(b) shows the calibration curve obtained by plotting photoelectric magnitude against GALAXY M-value. This is very nearly a straight line. This property of M-value minimises the magnitude dependence of the effect of variable BFL on photographic magnitude.

The four U plates were measured in GALAXY and the calibration curves, photoelectric magnitude against M-value, were plotted. The mean curve for all four plates was plotted and deviations from this curve of the points representing the standard stars

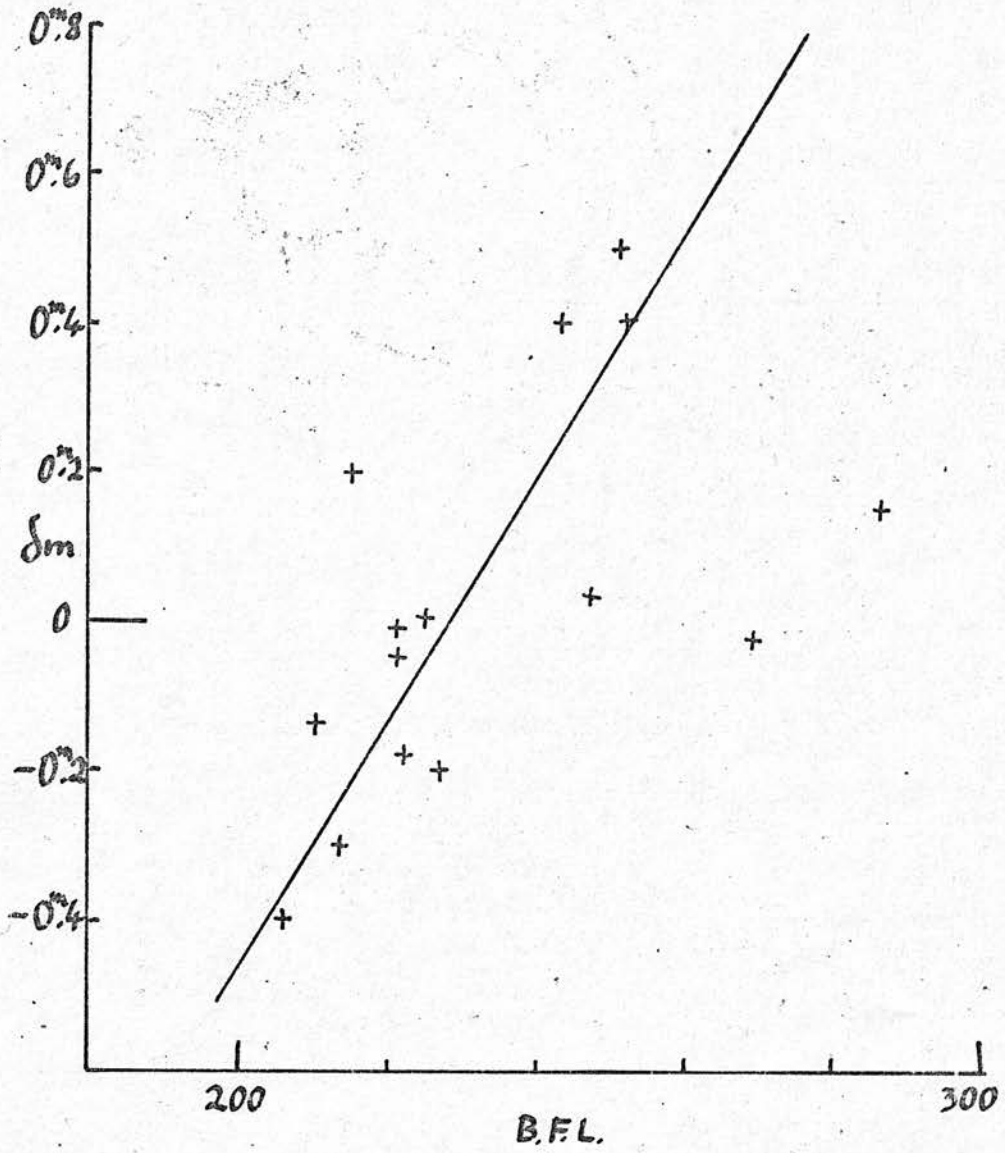

FIG 18 : The Error in Measured Magnitude is Shown Plotted Against Plate Background Fog Level for Photoelectric Standard Stars.

were plotted against BFL. This BFL was measured alongside each star image using the Becker iris photometer. The plot is shown in fig 18. The relationship between BFL and δm, the magnitude error, is apparently linear. The mean U magnitudes of all stars measured by GALAXY were corrected according to this relationship. The BFLs alongside each star image had been measured in the earlier runs on the semi-automatic Becker iris photometer.

The errors in the corrected U magnitudes are difficult to estimate for the individual stars but the scatter about the line of best fit on fig 18 indicates an rms error of about $0^{m}.11$ in general.

The V, B and U magnitudes of all the stars observed are shown in table 3.

TABLE 3

Star No.	V	No.of Plates	r.m.s. Error	B	No.of Plates	r.m.s. Error	GALAXY U
1	9.64	4	0.02	10.41	4	0.02	10.05
2	14.84	4	0.13	16.38	3	0.04	-
3	15.80	2	0.45	17.48	3	0.04	-
4	14.02	4	0.04	14.94	4	0.02	15.42
5	14.99	4	0.09	16.33	4	0.04	-
6	13.17	4	0.04	14.00	4	0.05	13.91
7	15.34	3	0.25	16.22	4	0.08	16.78
8	15.70	2	0.04	17.18	4	0.07	-
9	13.62	4	0.03	14.32	4	0.02	14.33
10	15.25	4	0.20	16.23	4	0.06	-
11	15.66	4	0.14	17.27	4	0.08	-
12	12.33	4	0.02	14.46	4	0.03	-
13	11.79	4	0.04	12.32	4	0.04	12.68
14	12.36	4	0.06	14.23	4	0.04	-
15	15.62	4	0.13	16.99	4	0.06	-
16	16.04	1	0.00	17.64	3	0.14	-
17	14.07	4	0.08	16.08	4	0.06	-
18	15.50	2	0.72	17.42	4	0.06	-
19	15.55	2	0.25	16.59	4	0.07	-
20	15.74	1	0.00	17.12	3	0.04	-
21	14.18	4	0.10	16.28	4	0.05	-
22	12.02	4	0.02	12.99	4	0.05	13.10
23	14.49	4	0.04	15.38	4	0.03	15.31
24	15.26	4	0.06	17.14	4	0.06	-
25	15.57	2	0.06	16.87	3	0.15	-
26	12.35	4	0.04	12.80	4	0.04	13.08
27	12.06	4	0.03	12.48	4	0.03	13.22
28	15.73	3	0.21	17.09	3	0.06	-
29	13.18	4	0.05	13.92	4	0.03	14.53
30	14.76	3	0.12	15.58	4	0.04	15.81
31	15.69	3	0.05	17.14	4	0.11	-
32	14.09	4	0.05	14.96	4	0.14	14.81
33	15.49	3	0.26	16.67	4	0.08	-
34	16.04	1	0.00	17.43	4	0.07	-
35	16.07	2	0.44	17.18	4	0.14	-
36	14.07	4	0.11	14.86	4	0.05	15.34
37	15.40	1	0.00	17.43	4	0.05	-
38	15.97	2	0.03	17.09	4	0.09	-
39	15.56	3	0.09	16.46	4	0.07	-
40	14.91	1	0.00	17.16	4	0.11	-
41	15.23	1	0.00	16.62	4	0.06	-
42	15.50	2	0.00	16.96	4	0.04	-
43	15.80	2	0.21	16.82	4	0.06	-
44	10.32	4	0.02	10.99	4	0.05	10.92
45	14.42	4	0.06	14.86	4	0.05	14.85

m = 0.00 means the images could not be measured.

Star No.	V	No.of Plates	r.m.s. Error	B	No.of. Plates	r.m.s. Error	GALAXY U
46	12.79	4	0.06	14.78	4	0.02	-
47	16.14	2	0.16	17.38	3	0.01	-
48	16.10	2	0.33	17.46	3	0.08	-
49	14.67	4	0.13	15.19	4	0.03	-
50	15.79	2	0.46	17.37	4	0.12	-
51	16.10	1	0.00	17.12	3	0.44	-
52	13.15	4	0.04	13.92	4	0.03	13.71
53	10.61	4	0.02	11.78	4	0.03	12.83
54	13.89	4	0.03	15.16	4	0.02	-
55	11.67	4	0.04	12.27	4	0.01	12.14
56	14.30	4	0.07	15.70	4	0.04	16.52
57	13.07	4	0.02	13.62	4	0.04	14.23
58	15.38	3	0.11	17.10	2	0.16	-
59	15.40	3	0.10	16.74	4	0.11	-
60	9.71	4	0.03	10.27	4	0.01	10.71
61	15.83	3	0.23	16.53	4	0.05	-
62	14.47	4	0.12	15.19	4	0.03	-
63	12.84	4	0.04	13.93	4	0.06	13.00
64	15.80	3	0.04	16.78	4	0.12	-
65	15.98	2	0.16	17.31	4	0.04	-
66	15.52	3	0.15	16.98	4	0.04	-
67	15.44	3	0.11	16.94	4	0.07	-
68	15.39	4	0.22	16.37	4	0.03	-
69	12.93	4	0.07	13.84	4	0.03	13.71
70	16.04	1	0.00	17.12	4	0.11	-
71	15.56	4	0.23	16.53	4	0.07	-
72	11.66	4	0.02	12.37	4	0.01	12.48
73	16.24	1	0.00	17.23	4	0.07	-
74	16.70	1	0.00	17.51	4	0.21	-
75	16.14	2	0.01	17.45	2	0.25	-
76	18.56	1	0.00	17.66	3	0.27	-
77	15.77	3	0.12	17.42	3	0.09	-
78	13.55	4	0.03	15.51	4	0.03	-
79	15.79	3	0.15	17.31	3	0.08	-
80	12.86	4	0.01	13.46	4	0.03	13.43
81	14.87	4	0.09	15.51	4	0.06	15.84
82	11.55	4	0.04	11.97	4	0.04	-
83	14.10	4	0.07	15.02	4	0.06	15.37
84	16.00	3	0.03	17.00	4	0.04	-
85	14.22	4	0.09	15.02	4	0.01	15.55
86	11.33	4	0.04	11.84	4	0.01	11.32
87	15.37	4	0.27	15.86	4	0.02	16.00
88	11.04	4	0.02	11.46	4	0.03	11.64
89	15.17	3	0.24	17.03	4	0.12	11.85
90	11.54	4	0.03	12.03	4	0.02	12.50

Star No.	V	No.of Plates	r.m.s. Error	B	No.of Plates	r.m.s. Error	GALAXY U
91	11.67	4	0.02	12.21	4	0.04	12.19
92	13.51	4	0.07	14.23	4	0.05	13.89
93	14.19	4	0.09	15.67	4	0.08	-
94	15.07	4	0.13	15.88	4	0.03	16.52
95	15.98	3	0.15	17.57	3	0.19	-
96	16.17	3	0.20	17.39	4	0.05	-
97	12.53	4	0.03	13.78	4	0.03	14.39
98	14.49	4	0.10	15.09	4	0.03	14.97
99	14.10	4	0.09	14.71	4	0.04	14.77
100	14.76	4	0.07	16.04	4	0.04	16.46
101	15.84	4	0.14	16.74	4	0.14	-
102	15.68	4	0.05	16.64	4	0.05	-
103	15.88	1	0.00	18.19	1	0.00	-
104	14.64	4	0.10	16.40	4	0.04	-
105	15.65	4	0.19	16.92	4	0.06	16.66
106	15.76	4	0.29	16.52	4	0.04	-
107	16.26	2	0.36	17.75	4	0.15	-
108	16.70	2	0.20	17.70	3	0.17	-
109	0.00	0	0.00	17.49	4	0.04	-
110	13.91	1	0.00	17.72	3	0.14	-
111	15.08	1	0.00	17.41	4	0.20	-
112	14.15	4	0.18	14.87	4	0.06	-
113	13.97	4	0.42	15.16	4	0.03	15.30
114	14.53	3	0.17	15.58	4	0.06	16.35
115	12.66	4	0.04	14.20	4	0.02	15.18
116	15.89	3	0.56	17.36	4	0.09	-
117	13.02	4	0.42	13.18	4	0.03	12.97
118	14.78	3	0.19	15.64	4	0.03	16.22
119	14.27	3	0.06	14.93	4	0.03	15.09
120	15.54	3	0.12	16.74	4	0.05	-
121	12.51	4	0.04	13.25	4	0.01	13.59
122	11.40	4	0.04	11.98	4	0.02	12.06
123	13.36	4	0.04	14.53	4	0.02	14.87
124	15.59	4	0.30	16.11	4	0.03	-
125	15.54	4	0.22	16.61	4	0.08	-
126	15.59	4	0.16	16.29	4	0.07	-
127	15.00	3	0.07	15.57	4	0.05	15.50
128	15.55	3	0.13	16.36	4	0.01	-
129	13.44	4	0.06	14.23	4	0.04	14.40
130	15.77	3	0.18	16.48	4	0.09	-
131	10.12	4	0.02	10.50	4	0.01	10.91
132	15.60	2	0.13	16.69	4	0.10	-
133	15.45	4	0.22	16.27	4	0.05	17.48
134	16.16	2	0.19	17.70	3	0.25	-
135	16.52	2	0.02	17.46	4	0.16	-

Star No.	V	No. of Plates	r.m.s. Error	B	No. of Plates	r.m.s. Error	GALAXY U
136	13.74	4	0.10	14.46	4	0.03	14.12
137	13.77	4	0.02	14.25	4	0.07	14.27
138	15.88	2	0.30	16.94	4	0.08	-
139	16.20	2	0.24	17.15	4	0.06	-
140	14.81	4	0.04	16.40	4	0.11	-
141	16.44	1	0.00	17.11	4	0.12	-
142	16.14	1	0.00	17.43	4	0.21	-
143	15.78	1	0.00	16.83	4	0.03	17.23
144	15.17	4	0.19	16.18	4	0.07	17.36
145	15.66	4	0.19	16.84	4	0.07	-
146	15.18	4	0.23	15.78	4	0.04	16.25
147	15.14	4	0.06	16.59	4	0.10	-
148	15.21	4	0.19	16.10	4	0.06	16.34
149	15.71	2	0.33	17.12	4	0.07	-
150	15.83	3	0.14	16.94	4	0.02	-
151	0.00	0	0.00	17.69	3	0.18	-
152	16.06	2	0.06	16.73	4	0.07	-
153	12.27	4	0.03	13.91	4	0.02	15.14
154	16.16	3	0.16	17.37	4	0.10	-
155	15.62	4	0.12	17.01	4	0.08	-
156	14.07	4	0.08	14.88	4	0.02	15.22
157	15.66	2	0.45	17.64	4	0.13	-
158	11.79	4	0.01	12.16	4	0.04	12.28
159	15.57	2	0.17	17.51	4	0.12	-
160	15.39	4	0.34	16.21	4	0.05	16.59
161	16.17	2	0.04	17.52	4	0.17	-
162	15.86	4	0.12	16.81	4	0.14	-
163	14.66	4	0.07	16.57	4	0.05	-
164	14.22	4	0.12	14.91	4	0.04	15.29
165	15.70	3	0.17	16.55	4	0.05	-
166	15.42	4	0.14	17.07	4	0.08	-
167	16.17	1	0.00	17.87	3	0.11	-
168	15.07	3	0.14	15.74	4	0.08	15.87
169	15.83	2	0.42	16.83	4	0.10	-
170	15.97	3	0.50	17.56	3	0.25	-
171	15.53	4	0.13	16.10	4	0.05	16.32
172	15.59	1	0.00	16.49	4	0.05	-
173	15.79	2	0.17	16.43	4	0.07	-
174	15.98	1	0.00	17.54	4	0.14	-
175	15.62	3	0.25	17.02	4	0.06	-
176	13.77	4	0.12	14.26	4	0.02	14.22
177	12.12	4	0.04	13.71	4	0.01	15.13
178	15.44	4	0.25	16.39	4	0.04	16.96
179	12.73	4	0.03	14.27	4	0.04	15.51
180	15.33	3	0.10	16.31	4	0.04	16.94

Star No.	V	No.of Plates	r.m.s. Error	B	No.of Plates	r.m.s. Error	GALAXY U
181	14.81	4	0.18	15.79	4	0.06	16.00
182	15.66	2	0.29	17.08	4	0.13	-
183	16.26	2	0.26	17.08	4	0.12	-
184	15.95	3	0.20	17.40	4	0.19	-
185	15.09	1	0.00	17.30	3	0.11	-
186	15.90	2	0.07	16.87	4	0.11	-
187	16.05	2	0.04	17.36	4	0.08	-
188	15.76	4	0.13	16.35	4	0.08	-
189	16.09	2	0.23	17.79	3	0.30	-
190	13.60	4	0.08	14.31	4	0.04	13.85
191	15.74	3	0.29	16.79	4	0.11	-
192	9.88	4	0.02	10.56	4	0.02	10.59
193	14.58	4	0.12	15.57	4	0.03	15.16
194	15.93	2	0.20	17.13	4	0.08	-
195	15.18	3	0.15	16.50	4	0.08	-
196	13.28	4	0.08	14.15	4	0.00	13.70
197	15.16	4	0.14	16.62	4	0.07	-
198	16.00	1	0.00	17.53	3	0.04	-
199	12.46	4	0.03	13.54	4	0.02	13.92
200	15.92	4	0.31	17.53	4	0.18	-
201	15.48	2	0.10	16.46	4	0.10	17.11
202	16.13	1	0.00	17.96	2	0.33	-
203	15.99	4	0.14	16.96	4	0.11	-
204	16.05	2	0.53	17.37	4	0.15	-
205	15.30	4	0.24	16.15	4	0.03	16.87
206	16.56	1	0.00	17.87	2	0.21	-
207	16.44	1	0.00	17.52	4	0.23	-
208	15.83	1	0.00	17.57	4	0.10	-
209	16.27	2	0.14	17.48	4	0.20	-
210	15.66	4	0.19	16.65	4	0.06	-
211	15.98	2	0.26	17.73	3	0.25	-
212	16.18	1	0.00	17.93	3	0.28	-
213	15.87	3	0.33	17.33	4	0.09	-
214	15.26	4	0.06	16.69	4	0.11	-
215	14.94	4	0.13	17.04	4	0.07	-
216	15.67	2	0.05	16.87	4	0.07	-
217	15.47	2	0.03	17.49	4	0.20	-
218	16.26	2	0.28	17.77	3	0.28	-
219	0.00	0	0.00	17.97	2	0.27	-
220	0.00	0	0.00	17.54	4	0.06	-
221	14.82	4	0.13	15.87	4	0.04	15.96
222	11.45	4	0.02	13.62	4	0.03	15.61
233	15.39	3	0.28	16.57	4	0.04	-
224	15.52	2	0.09	16.18	4	0.10	16.49
225	14.14	4	0.06	15.16	3	0.02	15.32

Star No.	V	No. of Plates	r.m.s. Error	B	No. of Plates	r.m.s. Error	GALAXY U
226	15.13	4	0.17	16.05	4	0.07	16.28
227	15.84	3	0.13	17.46	4	0.20	-
228	15.87	2	0.10	18.09	2	0.05	-
229	16.32	3	0.15	17.64	2	0.36	-
230	16.30	1	0.00	17.72	4	0.14	-
231	14.46	4	0.07	15.36	4	0.25	15.92
232	16.29	2	0.43	17.65	4	0.25	-
233	15.60	3	0.18	16.75	4	0.07	-
234	15.83	2	0.15	17.19	4	0.10	-
235	15.78	3	0.35	17.27	4	0.17	-
236	15.84	3	0.47	17.47	3	0.23	-
237	16.26	1	0.00	17.33	4	0.14	-
238	12.87	4	0.05	13.59	4	0.05	13.30
239	15.48	3	0.02	16.21	4	0.02	16.84
240	12.70	4	0.02	13.65	4	0.03	13.78
241	13.16	4	0.06	13.84	4	0.02	13.49
242	16.18	2	0.18	17.18	4	0.08	-
243	15.83	3	0.02	16.57	4	0.12	16.77
244	14.86	4	0.07	15.64	4	0.02	15.38
245	15.98	2	0.30	17.74	3	0.33	-
246	15.58	3	0.15	17.21	4	0.09	-
247	15.69	3	0.24	16.78	4	0.13	-
248	15.84	3	0.06	17.26	4	0.14	-
249	13.01	4	0.08	13.71	4	0.01	13.42
250	15.05	4	0.15	15.74	4	0.05	15.84
251	12.80	4	0.06	14.71	4	0.04	16.79
252	15.20	4	0.09	15.79	4	0.04	15.89
253	15.55	4	0.10	16.25	4	0.09	16.74
254	16.28	2	0.24	17.30	3	0.20	-
255	15.87	2	0.01	17.19	4	0.16	-
256	14.97	4	0.11	16.19	4	0.05	-
257	14.02	4	0.10	14.66	4	0.04	14.67
258	15.42	2	0.07	16.68	4	0.08	-
259	15.18	4	0.08	16.79	4	0.10	-
260	14.16	4	0.09	15.43	4	0.07	-
261	15.81	3	0.27	17.49	3	0.03	-
262	15.53	3	0.22	16.33	4	0.04	-
263	15.39	4	0.32	16.32	4	0.05	-
264	15.62	4	0.06	16.74	4	0.09	-
265	15.87	4	0.13	17.51	2	0.45	-
266	16.07	2	0.10	17.12	4	0.14	-
267	14.77	4	0.13	16.19	4	0.05	-
268	15.55	3	0.20	16.53	4	0.03	-
269	11.10	4	0.01	12.45	4	0.04	13.21
270	13.19	4	0.04	14.07	4	0.01	14.19

Star No.	V	No.of Plates	r.m.s. Error	B	No.of Plates	r.m.s. Error	GALAXY U
271	15.9o	4	0.21	17.41	4	0.11	-
272	16.00	1	0.00	16.79	4	0.07	-
273	15.63	3	0.12	17.23	4	0.07	-
274	15.78	3	0.20	17.14	4	0.13	-
275	15.98	1	0.00	16.38	4	0.03	-
276	15.92	3	0.12	16.57	4	0.06	17.28
277	15.24	4	0.08	17.13	4	0.12	-
278	14.54	4	0.12	15.92	4	0.04	-
279	14.97	4	0.07	15.85	4	0.02	15.82
280	13.49	4	0.02	14.18	4	0.04	14.14
281	15.87	3	0.28	17.14	4	0.17	16.79
282	15.51	4	0.03	16.67	4	0.01	-
283	15.46	4	0.23	15.89	4	0.03	15.86
284	16.05	2	0.15	17.31	4	0.10	-
285	15.38	4	0.30	16.73	4	0.08	-
286	15.04	4	0.20	15.97	4	0.04	-
287	15.41	3	0.10	16.48	4	0.15	-
288	15.73	4	0.06	16.69	4	0.05	-
289	15.72	1	0.00	17.52	3	0.20	-
290	15.68	4	0.21	16.74	4	0.06	-
291	13.72	4	0.06	14.47	4	0.05	14.46
292	14.52	4	0.13	15.65	4	0.05	16.19
293	15.92	3	0.10	17.12	4	0.15	-
294	14.58	4	0.07	15.36	4	0.02	-
295	16.12	3	0.20	17.57	4	0.18	-
296	15.96	3	0.12	17.26	3	0.09	-
297	11.11	4	0.02	11.71	4	0.04	11.57
298	11.28	4	0.01	11.99	4	0.05	12.27
299	16.44	1	0.00	17.34	4	0.11	-
300	15.90	2	0.07	17.32	3	0.21	-
301	14.27	4	0.05	15.18	4	0.02	15.68
302	13.69	4	0.10	14.56	4	0.04	14.81
303	15.95	4	0.10	16.85	4	0.05	-
304	15.69	3	0.16	17.18	4	0.14	-
305	15.82	3	0.11	17.10	4	0.10	-
306	15.76	4	0.13	16.95	4	0.13	17.12
307	15.72	3	0.16	17.69	3	0.13	-
308	14.17	4	0.03	14.79	4	0.06	14.67
309	16.01	2	0.03	17.79	4	0.16	-
310	16.20	1	0.00	17.36	4	0.11	-
311	15.36	3	0.07	15.95	4	0.10	16.14
312	15.99	4	0.15	17.48	4	0.11	-
313	15.87	3	0.17	17.60	3	0.22	-
314	15.79	4	0.17	17.34	4	0.05	15.59
315	16.07	2	0.30	17.63	4	0.20	-

Star No.	V	No.of Plates	r.m.s. Error	B	No.of Plates	r.m.s. Error	GALAXY U
316	15.86	4	0.15	17.19	4	0.07	-
317	14.35	4	0.09	15.20	4	0.03	15.23
318	13.95	4	0.02	14.83	4	0.03	15.10
319	16.52	1	0.00	17.47	4	0.12	-
320	15.95	2	0.65	17.65	4	0.23	-
321	15.36	3	0.08	16.97	4	0.13	-
322	15.83	2	0.11	17.15	4	0.13	-
323	15.75	3	0.10	17.42	4	0.15	-
324	13.65	4	0.01	14.39	4	0.02	14.33
325	10.54	4	0.02	10.84	4	0.04	11.17
326	15.19	2	0.25	15.74	4	0.06	15.96
327	15.63	4	0.19	16.37	4	0.06	16.33
328	15.93	3	0.18	17.28	4	0.14	-
329	14.69	4	0.14	15.63	4	0.03	-
330	16.44	1	0.00	17.74	4	0.21	-
331	9.62	4	0.02	10.15	3	0.03	9.76
332	13.75	4	0.09	14.53	4	0.06	14.94
333	13.49	4	0.08	14.40	4	0.21	14.52
334	14.38	4	0.03	15.01	4	0.03	14.72
335	12.74	4	0.03	13.45	4	0.03	13.29
336	15.47	3	0.08	16.86	4	0.05	-
337	15.97	3	0.20	17.20	4	0.09	-
338	14.99	4	0.11	15.67	4	0.03	16.17
339	14.97	3	0.25	16.68	4	0.08	-
340	14.83	4	0.10	15.39	4	0.04	15.61
341	15.47	3	0.26	17.04	4	0.04	16.05
342	14.72	4	0.15	15.62	4	0.04	15.35
343	15.68	4	0.31	17.30	4	0.13	-
344	15.88	3	0.17	17.31	4	0.11	-
345	0.00	0	0.00	17.37	4	0.08	-
346	15.57	3	0.10	16.17	4	0.08	16.90
347	15.95	4	0.30	17.41	4	0.09	-
348	16.01	2	0.39	17.28	4	0.09	-
349	13.88	4	0.03	15.88	4	0.02	-
350	15.04	4	0.12	16.54	4	0.09	-
351	15.65	4	0.14	16.90	4	0.07	-
352	16.35	2	0.18	17.58	4	0.25	-
353	16.30	2	0.30	16.90	3	0.11	-
354	15.60	3	0.11	16.72	3	0.07	-
355	12.50	4	0.05	14.23	4	0.01	15.21
356	15.80	3	0.20	17.37	4	0.09	-
357	15.49	3	0.16	17.11	4	0.12	-
358	14.70	4	0.13	16.40	4	0.02	-
359	15.54	4	0.12	16.15	4	0.06	-
360	15.76	3	0.19	17.18	3	0.14	-

Star No.	V	No.of Plates	r.m.s. Error	B	No.of Plates	r.m.s. Error	GALAXY U
361	16.24	2	0.14	17.22	2	0.04	-
362	15.79	3	0.06	17.70	3	0.14	-
363	15.09	4	0.06	16.40	4	0.05	-
364	12.25	4	0.05	13.09	4	0.05	13.14
365	13.49	4	0.02	14.48	4	0.04	15.35
366	15.86	4	0.21	17.36	4	0.15	-
367	15.70	4	0.15	17.03	4	0.09	-
368	15.47	4	0.18	16.94	4	0.08	-
369	15.18	4	0.18	16.34	4	0.05	15.57
370	13.57	4	0.05	14.29	4	0.02	14.18
371	14.33	4	0.04	15.00	4	0.05	-
372	14.64	3	0.21	16.05	4	0.10	-
373	15.61	4	0.44	16.43	4	0.08	-
374	16.28	3	0.28	17.07	4	0.06	-
375	14.85	4	0.14	15.79	4	0.07	-
376	14.79	4	0.16	15.62	4	0.05	
377	15.96	2	0.10	16.75	4	0.04	-
378	12.47	4	0.01	13.92	4	0.02	15.15
379	15.66	1	0.00	17.61	3	0.06	-
380	14.98	4	0.15	15.97	4	0.41	-
381	15.92	4	0.18	17.34	4	0.10	-
382	12.39	4	0.06	13.21	4	0.03	13.36
383	13.07	4	0.08	14.04	4	0.04	14.69
384	15.52	4	0.12	16.27	4	0.03	-
385	14.97	4	0.40	16.00	4	0.07	-
386	11.91	4	0.03	12.10	4	0.04	12.00
387	15.54	2	0.28	16.76	4	0.09	-
388	12.89	4	0.05	13.32	4	0.03	13.22
389	15.92	4	0.26	16.61	4	0.07	-
390	14.84	4	0.19	15.45	4	0.02	-
391	16.19	4	0.22	17.37	4	0.12	-
392	16.35	3	0.322	17.05	4	0.12	-
393	16.18	3	0.16	17.33	4	0.09	-
394	16.45	3	0.24	16.70	4	0.05	-
395	14.22	4	0.12	15.22	4	0.05	16.30
396	15.66	3	0.36	16.71	4	0.07	-
397	15.88	2	0.03	16.67	4	0.06	16.55
398	15.42	3	0.26	16.51	4	0.08	16.74
399	15.68	2	0.24	16.77	4	0.09	-
400	13.19	4	0.07	14.82	4	0.05	16.61
401	16.05	2	0.27	17.22	4	0.12	-
402	16.07	3	0.17	17.00	4	0.18	12.78
403	15.22	4	0.12	15.86	4	0.02	15.51
404	12.47	4	0.07	13.03	4	0.05	12.80
405	14.41	4	0.07	15.61	4	0.04	16.32

Star No.	V	No.of Plates	r.m.s. Error	B	No.of Plates	r.m.s. Error	GALAXY U
406	15.93	3	0.34	17.41	3	0.19	-
407	16.30	3	0.40	17.36	4	0.03	15.44
408	16.41	3	0.24	17.05	4	0.11	-
409	16.30	4	0.32	17.37	4	0.18	-
410	0.00	0	0.00	17.54	4	0.29	-
411	15.31	3	0.16	16.02	4	0.07	-
412	15.19	4	0.53	16.92	4	0.13	-
413	14.15	4	0.48	14.88	4	0.02	15.24
414	16.13	2	0.16	17.21	4	0.03	-
415	16.20	3	0.26	16.66	4	0.09	15.82
416	15.94	3	0.15	17.42	4	0.11	-
417	16.94	2	0.14	17.07	4	0.08	-
418	16.22	2	0.45	17.48	3	0.24	-
419	14.83	4	0.24	16.28	4	0.02	-
420	15.93	2	0.32	17.51	4	0.13	-
421	15.83	4	0.22	16.69	4	0.08	-
422	16.43	3	0.24	16.97	4	0.09	15.52
423	15.66	3	0.31	16.43	4	0.07	-
424	15.83	4	0.30	17.70	2	0.49	-
425	14.20	4	0.09	15.09	4	0.01	-
426	15.80	4	0.26	16.56	4	0.07	-
427	15.84	2	0.33	17.49	4	0.11	-
428	16.58	1	0.00	17.68	4	0.21	-
429	10.64	4	0.04	12.47	4	0.06	14.71
430	15.99	3	0.19	17.47	4	0.18	-
431	14.77	4	0.19	15.31	4	0.01	15.22
432	12.42	4	0.07	13.22	4	0.05	-
433	16.09	2	0.25	17.51	4	0.08	-
434	16.21	2	0.27	17.48	4	0.11	-
435	16.39	3	0.28	17.63	3	0.21	-
436	16.46	1	0.00	17.47	4	0.13	-
437	16.21	3	0.25	17.43	4	0.17	-
438	16.17	2	0.23	17.34	4	0.09	-
439	16.20	2	0.34	17.66	3	0.14	-
440	16.25	3	0.39	16.55	4	0.08	16.97
441	15.00	4	0.18	15.51	4	0.05	15.07
442	14.80	4	0.23	15.34	4	0.02	15.37
443	15.50	4	0.16	16.28	4	0.05	16.98
444	15.82	4	0.21	16.80	4	0.12	-
445	15.93	3	0.25	16.93	4	0.04	-
446	14.98	4	0.18	15.92	4	0.04	15.96
447	11.86	4	0.07	13.76	4	0.07	15.42
448	14.63	4	0.14	16.28	4	0.10	-
449	13.38	4	0.10	14.75	4	0.00	15.49
450	11.65	4	0.07	11.92	4	0.06	12.11

Star No.	V	No.of Plates	r.m.s. Error	B	No.of Plates	r.m.s. Error	GALAXY U
451	15.43	4	0.23	15.89	4	0.03	-
452	14.05	4	0.12	14.89	4	0.05	15.25
453	15.23	4	0.26	16.44	4	0.05	-
454	16.40	3	0.16	17.10	4	0.07	-
455	15.96	2	0.18	16.28	4	0.04	-
456	14.97	4	0.18	16.15	4	0.03	-
457	0.00	0	0.00	17.59	4	0.14	-
458	15.74	1	0.00	17.70	3	0.36	-
459	16.44	2	0.23	17.34	4	0.12	-
460	13.85	4	0.02	15.34	4	0.02	16.34
461	16.38	1	0.00	17.40	4	0.17	-
462	16.13	2	0.18	17.19	4	0.08	-
463	16.28	2	0.16	16.35	4	0.05	-
464	0.00	0	0.00	17.48	4	0.13	-
465	15.29	3	0.43	16.06	4	0.03	16.61
466	15.62	4	0.20	16.97	4	0.06	-
467	15.77	3	0.20	17.30	4	0.07	-
468	16.36	2	0.52	17.60	3	0.24	16.38
469	13.89	4	0.18	14.58	4	0.06	14.41
470	16.07	3	0.07	17.06	4	0.04	-
471	13.81	4	0.10	14.32	4	0.03	14.46
472	15.91	3	0.16	16.97	4	0.05	-
473	15.24	4	0.31	16.08	4	0.05	-
474	14.84	4	0.16	16.16	4	0.08	-
475	16.01	2	0.39	17.58	4	0.18	-
476	16.15	3	0.22	17.76	4	0.22	-
477	15.63	4	0.19	17.00	4	0.19	-
478	15.11	4	0.30	15.74	4	0.04	15.54
479	13.48	4	0.09	14.98	4	0.03	15.91
480	16.12	2	0.57	17.58	4	0.23	-
481	16.37	3	0.29	16.96	4	0.06	-
482	15.97	4	0.26	16.65	4	0.08	-
483	16.21	4	0.30	17.42	4	0.07	-
484	15.49	4	0.23	16.57	4	0.08	16.37
485	10.44	4	0.06	12.09	4	0.05	14.51
486	15.76	4	0.17	16.82	4	0.12	-
487	15.73	4	0.29	16.63	4	0.06	-
488	16.22	3	0.18	16.94	4	0.09	-
489	16.36	1	0.00	17.09	4	0.03	-
490	14.90	4	0.10	15.75	4	0.07	-
491	16.06	3	0.31	17.17	4	0.13	-
492	15.85	2	0.19	17.18	4	0.06	-
493	16.07	2	0.05	17.08	4	0.08	-
494	16.13	3	0.22	17.35	4	0.17	-
495	16.47	3	0.20	17.56	4	0.19	-

Star No.	V	No. of Plates	r.m.s. Error	B	No. of Plates	r.m.s. Error	GALAXY U
496	15.64	4	0.26	16.30	4	0.03	16.30
497	15.98	3	0.39	17.38	4	0.09	-
498	15.94	1	0.00	17.25	4	0.02	-
499	15.10	4	0.26	16.06	4	0.05	-
500	13.33	4	0.06	14.61	4	0.05	15.73
501	16.13	3	0.30	16.95	4	0.09	-
502	15.92	2	0.42	17.48	4	0.05	-
503	0.00	0	0.00	17.60	4	0.20	-
504	15.59	4	0.15	16.48	4	0.03	16.32
505	16.06	3	0.19	16.93	4	0.10	-
506	15.62	4	0.39	16.78	4	0.01	-
507	16.46	1	0.00	17.52	4	0.10	-
508	16.41	3	0.17	17.80	3	0.15	-
509	15.72	1	0.00	17.46	4	0.14	-
510	12.05	4	0.09	13.52	4	0.02	14.20
511	15.52	2	0.06	17.28	4	0.21	-
512	16.58	1	0.00	17.49	4	0.22	-
513	15.84	3	0.38	16.95	4	0.08	-
514	13.97	4	0.17	15.11	4	0.02	15.95
515	12.81	4	0.07	13.25	4	0.05	13.09
516	11.54	4	0.06	11.84	4	0.05	11.59
517	15.70	3	0.28	17.39	4	0.15	-
518	16.06	3	0.28	17.04	4	0.11	-
519	15.83	4	0.12	16.80	4	0.06	-
520	15.82	4	0.25	16.73	4	0.06	-
521	15.30	4	0.24	15.92	4	0.02	15.78
522	14.18	4	0.11	15.41	4	0.06	15.52
523	15.92	4	0.25	16.57	4	0.06	-
524	15.99	2	0.02	17.07	4	0.15	-
525	12.45	4	0.05	13.24	4	0.03	13.26
526	15.86	3	0.12	16.63	4	0.10	-
527	15.81	4	0.21	16.88	4	0.08	-
528	14.31	4	0.09	15.38	4	0.09	16.49
529	15.38	3	0 08	16.58	4	0.05	16.43
530	14.19	4	0.18	14.89	4	0.04	14.83
531	13.30	4	0.07	13.80	4	0.06	13.55
532	13.95	4	0.08	14.60	4	0.06	14.79
533	15.45	4	0.26	16.43	4	0.06	16.32
534	14.52	4	0.15	15.02	4	0.02	14.99
535	14.42	4	0.13	15.24	4	0.03	15.37
536	16.30	1	0.00	17.63	4	0.26	-
537	16.34	1	0.00	17.46	4	0.21	-
538	16.63	1	0.00	17.42	4	0.19	-
539	15.84	2	0.22	17.24	4	0.19	-
540	15.97	2	0.45	17.55	4	0.31	-

Star No.	V	No.of Plates	r.m.s. Error	B	No.of Plates	r.m.s. Error	GALAXY U
541	15.46	4	0.42	16.58	4	0.07	-
542	15.29	4	0.14	15.83	4		
543	15.52	4	0.16	16.12	4	0.03	15.11
544	14.93	4	0.20	15.52	4	0.03	15.67
545	15.02	4	0.18	15.58	4	0.02	15.90
546	16.40	3	0.26	17.69	4	0.23	-
547	15.77	3	0.13	16.95	4	0.15	-
548	14.20	4	0.09	15.44	4	0.05	16.21
549	16.13	1	0.00	17.43	4	0.18	-
550	16.07	4	0.07	17.26	4	0.14	-
551	14.98	4	0.24	15.87	4	0.03	16.67
552	15.93	4	0.28	16.31	4	0.04	13.44
553	16.15	4	0.33	17.22	4	0.09	-
554	16.70	1	0.00	17.43	4	0.15	-
555	13.01	4	0.03	13.79	4	0.03	-
556	15.92	2	0.18	17.27	4	0.11	-
557	15.99	4	0.32	16.98	4	0.11	-
558	14.90	4	0.25	16.19	4	0.03	-
559	14.88	4	0.19	15.53	4	0.03	15.55
560	14.97	4	0.17	15.79	4	0.12	-
561	15.39	2	0.14	16.92	4	0.19	-
562	16.27	2	0.27	17.45	4	0.10	-
563	15.90	2	0.07	16.88	4	0.15	-
564	15.40	4	0.11	16.22	4	0.08	16.27
565	15.35	3	0.25	16.08	4	0.07	-
566	15.42	3	0.12	17.61	4	0.13	-
567	15.68	1	0.00	17.74	2	0.26	-
568	15.50	1	0.00	17.21	2	0.15	-
569	15.25	4	0.12	16.39	4	0.15	-
570	15.24	2	0.32	17.03	3	0.15	-
571	11.70	4	0.03	12.59	4	0.05	12.68
572	16.06	2	0.50	17.42	4	0.14	-
573	15.96	3	0.26	17.65	4	0.13	-
574	15.06	4	0.11	16.75	4	0.05	-
575	15.50	4	0.17	16.83	4	0.11	-
576	15.38	3	0.11	15.92	4	0.28	-
577	15.72	3	0.23	17.14	4	0.36	-
578	15.89	3	0.20	17.40	4	0.16	-
579	14.63	4	0.13	15.63	4	0.08	16.08
580	15.60	4	0.17	17.07	4	0.08	-
581	15.21	4	0.19	15.98	4	0.07	16.44
582	14.17	4	0.04	15.14	4	0.07	15.57
583	12.45	4	0.03	14.11	4	0.03	15.43
584	15.50	4	0.13	16.84	4	0.14	-
585	14.63	4	0.06	16.51	4	0.10	-

Star No.	V	No.of Plates	r.m.s. Error	B	No.of Plates	r.m.s. Error	GALAXY U
586	15.58	1	0.00	17.97	2	0.27	-
587	11.18	4	0.02	11.75	4	0.03	11.70
588	14.08	4	0.04	14.95	4	0.03	15.00
589	13.22	4	0.04	14.04	4	0.02	14.35
590	14.40	4	0.05	16.23	4	0.01	-
591	15.55	4	0.17	16.82	4	0.12	-
592	15.02	4	0.15	15.81	4	0.04	16.66
593	11.28	4	0.05	11.61	4	0.02	11.74
594	15.62	3	0.26	16.90	4	0.05	-
595	15.42	3	0.13	16.59	4	0.04	17.15
596	15.52	4	0.11	16.97	4	0.04	-
597	15.57	2	0.41	17.54	2	0.22	-
598	15.45	2	0.11	17.62	3	0.17	-
599	15.93	3	0.30	17.52	4	0.11	-
600	14.00	4	0.06	15.72	4	0.05	-
601	15.64	3	0.24	16.97	4	0.06	-
602	12.95	4	0.06	14.70	4	0.01	16.46
603	15.69	2	0.36	17.90	1	0.00	-
604	15.94	1	0.00	17.98	2	0.21	-
605	15.26	4	0.18	16.20	4	0.05	-
606	15.53	4	0.06	16.80	4	0.07	-
607	15.53	4	0.12	17.17	4	0.12	-
608	14.68	4	0.07	15.54	4	0.05	15.98
609	13.78	4	0.03	14.45	4	0.03	14.43
610	16.07	3	0.09	17.53	4	0.14	-
611	16.00	3	0.05	17.09	4	0.05	-
612	15.58	4	0.11	16.57	4	0.06	-
613	12.63	4	0.06	13.36	4	0.04	13.91
614	16.10	2	0.06	17.28	4	0.07	13.91
615	15.07	4	0.11	16.63	4	0.09	-
616	15.61	4	0.19	17.14	4	0.08	-
617	12.97	4	0.04	14.57	4	0.05	15.99
618	15.34	4	0.06	16.98	4	0.11	14.77
619	14.91	4	0.08	15.99	4	0.03	16.41
620	15.25	3	0.18	15.97	4	0.05	16.07
621	16.21	2	0.53	17.30	4	0.16	-
622	14.30	4	0.10	15.16	4	0.04	15.41
623	14.94	4	0.06	15.96	4	0.05	15.97
624	10.95	4	0.03	12.56	4	0.06	14.10
625	14.58	4	0.14	16.16	4	0.05	-
626	15.42	4	0.15	16.49	4	0.08	-
627	15.36	4	0.39	16.45	4	0.05	17.00
628	14.04	4	0.43	15.25	4	0.03	15.14
629	12.79	4	0.01	13.49	4	0.02	13.36
630	15.68	3	0.13	16.95	4	0.02	-

Star No.	V	No. of Plates	r.m.s. Error	B	No. of Plates	r.m.s. Error	GALAXY U
631	13.67	4	0.07	15.83	4	0.02	-
632	15.91	3	0.08	17.03	4	0.14	-
633	15.75	3	0.31	17.27	4	0.16	-
634	15.46	4	0.13	16.50	4	0.06	-
635	15.39	4	0.14	16.62	4	0.05	-
636	16.02	2	0.34	17.28	4	0.18	-
637	13.34	4	0.08	15.74	4	0.07	-
638	15.57	3	0.16	16.92	4	0.17	-
639	13.97	4	0.10	15.10	4	0.02	15.38
640	13.09	4	0.07	14.67	4	0.03	15.80
641	15.08	4	0.26	16.55	4	0.07	-
642	15.56	2	0.00	17.99	2	0.35	-
643	15.71	4	0.11	17.60	4	0.11	-
644	14.96	4	0.11	16.61	4	0.05	-
645	16.08	2	0.18	17.48	4	0.09	-
646	15.53	4	0.17	16.62	4	0.07	-
647	16.08	2	0.24	17.14	4	0.08	-
648	14.97	4	0.31	15.67	4	0.04	16.08
649	15.62	3	0.17	17.53	4	0.09	-
650	14.36	4	0.07	15.50	4	0.05	-
651	15.88	3	0.31	17.02	4	0.11	-
652	15.76	3	0.13	17.02	4	0.08	-
653	15.64	4	0.17	17.38	4	0.08	-
654	13.39	4	0.03	15.07	4	0.02	16.96
655	15.12	4	0.12	16.71	4	0.08	-
656	12.95	4	0.02	14.04	4	0.03	14.39
657	15.90	2	0.04	16.98	4	0.06	-
658	15.32	4	0.18	16.49	4	0.08	-
659	11.09	4	0.01	13.06	4	0.03	15.23
600	13.07	4	0.05	14.80	4	0.03	16.25
661	14.37	3	0.12	16.13	4	0.11	-
662	13.61	4	0.06	14.75	4	0.03	14.55
663	12.10	4	0.04	12.54	4	0.01	12.62
664	10.66	4	0.02	11.96	4	0.03	13.30
665	13.97	4	0.12	14.97	4	0.02	15.98
666	13.93	4	0.03	15.28	3	0.03	16.21
667	13.87	4	0.12	14.39	4	0.04	14.06
668	15.75	4	0.19	16.99	4	0.13	-
669	14.64	4	0.25	15.87	4	0.03	16.86
670	15.50	3	0.24	16.71	4	0.04	-
671	13.91	4	0.05	15.61	4	0.04	-
672	12.60	4	0.07	13.43	4	0.01	-
673	15.52	4	0.09	16.13	4	0.10	13.65
674	13.14	4	0.04	13.88	4	0.02	13.66
675	15.83	1	0.00	17.45	4	0.17	-

Star No.	V	No. of Plates	r.m.s. Error	B	No. of Plates	r.m.s. Error	GALAXY U
676	16.23	2	0.35	17.18	4	0.12	-
677	14.40	4	0.07	14.97	4	0.04	-
678	15.26	4	0.07	15.94	4	0.02	-
679	15.91	3	0.19	17.32	4	0.11	-
680	15.91	1	0.00	17.52	4	0.16	-
681	15.50	1	0.00	17.40	4	0.06	-
682	15.82	1	0.00	17.52	3	0.10	-
683	15.59	4	0.15	17.37	4	0.16	-
684	15.12	4	0.11	16.03	4	0.09	16.54
685	13.77	4	0.05	14.63	4	0.40	14.77
686	16.00	3	0.21	17.34	4	0.03	-
687	15.27	4	0.08	15.88	3	0.01	15.87
688	13.11	4	0.05	13.98	4	0.04	13.94
689	12.67	4	0.05	13.32	4	0.06	13.33
690	16.16	3	0.14	17.07	4	0.07	-
691	15.15	4	0.08	16.04	4	0.05	15.96
692	15.72	3	0.16	16.37	4	0.05	16.52
693	16.40	1	0.00	17.56	4	0.16	-
694	14.79	4	0.04	16.04	4	0.09	-
695	15.77	3	0.10	17.53	4	0.37	-
696	15.85	3	0.14	17.34	4	0.08	-
697	16.00	2	0.14	17.34	4	0.13	-
698	15.37	3	0.29	16.72	4	0.03	-
699	15.81	3	0.27	17.56	4	0.08	-
700	11.55	4	0.02	12.89	4	0.02	13.75
701	15.60	3	0.14	17.06	3	0.17	-
702	13.94	4	0.08	14.80	4	0.02	15.17
703	14.94	4	0.09	15.72	4	0.04	16.11
704	13.86	4	0.04	14.64	3	0.02	-
705	15.53	3	0.28	17.36	4	0.12	-
706	15.76	3	0.33	17.30	4	0.22	-
707	15.16	4	0.18	16.61	4	0.05	-
708	15.61	3	0.22	16.67	4	0.08	-
709	16.25	2	0.43	17.56	4	0.18	-
710	15.83	3	0.18	16.76	4	0.06	-
711	14.96	4	0.10	15.62	4	0.05	15.93
712	15.87	3	0.21	16.62	4	0.04	-
713	15.80	4	0.23	17.25	4	0.08	-
714	16.13	1	0.00	17.76	3	0.17	-
715	15.85	4	0.34	17.50	3	0.13	-
716	16.30	1	0.00	17.55	3	0.15	-
717	15.98	4	0.35	17.44	3	0.17	-
718	16.22	4	0.21	17.65	3	0.15	-
719	15.75	4	0.03	16.57	4	0.04	-
720	16.03	2	0.15	17.10	4	0.08	-

Star No.	V	No.of Plates	r.m.s. Error	B	No.of Plates	r.m.s. Error	GALAXY U
721	15.94	2	0.33	16.95	4	0.11	-
722	16.31	2	0.09	17.62	3	0.20	-
723	0.00	0	0.00	17.72	3	0.12	-
724	15.89	2	0.07	16.71	4	0.06	-
725	15.79	3	0.11	16.27	4	0.10	16.40
726	13.63	4	0.04	14.09	4	0.02	14.20
727	15.07	4	0.11	16.59	4	0.04	-
728	14.98	4	0.03	15.82	4	0.05	15.83
729	15.26	4	0.08	16.01	4	0.03	16.09
730	14.19	4	0.04	14.76	4	0.04	14.81
731	14.19	4	0.09	14.86	4	0.03	15.10
732	15.88	3	0.01	17.23	4	0.15	-
733	16.26	1	0.00	17.49	4	0.10	-
734	16.03	2	0.15	17.51	4	0.12	-
735	15.67	4	0.22	16.51	4	0.12	16.60
736	15.77	3	0.22	16.95	4	0.13	-
737	16.37	2	0.33	17.73	3	0.16	-
738	14.73	4	0.12	15.61	4	0.02	15.38
739	16.45	3	0.21	17.60	4	0.06	-
740	13.91	4	0.09	14.42	4	0.05	-
741	15.40	4	0.31	16.53	4	0.06	-
742	16.36	2	0.19	17.46	4	0.08	-
743	13.39	4	0.03	15.44	4	0.01	-
744	15.74	3	0.25	16.67	4	0.07	-
745	16.23	3	0.23	17.36	4	0.06	-
746	15.86	3	0.29	17.64	4	0.27	-
747	14.21	4	0.07	15.10	4	0.02	14.78
748	16.18	4	0.23	17.43	3	0.06	-
749	15.75	4	0.13	16.88	4	0.05	-
750	16.15	3	0.11	17.16	4	0.07	-
751	15.73	4	0.10	15.86	4	0.04	-
752	16.15	2	0.63	17.43	4	0.11	16.32
753	15.83	4	0.05	16.54	4	0.03	-
754	15.00	4	0.08	15.43	4	0.03	16.57
755	13.35	4	0.08	13.98	4	0.02	-
756	16.20	3	0.35	17.18	4	0.04	-
757	14.21	4	0.12	15.90	4	0.03	-
758	15.21	4	0.15	16.28	4	0.05	-
759	16.09	3	0.07	16.88	4	0.03	-
760	15.91	2	0.17	17.34	3	0.05	-
761	16.21	3	0.20	17.13	4	0.07	-
762	15.87	3	0.27	17.23	4	0.04	-
763	16.36	2	0.06	17.79	3	0.32	-
764	16.51	2	0.38	17.82	2	0.52	-
765	16.39	2	0.37	17.67	3	0.09	-

Star No.	V	No.of Plates	r.m.s. Error	B	No.of Plates	r.m.s. Error	GALAXY U
766	15.48	3	0.31	16.19	3	0.11	-
767	15.60	4	0.16	16.32	4	0.07	-
768	14.48	4	0.18	15.86	4	0.05	16.85
769	15.39	4	0.28	16.34	4	0.04	-
770	15.12	4	0.14	16.88	4	0.14	-
771	14.86	4	0.15	15.73	4	0.02	15.90
772	14.38	4	0.11	15.13	4	0.02	15.69
773	16.08	2	0.45	17.56	4	0.10	-
774	15.97	2	0.01	17.45	4	0.08	-
775	10.74	4	0.04	11.38	4	0.05	11.29
776	16.10	3	0.27	17.34	3	0.09	-
777	15.42	4	0.08	16.58	4	0.04	-
778	15.64	4	0.09	17.32	4	0.13	-
779	15.62	4	0.07	16.69	4	0.04	-
780	16.40	2	0.41	17.78	3	0.21	-
781	11.46	4	0.02	12.07	4	0.03	11.87
782	12.99	4	0.04	13.80	4	0.04	14.22
783	12.52	4	0.02	13.32	4	0.02	13.42
784	16.02	2	0.30	17.52	3	0.16	-
785	16.16	3	0.13	17.20	4	0.08	-
786	15.87	3	0.13	17.16	4	0.09	-
787	16.05	3	0.28	17.54	3	0.09	-
788	14.38	4	0.15	16.42	4	0.02	-
789	15.92	3	0.15	17.68	3	0.23	-
790	15.46	4	0.06	16.73	3	0.06	-
791	15.86	4	0.12	17.13	4	0.10	-
792	15.97	3	0.10	17.27	4	0.10	-
793	15.62	1	0.00	17.26	3	0.16	-
794	12.03	4	0.04	13.20	4	0.03	14.00
795	12.04	4	0.04	12.84	4	0.06	13.20
796	15.94	4	0.17	17.59	4	0.09	-
797	15.95	2	0.05	17.83	3	0.30	-
798	16.05	3	0.24	17.60	3	0.13	-
799	15.95	3	0.20	17.00	4	0.09	-
800	16.24	4	0.02	17.22	4	0.09	14.57
801	16.15	3	0.15	17.46	4	0.11	-
802	14.89	4	0.11	15.80	4	0.06	16.16
803	15.42	3	0.14	16.70	4	0.10	-
804	16.50	1	0.00	17.24	4	0.19	-
805	16.11	2	0.34	17.15	4	0.08	-
806	15.58	3	0.06	16.82	4	0.06	-
807	15.28	4	0.16	15.97	4	0.07	15.49
808	16.32	3	0.29	17.51	4	0.06	-
809	12.26	4	0.04	13.16	4	0.01	-
810	15.27	4	0.15	16.09	4	0.07	16.39

Star No.	V	No.of Plates	r.m.s. Error	B	No.of Plates	r.m.s. Error	GALAXY U
811	14.99	4	0.09	15.26	4	0.03	15.43
812	15.23	4	0.11	16.10	4	0.05	16.71
813	14.27	4	0.10	15.06	4	0.06	15.31
814	15.03	4	0.04	16.26	4	0.05	-
815	15.78	3	0.15	16.97	4	0.07	-
816	15.44	3	0.05	16.37	4	0.04	16.34
817	16.43	2	0.17	17.43	3	0.13	-
818	16.37	2	0.03	18.14	1	0.00	-
819	15.88	3	0.13	17.31	4	0.14	-
820	15.27	4	0.17	15.95	4	0.08	-
821	16.17	3	0.26	17.50	3	0.21	12.55
822	15.28	4	0.07	15.63	4	0.04	-
823	15.83	2	0.39	17.03	4	0.04	16.21
824	14.03	4	0.06	14.79	4	0.03	14.70
825	14.19	4	0.03	15.58	4	0.04	16.79
826	16.23	2	0.26	17.81	2	0.15	-
827	16.09	3	0.34	17.58	4	0.26	-
828	16.04	3	0.04	17.50	4	0.16	-
829	16.03	2	0.47	17.53	2	0.07	-
830	15.13	4	0.03	16.06	4	0.10	-
831	15.19	3	0.04	16.66	4	0.09	16.42
832	15.23	3	0.25	15.99	4	0.06	16.47
833	15.86	3	0.18	17.53	3	0.13	-
834	15.42	3	0.28	16.32	3	0.06	-
835	15.28	4	0.11	16.16	3	0.05	17.00
836	15.15	4	0.25	15.72	4	0.24	15.38
837	15.38	4	0.06	16.06	4	0.13	16.40
838	16.18	2	0.13	17.65	3	0.12	-
839	16.08	3	0.33	17.86	2	0.33	-
840	15.87	4	0.20	17.41	4	0.09	-
841	15.75	4	0.16	16.81	4	0.12	-
842	16.31	2	0.09	17.59	3	0.12	-
843	12.83	4	0.08	13.71	4	0.03	-
844	15.82	4	0.24	17.67	3	0.12	-
845	15.88	1	0.00	17.27	2	0.40	-
846	14.24	4	0.08	15.62	4	0.02	-
847	15.41	3	0.13	16.71	4	0.03	-
848	15.33	3	0.03	16.42	4	0.08	-
849	15.64	4	0.21	16.22	4	0.05	-
850	15.52	3	0.09	16.74	4	0.02	-
851	15.91	3	0.21	17.53	4	0.11	-
852	15.77	1	0.00	17.31	3	0.02	-
853	15.83	2	0.18	17.12	4	0.04	-
854	16.13	4	0.25	17.45	4	0.16	-
855	12.74	4	0.02	13.33	4	0.04	14.10

Star No.	V	No.of Plates	r.m.s. Error	B	No.of Plates	r.m.s. Error	GALAXY U
856	13.79	4	0.08	16.30	4	0.07	-
857	10.73	4	0.01	13.27	4	0.06	13.20
858	12.83	4	0.09	13.65	4	0.03	-
859	15.54	2	0.06	16.93	4	0.02	-
860	0.00	0	0.00	17.29	4	0.06	-
861	13.46	4	0.09	14.22	4	0.04	14.28
862	14.89	4	0.08	15.57	4	0.08	15.85
863	16.07	2	0.05	17.10	4	0.08	-
864	15.50	4	0.12	16.10	4	0.04	16.47
865	15.88	2	0.25	16.56	4	0.05	-
866	15.29	4	0.36	16.65	4	0.08	-
867	16.52	2	0.01	17.31	4	0.06	-
868	15.84	4	0.11	17.21	4	0.06	-
869	14.44	4	0.14	15.17	4	0.03	15.75
870	15.14	4	0.18	15.85	4	0.12	16.70
871	15.54	4	0.27	16.35	4	0.03	15.74
872	11.77	4	0.03	12.73	4	0.01	13.09
873	15.46	3	0.30	17.09	4	0.07	-
874	15.74	3	0.34	16.72	4	0.13	-
875	15.59	4	0.17	16.76	4	0.08	15.65
876	15.77	2	0.14	16.35	4	0.04	-
877	14.85	3	0.16	15.40	4	0.02	-
878	14.37	4	0.08	16.31	4	0.04	-
879	14.50	4	0.11	17.22	4	0.11	-
880	14.94	4	0.17	16.01	4	0.08	-
881	15.93	2	0.21	17.55	4	0.13	-
882	16.20	3	0.25	17.59	4	0.10	-
883	16.08	3	0.31	16.33	1	0.00	-
884	15.94	1	0.00	17.23	4	0.04	-
885	15.17	4	0.14	15.69	4	0.02	15.70
886	15.88	2	0.48	17.42	4	0.14	-
887	12.42	4	0.03	14.59	4	0.03	-
888	16.12	2	0.29	17.62	4	0.16	-
889	15.29	4	0.07	15.75	4	0.03	16.00
890	16.35	2	0.36	17.87	2	0.42	-
891	16.22	2	0.21	17.08	4	0.12	16.75
892	16.06	4	0.23	17.14	4	0.11	-
893	16.11	3	0.14	17.07	4	0.05	-
894	13.20	4	0.06	13.65	4	0.07	13.53
895	13.99	4	0.09	15.95	4	0.07	-
896	15.70	3	0.37	16.30	4	0.04	16.36
897	15.23	3	0.17	15.97	4	0.04	16.37
898	16.58	2	0.14	17.36	4	0.07	-
899	15.00	4	0.09	16.41	4	0.07	-
900	12.16	4	0.04	13.75	4	0.02	15.18

Star No.	V	No. of Plates	r.m.s. Error	B	No. of Plates	r.m.s. Error	GALAXY U
901	15.99	2	0.13	17.41	4	0.11	-
902	10.97	4	0.01	11.58	4	0.03	11.63
903	16.32	1	0.00	17.50	4	0.12	-
904	15.96	3	0.08	17.19	4	0.10	-
905	14.65	4	0.16	15.35	4	0.02	15.26
906	13.71	4	0.11	15.09	4	0.04	16.71
907	15.18	4	0.09	16.12	4	0.06	-
908	13.82	4	0.10	15.01	4	0.01	15.44
909	15.93	2	0.03	17.28	4	0.10	-
910	15.95	4	0.05	17.43	4	0.06	-
911	16.70	1	0.00	17.55	4	0.17	-
912	16.18	1	0.00	17.21	4	0.04	-
913	15.57	2	0.30	17.36	4	0.14	-
914	15.65	3	0.25	16.93	4	0.03	-
915	16.41	2	0.28	17.64	3	0.18	-
916	16.58	1	0.00	17.93	3	0.24	-
917	16.44	1	0.00	17.96	3	0.35	-
918	16.13	1	0.00	18.08	2	0.55	-
919	0.00	0	0.00	18.14	1	0.00	-
920	13.66	4	0.08	14.41	4	0.02	14.66
921	15.43	4	0.19	15.92	4	0.06	16.19
922	15.93	2	0.07	17.22	4	0.14	-
923	15.86	3	0.25	16.37	4	0.06	16.65
924	15.65	3	0.22	16.34	4	0.04	-
925	15.72	4	0.10	17.61	4	0.12	-
926	15.92	4	0.15	17.48	4	0.13	-
927	15.08	4	0.11	16.46	4	0.06	-
928	14.93	4	0.22	15.62	4	0.04	15.52
929	14.31	4	0.05	15.73	4	0.04	16.39
930	16.30	4	0.25	17.61	4	0.04	16.75
931	15.60	3	0.21	16.84	4	0.09	-
932	15.23	4	0.22	15.82	4	0.07	16.34
933	15.91	3	0.24	17.35	4	0.26	-
934	15.87	4	0.23	17.19	4	0.22	-
935	15.86	2	0.36	16.84	4	0.09	-
936	10.21	4	0.03	10.65	4	0.03	-
937	16.11	2	0.14	17.59	4	0.13	-
938	15.70	4	0.16	16.87	4	0.10	-
939	16.26	2	0.18	17.44	4	0.05	-
940	16.20	2	0.12	17.80	4	0.20	-
941	16.71	1	0.00	17.98	3	0.25	-
942	15.96	3	0.09	16.73	4	0.07	-
943	15.20	3	0.18	16.10	4	0.05	16.13
944	14.95	4	0.10	15.80	4	0.02	-
945	13.98	4	0.08	15.72	4	0.04	-
946	15.26	4	0.16	16.08	4	0.16	17.01

CHAPTER 6

THE POLARIZATION OF STARLIGHT

in IC 5146

Introduction

All the techniques used to measure the polarization of starlight in NGC 654 were repeated for IC 5146. All observations and reductions were performed in the same way, using the same equipment and computer programs. These techniques are fully described in Chapter [3] .

Data Collection

The data used for IC 5146 was rather better than that used for NGC 654 because seven good plates of the region were used, compared with the five plates of NGC 654. The plates were all taken when the moon was below the horizon so that polarized moonlight would not affect the results in any way.

The plates used are listed in the table on the following page:

Plate	Emulsion	Exposure	Date	Sidereal Time
843	IIaO	3x5 min	14.10.68	22^h40^m
844	IIaO	3x5 min	14.10.68	23^h14^m
846	IIaO	3x5 min	16.10.68	21^h49^m
847	IIaO	3x5 min	16.10.68	22^h22^m
854	IIaO	3x5 min	17.10.68	23^h37^m
855	IIaO	3x5 min	17.10.68	00^h07^m
870	IIaO	3x5 min	20.10.68	22^h15^m

Measurement of Images

All measurement of star images was done using the Computer Controlled Iris Photometer in its semi-automatic mode. This machine is described in Appendix 1.

245 stars were studied. These stars lie in the central region of the cluster and in three regions distributed around the cluster. As well as these stars, there are 100 in each of the three control regions and the 30 standard stars were measured 12 times during the measurement of a plate to keep a check on any calibration drift. There was thus a total of 2715 images to be measured on each plate, remembering that each star has three images. Fortunately, the Computer Controlled Iris Photometer's high rate of measurement made it possible to measure all the images on a plate by working overnight, when the workload on the computer is small.

The measurement of each plate was divided into six runs of between 400 and 500 measurements each. The standard stars were included at the beginning and end of runs which took about two hours each.

Reductions

The reductions of measurements were done using the same system of programs as was used for NGC 654.

The limiting magnitude on polarization plates is $15^{m}.00$ in the B waveband. Stars which did not have good measurements on three or more of the seven plates are rejected. The plates were all scrutinised for faulty images. The most common fault was the overlapping of star images. Other faults include emulsion defects and the involvement of certain images in nebulosity. The table below lists the stars with good polarization measures. The running numbers correspond to those on the charts used for UBV photometry.

No	Mpg	p	rms(p)	θo(deg)	Q	U	No of Plates used
1	10.32	0.060	0.014	-64	-0.036	-0.048	6
4	14.97	0.030	0.080	-62	0.030	-0.006	4
6	13.98	0.145	0.050	12	0.131	0.063	4
9	14.29	0.113	0.014	27	0.063	0.093	3
12	14.36	0.174	0.095	88	-0.174	0.011	3
13	12.34	0.080	0.014	74	-0.069	0.041	5
27	12.47	0.087	0.031	86	-0.086	0.011	6
36	14.93	0.031	0.049	- 2	0.031	-0.001	5
44	11.01	0.044	0.031	-79	-0.040	-0.017	4
46	14.73	0.203	0.046	-63	-0.119	-0.164	6
52	13.90	0.144	0.046	55	-0.051	0.135	4
53	11.78	0.018	0.093	38	0.004	0.018	6
55	12.23	0.033	0.033	-60	-0.017	-0.029	5
57	13.67	0.128	0.036	-45	0.004	-0.128	5
60	10.26	0.025	0.033	51	-0.005	0.024	6
63	13.50	0.132	0.055	-86	-0.131	-0.021	5
72	12.34	0.108	0.035	85	-0.107	0.017	6
83	14.80	0.226	0.035	14	0.198	0.109	3
85	14.98	0.024	0.129	53	-0.007	0.023	3
86	11.79	0.062	0.010	-45	0.002	-0.062	3
90	12.07	0.093	0.032	10	0.086	0.034	5
91	12.40	0.070	0.078	-76	-0.061	-0.034	3
92	14.12	0.034	0.039	-21	0.026	-0.022	6
190	14.27	0.034	0.027	36	0.010	0.032	6
192	10.60	0.054	0.007	-24	0.037	-0.039	4
196	14.06	0.040	0.080	-11	0.038	-0.014	6
199	13.44	0.149	0.039	-40	0.026	-0.147	5
222	13.33	0.052	0.064	-76	-0.045	-0.026	4
238	13.63	0.087	0.039	- 8	0.085	-0.022	4
700	12.79	0.092	0.055	8	0.088	0.027	4
702	14.80	0.134	0.040	83	-0.130	0.031	4
704	14.61	0.091	0.042	-35	0.032	-0.085	5
726	13.99	0.114	0.077	51	-0.028	0.111	5
731	14.87	0.037	0.003	-78	0.033	-0.016	5
861	14.20	0.119	0.064	-47	-0.006	-0.118	4
872	12.75	0.030	0.030	-76	-0.026	-0.014	5
887	14.53	0.040	0.069	60	-0.020	0.034	3
894	13.67	0.052	0.017	50	-0.009	0.051	6
900	13.65	0.134	0.026	55	-0.050	0.125	6
908	14.99	0.111	0.052	-75	-0.095	-0.056	3

p102

NN very happy.

Perhaps you ones
are going up with B.

c-f p18.

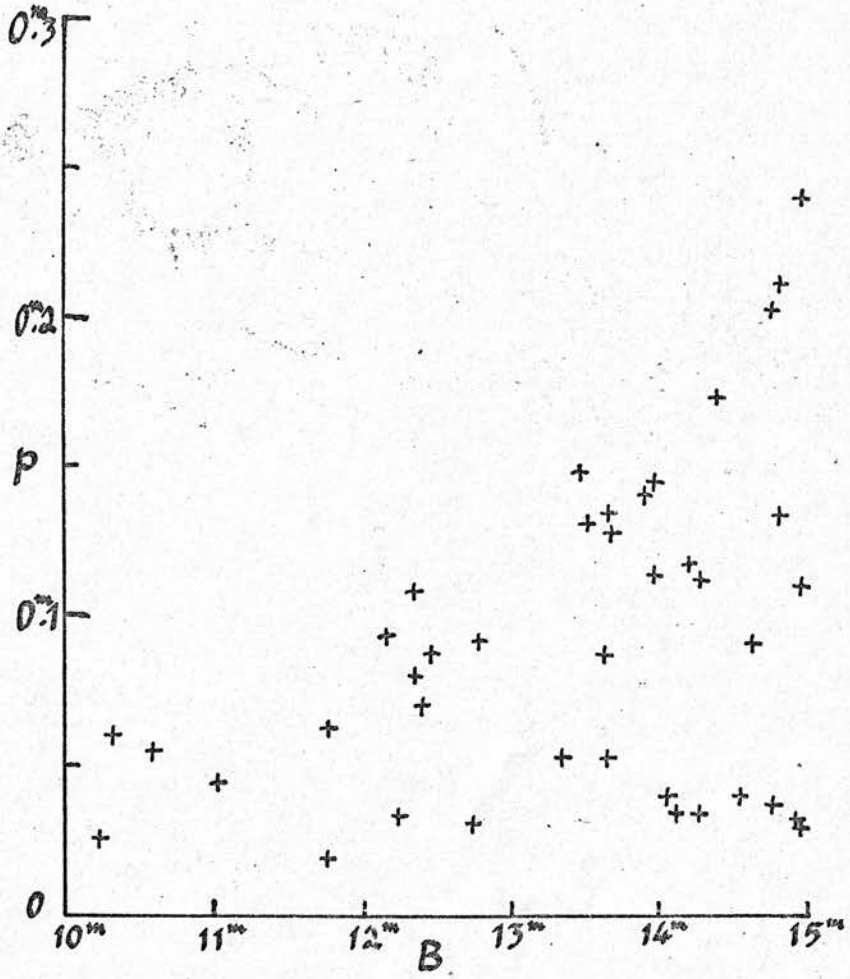

FIG 19 : Polarization Plotted Against B Magnitude for Stars in IC 5146.

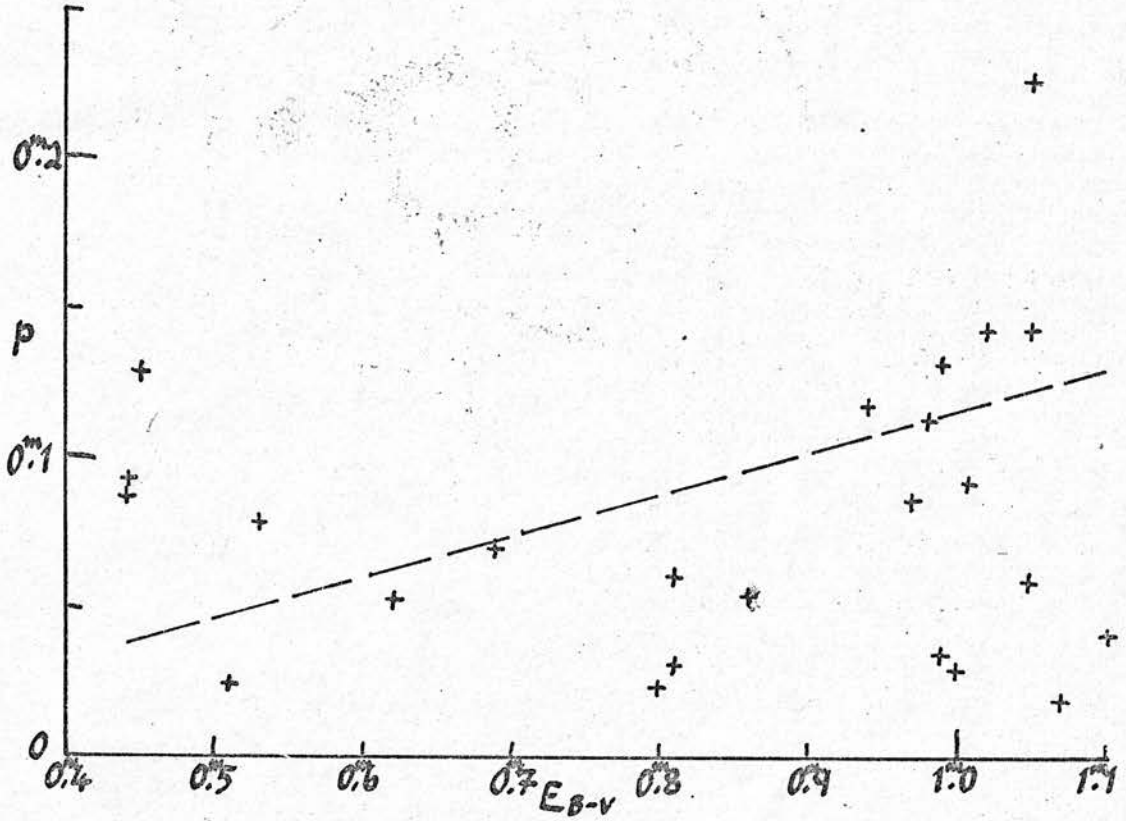

FIG 20 : Polarization Plotted Against Colour Excess for Stars in IC 5146.

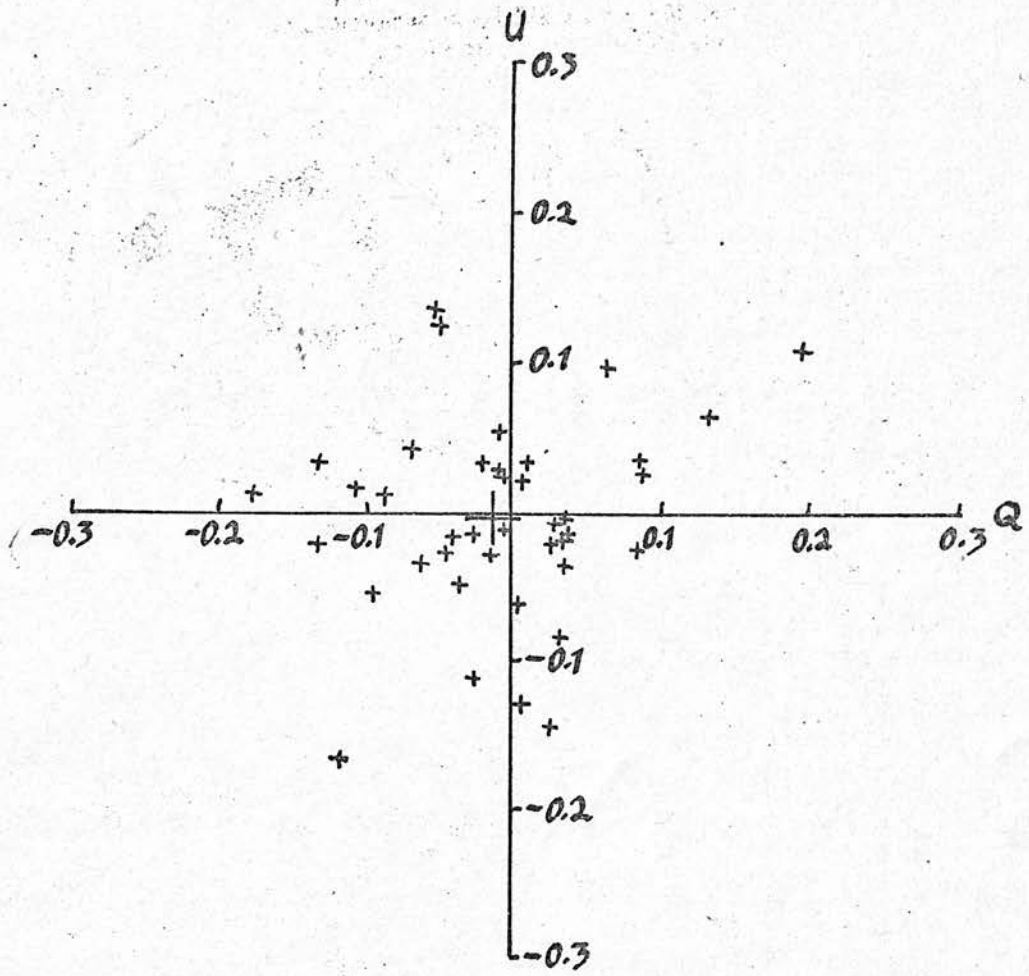

FIG 21 : The Stokes' Parameter U Plotted Against the Parameter Q for IC 5146.

Polarization and Magnitude

Fig 19 shows p, the polarization plotted against the B magnitude. The maximum polarization of faint stars is greater than that of brighter ones. This effect was found by Hall (23) who attached little significance to it because of observational selection. The relationship does however seem to be real and continues the relationship found by Hall to fainter magnitudes. The effect has also been found in the case of NGC 654 in this thesis.

Polarization and Colour Excess

Fig 20 shows p, the polarization plotted against colour excess, E_{B-V}. As in the case of NGC 654, the two quantities appear to be correlated. The slope of the line agrees with that found by Hall for stars at this galactic longitude.

The Stokes Parameters, Q and U

Fig 21 shows U plotted against Q, where

$$Q = p \cos 2\theta_o \text{ and } U = p \sin 2\theta_o.$$

The mean value of Q is $-0^m.012$ while that of U is $-0^m.001$. This means that the mean polarization $\bar{p}$ is about $0^m.01$ and the mean angle of the electric component to the equator, $\bar{\theta}_o$ is about 90^o. There are, at present, no photoelectric measurements of polarization for any of the stars studied, nor are there any measurements for nearby stars. Since, however, the measurements vary so much, it is likely that

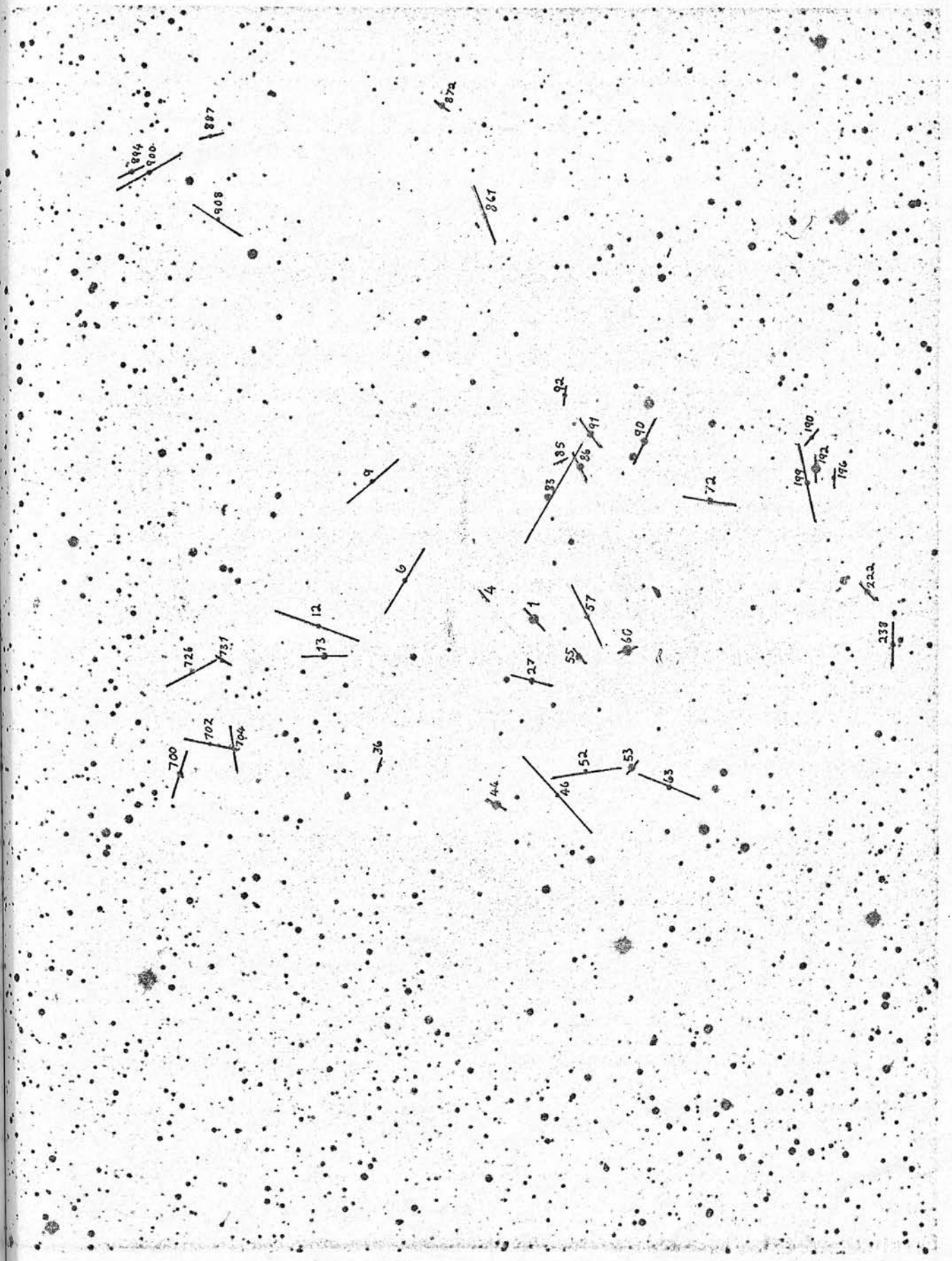

FIG 22 : Chart Showing Polarization Vectors for Stars in IC 5146. $0^m.1$ 1 cm. North to Left.

most of the polarization is produced in the immediate vicinity of the stars themselves and any comparisons would be irrelevant.

Discussion

Fig 22 shows the polarization vectors plotted on a photograph of the region of IC 5146. It can be seen that the polarization varies greatly from star to star in both magnitude and direction. This effect is most unusual, but has been observed by Hall (22) in one other H_{II} region - the Orion region. IC 5146, in common with Orion, lies well away from the Milky Way - about 6^{o} in the case of IC 5146. Most of the observed polarization therefore will be due to dust which is local to the cluster rather than to dust in intervening spiral arms. Because dust grains are lined up by the local magnetic field, the magnetic field in IC 5146 must be very complex indeed.

The most luminous stars in the region possess very small values of p, the polarization. This is also true in the case of the trapezium stars in Orion. Hall mentions that this may be due to a change in the particle distribution brought about by the radiation pressure from these stars.

Although polarization vectors vary a great deal in this region, it should be noticed that the stars tend to form

subsets with similar polarization vectors, eg 190, 192 and 196; 46, 52 and 63; 12 and 13; 887, 894 and 900.

CHAPTER 7

THE DARK NEBULA

Introduction

IC 5146 consists of a cluster of hot, young stars embedded in a bright nebula of ionised hydrogen and dust, surrounded by a larger dark nebula. The system is very nearly spherically symmetrical, broken only by a dark lane leaving the north west side of the nebula to become part of a complex of dust clouds which lie close to the nebula in this direction.

The high degree of symmetry of the IC 5146 system makes it ideal for calculations of mass and other properties based on optical and radio observations. Counts of stars seen through the dust allow estimates to be made of the amount of obscuration caused by different parts of the nebula. From this the mass of dust and, thence, the mass of hydrogen present can be estimated. Radio observations at 21 cms wavelength give the mass of neutral hydrogen present. The diameter of the sphere inside which the hydrogen is ionised, along with the spectral type of the exciting star give the density of hydrogen in the nebula. It is interesting to compare the masses found by these three techniques.

Fig 23

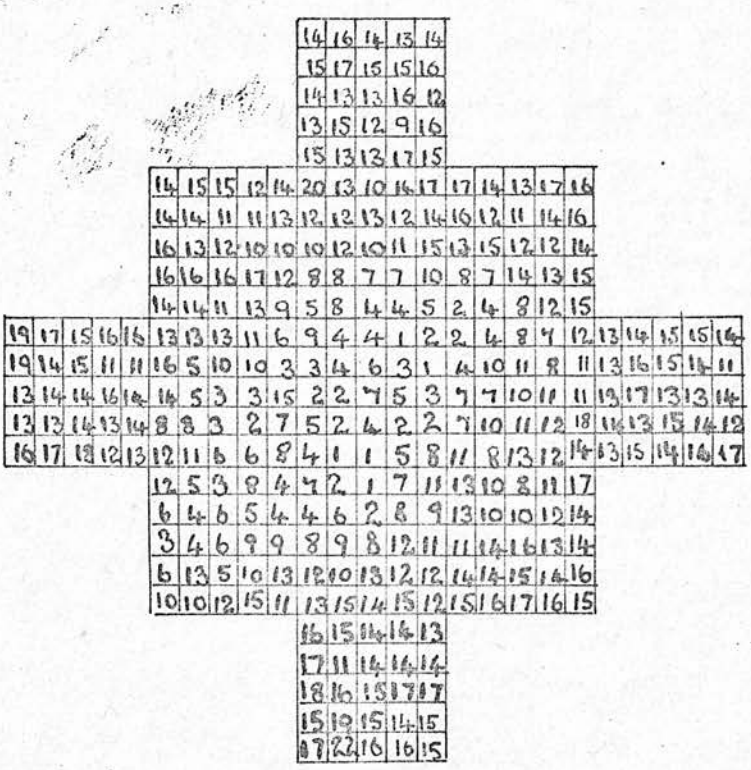

FIG 23 : Chart of IC 5146 Region Divided into 2 mm Squares on POSS O-print. The Numbers Indicate the no of Stars per mm^2.

Star Counts

The National Geographic Society - Palomar Observatory Sky Survey O-chart of the region of IC 5146 was used for star counts. The technique used was developed by Bok (27) for the study of dark nebulae seen against a background of stars. The expected number of stars is compared with the number of stars seen through the nebula and the absorption can be computed from this.

The reseau used for the star count has a grid of 1 mm squares. 1 mm corresponds to 67.14 are seconds on the POSS print and so we expect to count about 20 stars per reseau square in a relatively unobscured region, down to limiting magnitude.

The count was made using a binocular microscope with X5 magnification. All counting was done by one person, the author, because it is a rather subjective technique and people differ widely in their counts of stars in any one region.

An area of 1300 mm^2 was covered by the star counts. The number of stars per mm^2 fluctuates greatly from square to square and so these numbers are averaged over squares with 2 mm sides to show more clearly the trends over the region. Fig 23 shows the number of stars per mm^2 in each of the 2 mm side squares covering the region.

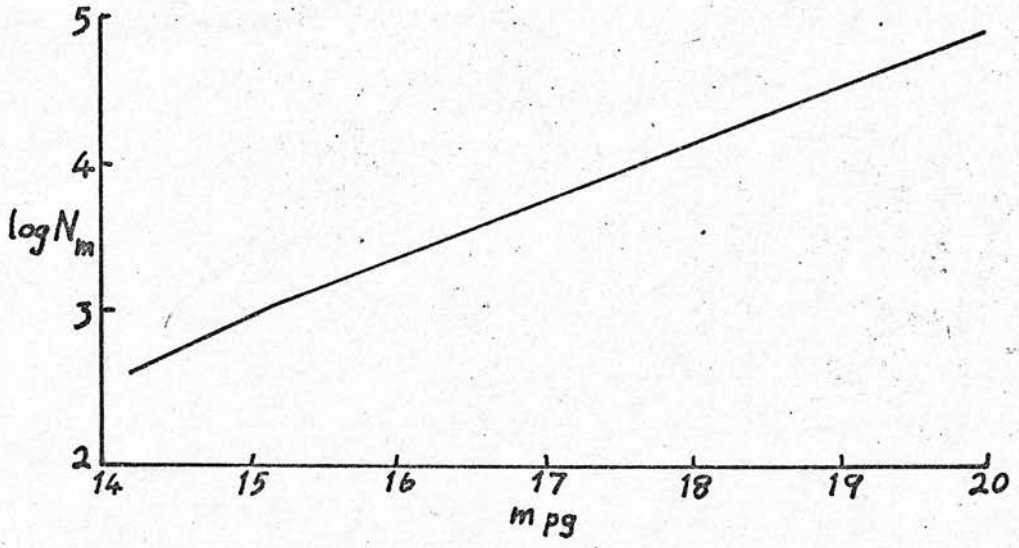

FIG 24 : The Log of N_m, the Number of Stars per Deg^2 to Limiting Magnitude m, Plotted Against Photographic Magnitude.

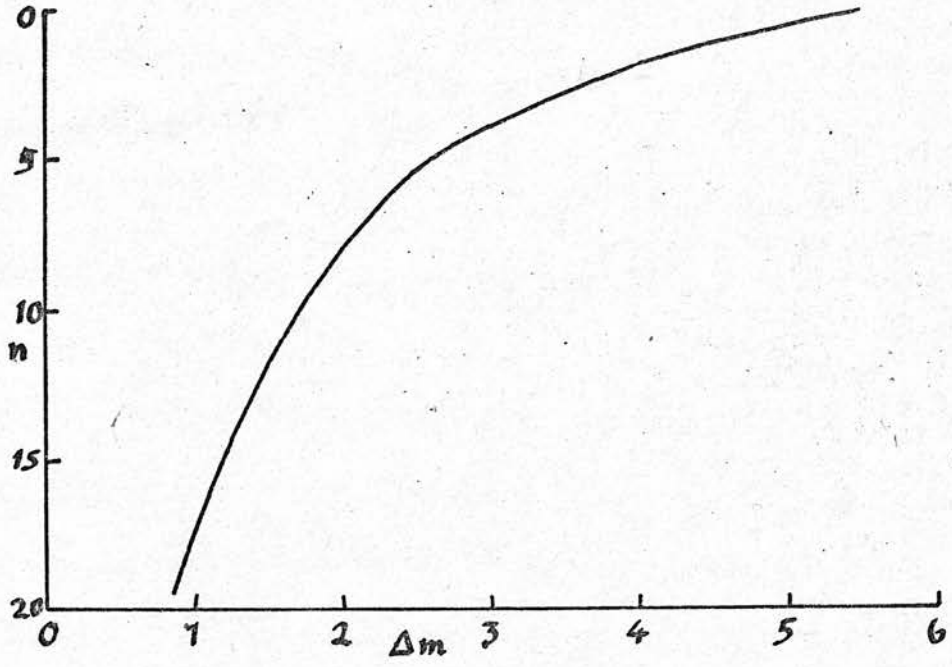

FIG 25 : n, the Number of Stars per mm^2 on the POSS O-print Plotted Against Δ m, the Number of Magnitudes of Absorption.

Van Rhijn (28) has published star counts at various galactic latitudes and longitudes. These counts can be used to predict the rate at which N, the number of stars per degree^2 varies with limiting magnitude in the region of IC 5146 if obscuration is not unduly high. From this we may then predict the variations in N due to a nearly dark nebula which absorbs $1\overset{m}{.}0$, $2\overset{m}{.}0$, $3\overset{m}{.}0$, etc.

Fig 24 shows the relationship between log N_m and pgm where N_m is the number of stars per degree^2 brighter than magnitude m. This relationship comes directly from the tables of van Rhijn. From this we can compute the relationship between n, the number of stars per mm^2 on the Palomar O-print, and the number of magnitudes of absorption. This relationship is shown on fig 25.

Two assumptions will be made for the computations of absorption:

(i) The number of stars which lie between us and the nebula is negligible compared with the number of background stars seen through the nebula.

(ii) The number of cluster members visible is negligible compared with the number of background stars visible.

In general, these two assumptions are very nearly true for all but the very central parts of the cluster where they will cause an underestimation of the value of the absorption.

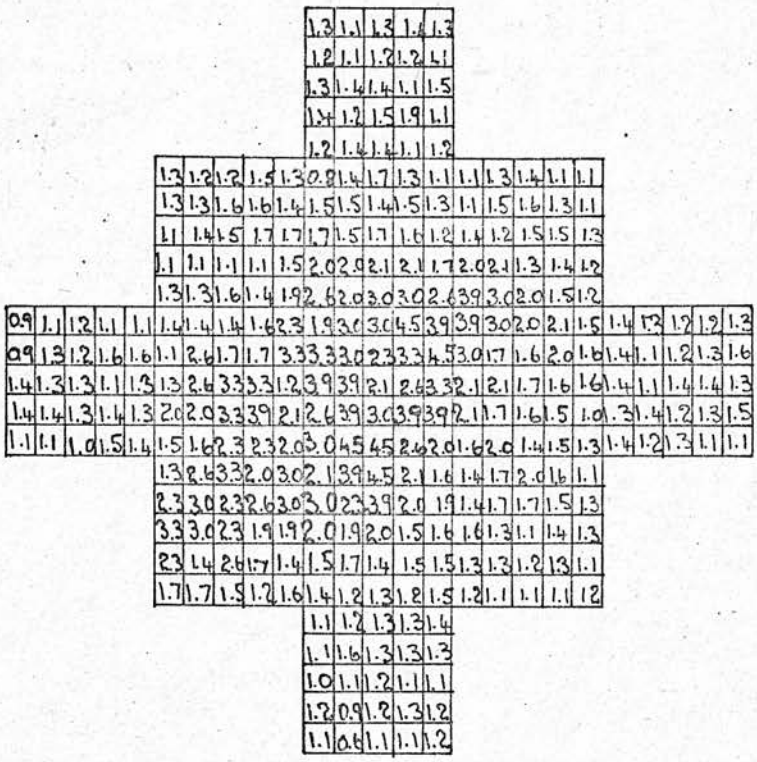

FIG 26 : Charts Showing Absorption in Magnitudes, Computed from Star Count Data on Fig 23.

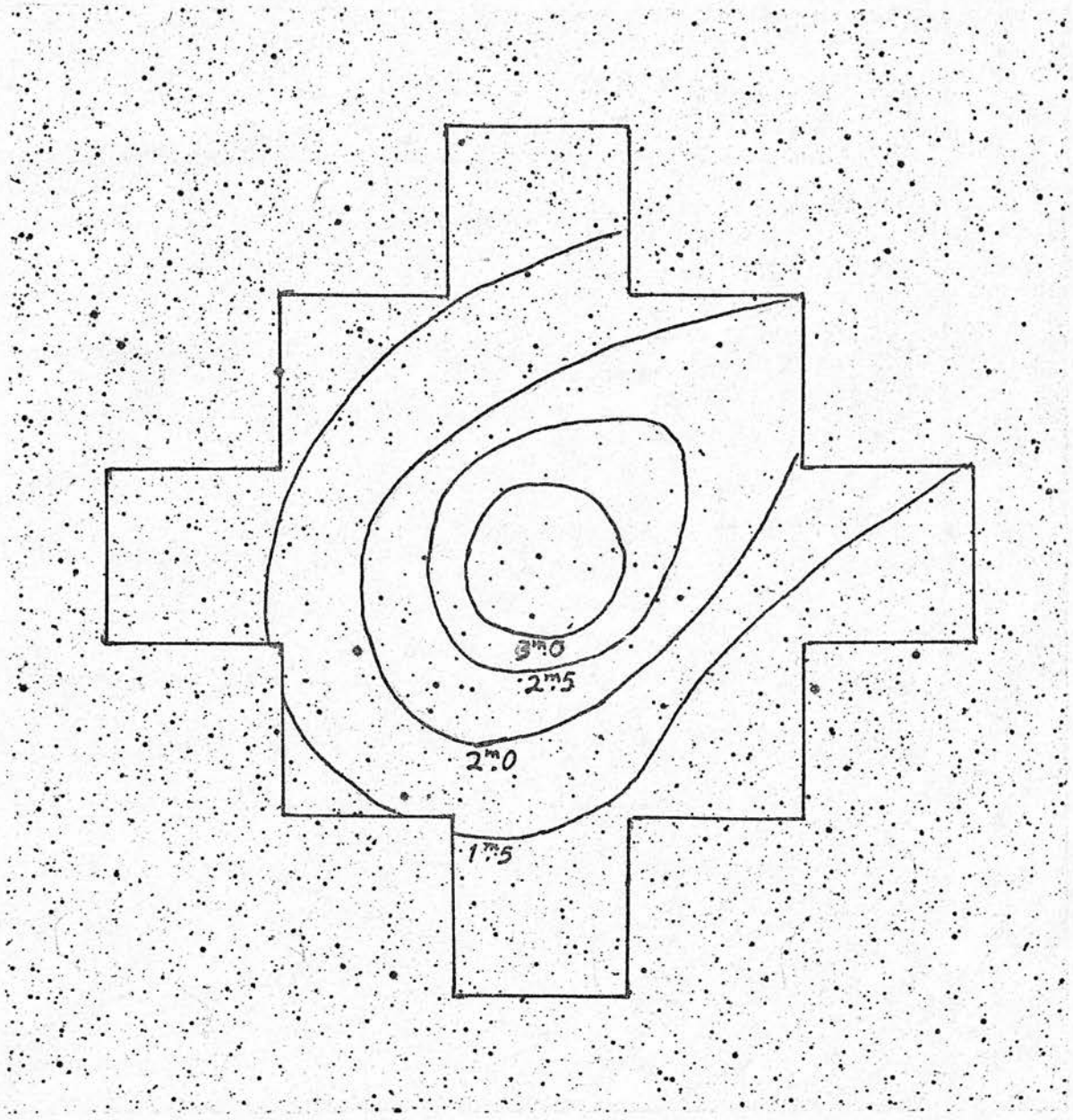

FIG 27 : Chart of IC 5146 Showing Contours of Equal Absorption Computed from Star Count Data on Figs 23 and 26.

This will, in turn, cause an underestimation of the mass of the nebula.

Fig 26 shows the area in which the star count was made divided into 2 mm squares and the value of the absorption in magnitudes is written in the squares, corresponding to the number of stars counted in them. In the outer squares the computed absorption is about $1^m.0$. This is because the star counts have not reached the nominal plate limit, but have stopped about $1^m.0$ short of this, ie at about $m_{pg} = 20.0$.

Using the data from fig 26, contours of equal absorption are plotted on a photograph of the area shown on fig 27. It can be clearly seen that the cluster and dark nebula are like a knob at the end of a dust lane. This dust lane goes on to become part of a large complex of dust clouds lying north west of the cluster. Unfortunately, no proper motion data are available to determine whether or not the cluster came from this complex initially. If it did, then the cluster would be moving away from the galactic plane.

Reddish (29) gives us a formula for the mass of a dark nebula in terms of its diameter, l, and the absorption in magnitudes, A_v, of starlight seen through the centre of the cloud:

$$M = 2.8 \times 10^{-3}\ l^2\ A_v\ g.$$

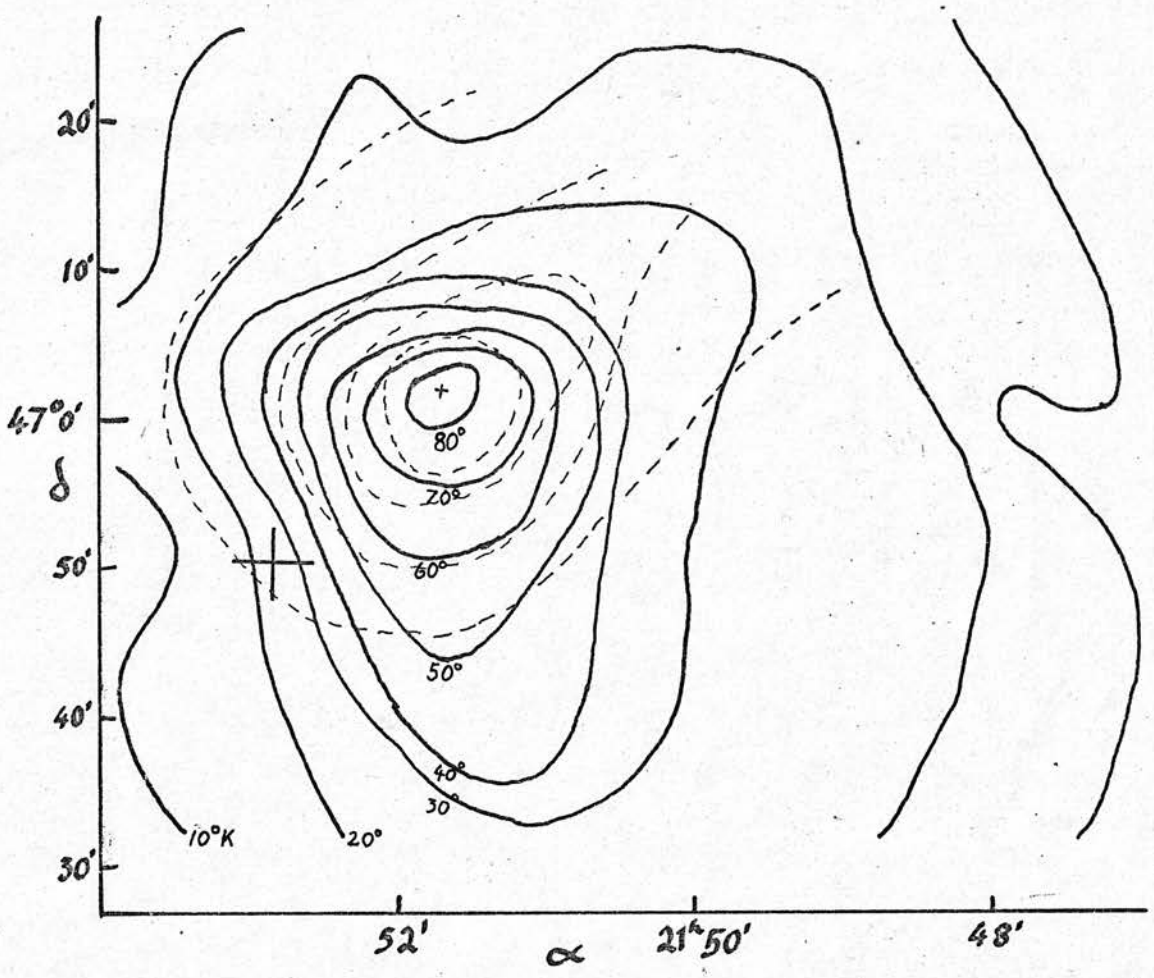

FIG 28 : Contours of Equal 21 cm Line Emission are Shown. Contours of Equal Absorption are Represented by Dashed Lines. The Heavy Cross Shows the Position of Radio Source CTA 97.

Now the absorption of starlight seen through the centre of IC 5146 is $\sim 1^{m}.5$ greater than that for starlight coming around the cloud. The diameter of the cloud is ~ 5 pc. We have:

$$M = 2.8 \times 10^{-3} \times (15 \times 10^{18})^2 \times 1.5 \text{ g}$$

$$9 \times 10^{35} \text{ g}$$

$$\underline{450\ M_{\odot}}$$

Alternatively, we may compute the mass of dust directly. For efficient scattering of light we have:

$$2\pi(\mu - 1)a \approx \lambda$$

where a is the radius of a grain, μ = refractive index of a grain and λ is the wavelength of incident radiation.

Now μ is typically 1.5 and maximum obscuration occurs at $\lambda \sim 2000\ \text{Å} = 2 \times 10^{-5}$cm

So $3a \approx \lambda = 2 \times 10^{-5}$cm

$\therefore$ $a \approx 7 \times 10^{-6}$cm

Now the optical cross section of a grain is

$$\pi a^2 Q_{ext}$$

$$\approx 1.5 \times 10^{-10} \text{cm}^2$$

Optical depth = $\tau = a^2 Q_{ext} n_g l$

$\approx \Delta m$, the obscuration in magnitudes,

where n_g is the number of grains and l is the distance travelled by the light.

Now the obscuration of starlight seen through the centre of IC 5146 is $\sim 1^{m}.5$ greater than that for starlight coming around the cloud,

so $\quad \Delta m = 1.5$

ie $\quad \pi a^2 Q_{ext} n_g l = 1.5$

now l, the cloud diameter ≈ 5 pc

$\therefore \quad n_g = 7 \times 10^{-10} cm^{-3}$.

M_g, the mass of a grain $= \frac{4}{3} \pi r^3 \rho$

Assuming $\rho \approx 2$ we have

$$m_g = 3 \times 10^{-15} g$$

Hence the total mass of interstellar grains

$$= V m_g n_g = \frac{4}{3} \pi (2.5 \times 3 \times 10^{18})^3 \times (7 \times 10^{-10}) \times (3 \times 10^{-15}) g$$

$$= 4 \times 10^{33} g$$

$$= \underline{2\ M_\odot}$$

Radio Observations

Riegel (16) has made a detailed study of IC 5146 at 21 cm wavelength using the 90 m transit radio telescope at the National Radio Astronomy Laboratory. He finds a very strong HI feature associated with IC 5146 whose position agrees precisely with the optical position of the cluster and nebula. He gives plots of R A vs radial velocity at 10' intervals in declination. The HI distribution is asymmetric and extends much farther to the south and west than to the north and east. Contours of equal 21 cm emission at 10^{o} intervals are shown on fig 28 and superimposed on this are the contours of equal absorption

found in the star count.

Clearly the dust and HI increase at the same rate as we approach the centre of the cloud, indicating that they are not effectively separated by radiation pressure from the embedded stars.

The masses of HI and HII computed by Riegel are:

M_{HI} = 670 $M_\odot$

M_{HII} = 20 $M_\odot$

Two assumptions were made in the calculations which could cast doubt on these computed masses:

(i) A spin temperature of 125°K is assumed for the background HI. Mebold (30) points out that the spin temperature is probably about 60°K in optically thick regions.

(ii) Continuum observations of the radio source CTA97 (17) are used for the computation of HII mass. CTA97 lies at a distance of about 15' from the optical HII region, right outside the dark cloud. Unless the stated position of this source is wrong it seems doubtful that it is physically connected with the optical HII region.

Churchwell, Felli and Mezger (18) were unable to detect IC 5146 at 15.4 GH_z in their search for compact HII

regions. Their observations put an upper limit of 0.67 on the flux density.

The Optical HII Region

The HII region in IC 5146 has an apparent diameter of 10', as seen on the POSS prints. This corresponds, at a distance of 1000 pc, to a diameter of 3 pc.

So, $R_{II} = 1.5$ pc

where R_{II} is the radius of the HII region.

Now, $R_{II} = Ro\ \eta^{\frac{1}{2}}\ N^{-2/3}$ (31)

where Ro = 17 pc for a B1V exciting star, η = the fraction of the sphere occupied by HII ≈ 1, and N is the number of hydrogen nuclei per cm^3

$\therefore \quad N = \left(\frac{17}{1.5}\right)^{3/2}$

$= 33$ hydrogen nuclei per cm^3.

The mass of hydrogen nucleus $\simeq 1.7 \times 10^{-24}$ g

the volume of the HII region $\sim 14\ pc^3$

$= 14 \times 9 \times 10^{54} cm^3$

$\therefore$ the mass of interstellar matter in the HII region $\approx 20 \times 10^{33}$g

$\approx$ 10 M⊙

This is rather smaller than Riegel's estimate of 20 M⊙ based on observations of CTA97.

If the density of interstellar matter were constant throughout the cloud, whose radius is 2.5 pc, we would

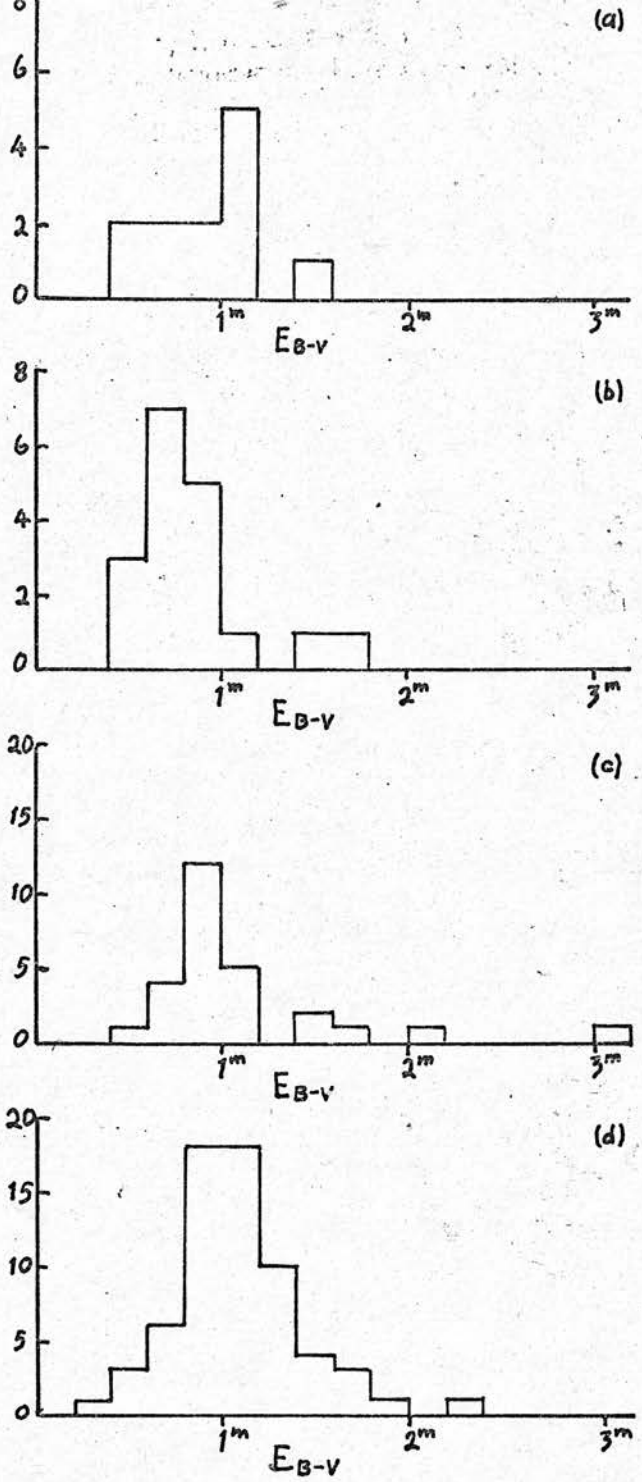

FIG 29 : Frequency Distributions of Colour Excess for Four Parts of IC 5146.

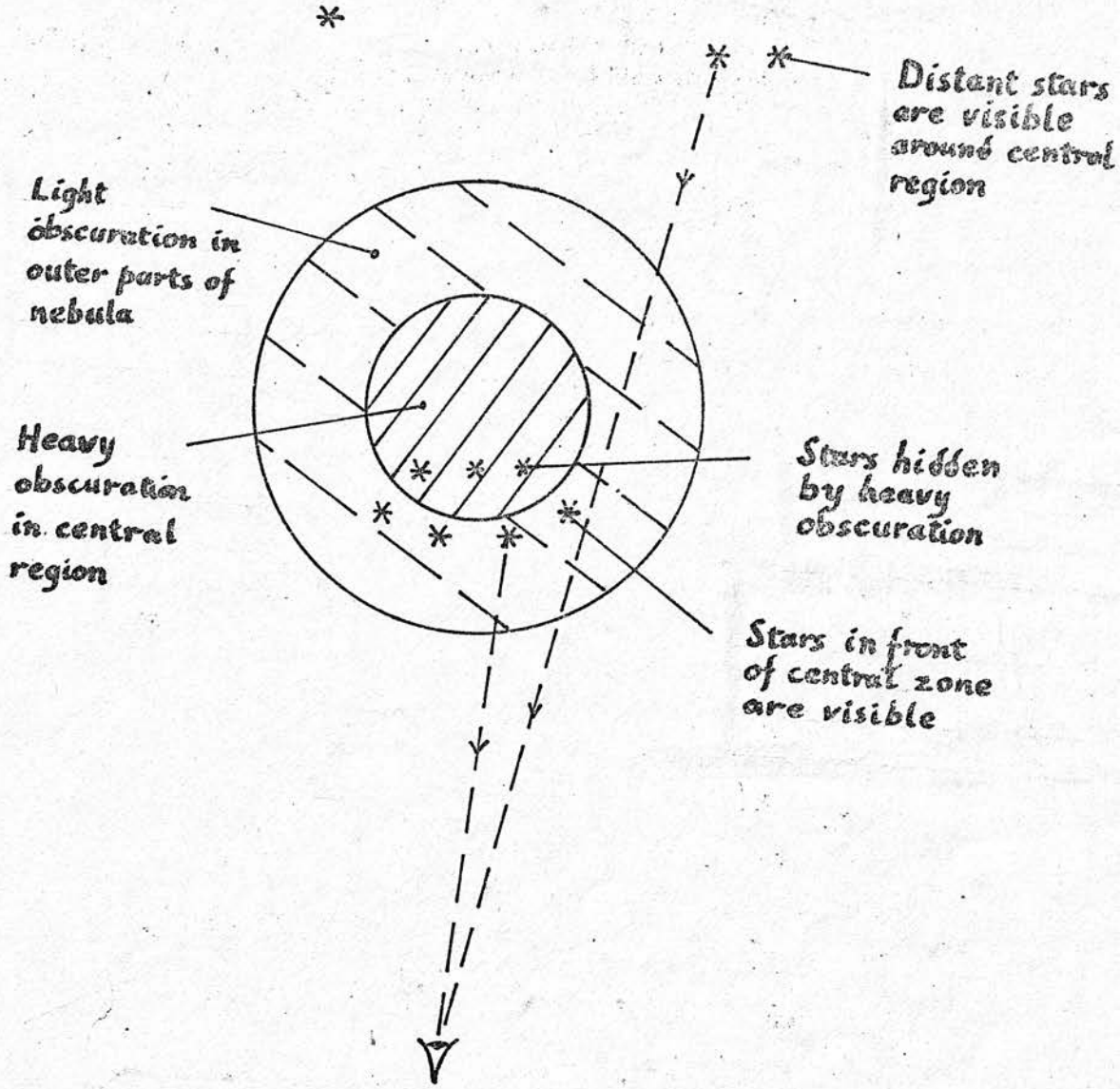

FIG 30 : Model of Dust Distribution in IC 5146.

find that the total mass of the cloud was about 40 $M_\odot$.

The Colour Excesses of Stars in and around IC 5146

The stars which were studied photometrically in Chapter 5 can be divided into four subsets. Referring to fig 27, which shows contours of equal absorption, we have:

(a) All stars within the $3^m.0$ contour.

(b) All stars between the $2^m.5$ and $3^m.0$ contours.

(c) All stars between the $2^m.0$ and $2^m.5$ contours.

(d) All stars between the $1^m.5$ and $2^m.0$ contours.

E_{B-V} was computed for the stars in these subsets. In (c) and (d) only those stars for which the colour excess could be determined unambiguously were used. In (a) and (b), however, stars were assumed to have the maximum of all possible reddenings in ambiguous cases and all stars were used. This is justifiable because most of the stars visible in (a) and (b) are cluster members and so are probably main sequence OB stars.

Fig 29 shows frequency distributions of colour excess in (a), (b), (c) and (d). Most of the stars in (a) and (b) have $E_{B-V} \leqslant 1^m.2$ while in (c) and (d) all but two of the stars have $E_{B-V} \leqslant 2^m.2$. At first glance it seems odd that the stars in (c) and (d) seen through the thinner parts of the cloud are more reddened than those in the

dense central parts. Fig 30 shows a model for the dust cloud which satisfies these conditions. The sudden onset of heavy obscuration in the central part of the system at an optical depth $A_V = 3 \times 1^m.2 = 3^m.6$ obscures all stars inside and behind it. Stars seen around this dense central region can be seen to a much greater optical depth, $A_V \approx 7^m.0$, because the build up of obscuration is much more gradual. In the centre, obscuration becomes effectively opaque in a distance containing relatively few stars. Outside, more stars can be seen to this optical depth.

From the above, we may conclude that the density of interstellar matter is much higher in the central part of the nebula than in the outer parts.

Conclusions

The mass of interstellar matter, principally hydrogen, has been computed three ways:

(i) The absorption of starlight has been measured by counting stars seen through the dark nebula. From this the mass of interstellar dust has been computed and is found to be about 0.2 M⊙. The mass of hydrogen corresponding to this is 450 M⊙.

(ii) Riegel (16) has observed the region at 21 cms wavelength and finds the masses of HI and HII to be:

M_{HI} = 670 M⊙

M_{HII} = 20 M⊙

(iii) Using the observed diameter of the HII region and the spectral type of the exciting star the density of hydrogen atoms near the centre of the nebula has been computed and from this we find

M_{HII} = 10 M⊙

If this density is constant throughout the cloud the total mass of interstellar matter is 40 M⊙.

(i) is probably an underestimate of the mass because it is assumed to that all stars counted are seen through the dark cloud. Of course a certain number of the stars lie in front of and within the cloud and so the absorption is underestimated, especially in the central parts where the proportion of stars in front of the cloud is highest.

(iii) probably overestimates the total mass of the cloud because the density of interstellar matter is much less near the outside of the cloud than in the central parts.

(ii) and (iii) give very different values for the mass of HII in IC 5146. The mass computed from radio observations cannot be completely trusted because continuum observations of CTA97 are used. CTA97 lies at a distance of 15' from the optical HII region, well outside the stated uncertainty

of the position measurement.

The mass of HI computed by Riegel seems to be accurate. The only possible reason for error is that the background spin temperature may have been overestimated.

We may conclude, then, that the mass of HI is close to Riegel's estimate of 670 $M_\odot$. Using this, plus the value of 0.2 $M_\odot$ for dust, we find a gas/dust ratio of $\sim$ 300 /1 by mass. The mass of HII is close to the one computed from the diameter of the HII region and the spectral type of the exciting star, ie about 10 $M_\odot$. This gives 1000 $M_\odot$ as the total mass of interstellar matter involved in IC 5146.

REFERENCES

(1) Reddish MNRAS 1967, 135, 251.

(2) Alter MNRAS 1941, 101, 97.

(3) Barkhatova AZh 1950, 27, 181.

(4) Muller ZfAp 1955, 110, 38.

(5) Pesch ApJ 1960, 132, 696.

(6) Hoag et al Pub US Nav Obs 1961, 17, 347.

(7) Johnson et al Low Obs Bull 1961, No 113.

(8) Hoag Ap J Supp 1965, No 107.

(9) Schmidt ZfAp 1961, 53, 32.

(10) Lindoff Ark f Ast 1968, 5, 1.

(11) Starikova Sov Ast AJ 1964, 8, 309.

(12) Walker Ap J 1959, 130, 57.

(13) Miller Ap J 1968, 151, 493.

(14) Williamson Ap & Sp Sc 1969, 6, 45.

(15) Georgelin and Georgelin Ast & Ap 1970, 6, 349.

(16) Riegel Ap J 1967, 148, 87.

(17) Kellermann A J 1964, 69, 205.

(18) Churchwell et al Ap L 1969, 4, 33.

(19) Pratt Pub R Obs Edin 1968, 6, 4.

(20) McKuskey and Houk A J 1964, 69, 412.

(21) Fitzgerald PhD Thesis 1967, Case Western Reserve Univ.

(22) Hall Pub US Nav Obs 1958, 17, 271.

(23) Hall and Mikesell Pub US Nav Obs, 1950, 17, 3.

(24) Lambrecht and Schmidt A N 1957, 284, 71.

(25) Salpeter Ap J 1955, 121, 161.

(26) Seddon and Jones Pub R Obs Edin 1966, 5, 99.

(27) Bok A J 1956, 61, 309.

(28) Van Rhijn Pub Ast Lab Gron 1929, No 43.

(29) Reddish Mem de la Soc Roy des Sc de Liege, 1970, 19, 283.

(30) Mebold Beit zur Radioast 1969, 1, 4.

(31) Allen Astrophysical Quantities 2nd ed 1963, London, Athlone Press.

(32) Walker Pub R Obs Edin 1971, 8, 103.

(33) Pratt Pub R Obs Edin 1971 8, 109.

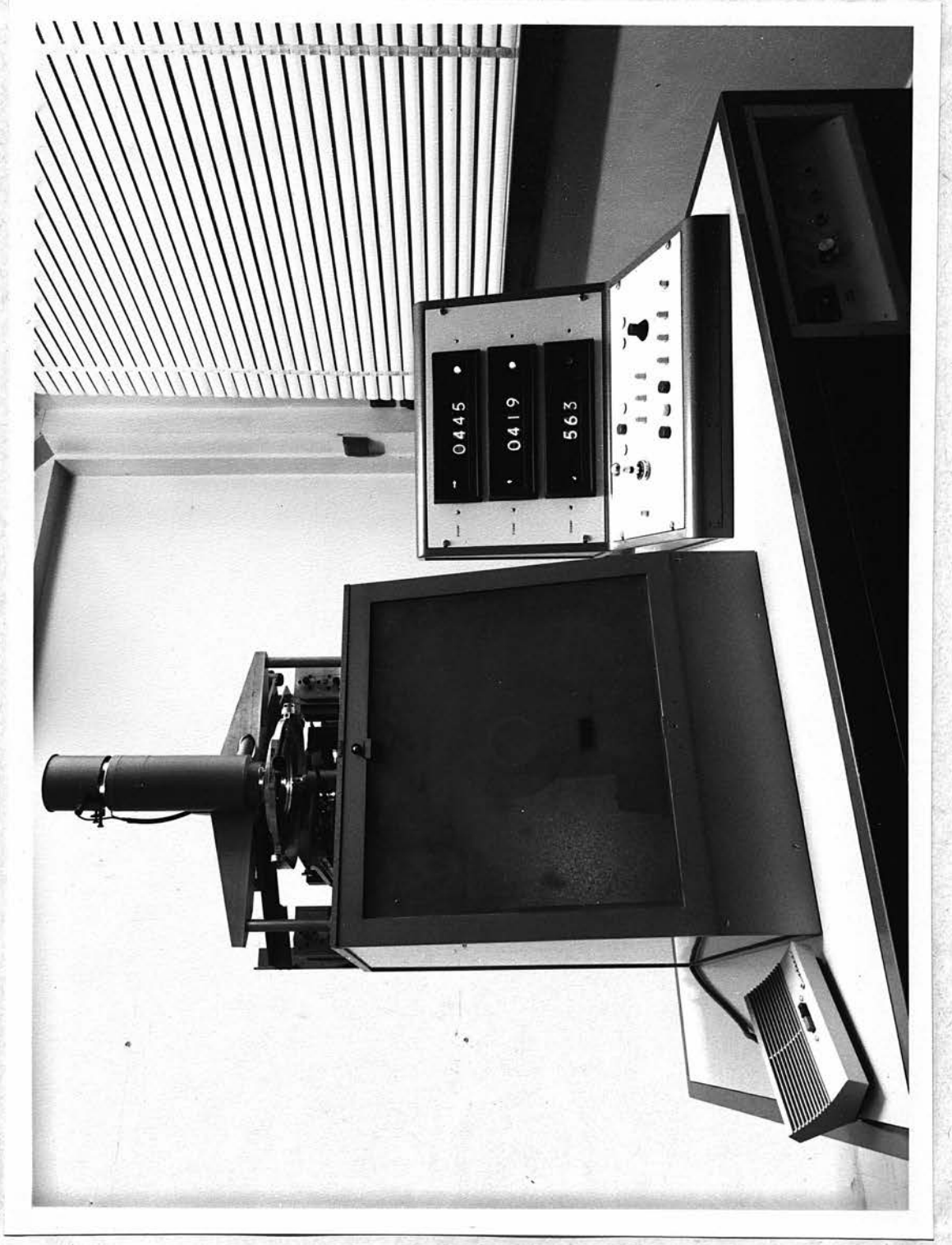

The Computer Controlled Iris Photometer.

PAPER TAPE READER

STAR COORDINATES INPUT ON PAPER TAPE

COMPUTER

TO X, Y MOTORS

FROM X, Y AND IRIS MOIRÉ READING HEADS

PAPER TAPE PUNCH

X, Y AND IRIS OUTPUT ON PAPER TAPE

LAMP

BEAM SPLITTER

REFERENCE BEAM

X MOTOR

Y CARRIAGE

STAR PLATE

Y READING HEAD

X CARRIAGE

Y GRATING

X READING HEAD

X GRATING

Y MOTOR

IRIS READING HEAD

IRIS DIAPHRAGM

IRIS GRATING

IRIS MOTOR

MIRROR

SIGNAL BEAM

OPTICAL CHOPPER

PHASE SENSITIVE DETECTOR

IRIS SERVO LOGIC

APPENDIX 1

The Computer Controlled Iris Photometer

Introduction

The Royal Observatory Edinburgh has, for a long time, been involved in the automation of astronomical equipment. Ideally, most of the Astrophysicist's time should be spent considering astrophysical matters, rather than in time-consuming observation and reduction. It is with this end in view that the Observatory's Instrumentation Division has been working on the automation of telescopes and measuring machines.

In their paper A SEMI-AUTOMATIC IRIS PHOTOMETER (26) Seddon and Jones conclude that the next step in the automation of iris photometers is to be the development of automatic setting and centring of star images within the iris. This is the task of the Computer Controlled Iris Photometer (CCIP).

A major source of fatigue in iris photometer operators has been the finding of star images, often scarcely visible, on the viewing screen prior to centring the image in the iris. The operator has to work from charts of the region being studied. These charts are usually printed from a different plate to the one being studied and this plate is often in a different colour sensitivity range. The

result is that the images seen on the screen often bear little resemblance to those on the chart. Another source of difficulty is a light which must be kept on to allow the operator to see the charts. At the same time the operator must maintain good enough dark-adaption to see the dim viewing screen. The fatigue induced by these factors can lead to inaccurate identification and measurement of images.

The CCIP is designed to cope with this problem in the following way - initially the operator uses the device in a manual mode. A good plate of the region under consideration is loaded and he selects stars by moving the table in X and Y to position the stars within the iris. By means of a signal to the computer the X and Y co-ordinates of the selected star are recorded by the computer, to be output on paper tape. This co-ordinate data tape can be input to the computer at a later stage to initiate automatic star finding on any plate of the same region.

Schematic Layout

A schematic layout of the CCIP is shown in the fold-out diagram.

Optics

The optical system of the CCIP is identical to that of a

standard Becker Iris Photometer. The signal beam, which passes through an adjustable iris diaphragm in the plane of the projected image of the star plate, is compared with a constant reference beam from the same source lamp. A star image is centred in the iris which is then opened or closed until the signal and reference beams are equal in intensity. In the standard Becker Iris Photometer the two beams are compared with an optical chopper and phase-sensitive detector arrangement. The iris is adjusted manually. In the CCIP the iris is adjusted by a servo arrangement which equalises the beams by adjusting the iris diameter.

Mechanical

In general, the structure and mechanical arrangements of a standard Becker Iris Photometer are unsuitable for automatic machine operation. This is largely due to lack of stiffness in the table.

The structure of the CCIP is much stronger than that of the Becker Iris Photometer, so that the table can be set with an accuracy of $\pm$ 10 μm.

A radial line moire grating is fixed directly on the iris mount, as is the drive from the servo. The iris opening is read with an accuracy of 1 part in 1,000.

Software

Software for the CCIP has been developed by Mr T Wallace at the Royal Observatory Edinburgh. There are basically two systems which can be used for control of the machine:

(a) The fully-automatic system.

(b) The semi-automatic system.

When the fully-automatic system is used the co-ordinate data tape is read into the computer. The machine then moves the star images, in turn, into the iris. Each image will be automatically scanned in X and Y until the maximum iris reading is found and this reading, along with the co-ordinates at which it was found, is stored by the computer. The measurements are output at the end of the run on paper tape. This entire procedure takes place without any intervention by the operator, who is free to continue with other work during the measurement.

In the fully-automatic system, measurement takes place at the rate of about 100 star images per hour. This speed is similar to that of a skilled operator on a standard Becker Iris Photometer. For a large programme of measurement, however, the amount of computer time used is prohibitive. It is for this reason that the semi-automatic system was developed.

The most time-consuming part of the fully automatic mode is the automatic centring of the images. It was found that the operator could centre the image manually in a much shorter time than the machine took. When the semi-automatic system is used, the machine centres the image with an accuracy of ± 10μm. At this stage the operator centres the image manually and sends a signal to the computer to record this iris reading and move the next image into the iris. A skilled operator can work at the rate of about 350 measurements per hour using the semi-automatic system. It is possible, too, to work for 2-3 hours at a stretch without excessive fatigue.

The rates of measurement quoted above include a measure of background fog level on the plate, at a point 200μm to the right of each image. If this facility is not used then about 500 measurements per hour could be made in the semi-automatic system.

Facility for Polarization Measurement

Plates used in the measurement of polarization of starlight have 3 images per star, separated in right ascension. The author has written a computer program, WSA9, which converts the co-ordinate data tape from a direct plate of a region into one for a polarization plate of the same region. The following information is read into the computer along with

the original co-ordinate data tape:

(1) The declination of the field centre.

(2) The co-ordinates of the second and third images of the star whose first image lies at (0,0).

This produces a new data tape with the co-ordinates of all three images of each star. Allowance is made for the curvature of lines of constant declination and for the decreasing effect of separation in right ascension as the poles are approached.

The GALAXY Machine.

APPENDIX 2

THE "GALAXY" MACHINE

The GALAXY machine (General Automatic Luminosity And XY Co-ordinate measuring machine) was developed jointly by Faul Coradi (Scotland) Ltd and the Royal Observatory Edinburgh. GALAXY is a high speed system for locating star images on photographic plates and measuring their positions, diameters and densities.

The four plates of IC 5146 in the U waveband were measured using GALAXY because of certain advantages, inherent in GALAXY's method of measuring image sizes and densities, over the iris readings produced by Becker-type iris photometers. One of these advantages is that it is easier to allow for the effects of nebulosity on star images.

The design and development of GALAXY has been described in detail by G S Walker (32). Briefly, the machine consists of:

(i) a precise, massive carriage which holds the photographic plate to be measured. The position of this carriage is measured by a moire fringe system.

(ii) two optical systems for location and measurement of star images. These systems use flying spot scanners.

(iii) an electronic system which controls all the operations of the machine.

The operation of the machine takes place in two stages:

(a) The search phase.

(b) The measurement phase.

In the search phase the photographic plate is positioned under the "search" optical system. The plate is scanned by a flying spot scanner which covers the plate at 17 cm^2 per hour. On a typical Schmidt plate this would record the positions of about 10,000 stars per hour with a precision of about 10 m. The co-ordinates are recorded on punched paper tape.

The co-ordinate tape from the search phase is fed into GALAXY during the measurement phase. Each image recorded in the search phase is moved under the measurement optical system where it is scanned in concentric circles and centred accurately. The image density profile is measured by comparing it with about one thousand model profiles and recording the one which fits best. The co-ordinates and "M-value", the profile number, are recorded on punched paper tape for processing by computer. The co-ordinates are recorded with an accuracy of ± 0.5μm rms, the image diameters with ± 0.2μm and the densities with ± 0.02.

The performance of GALAXY is described in detail by Pratt (33)

who wrote the computer programs which process GALAXY output for astronomical applications. These programs match up the images of stars on different plates of a region, taking into account such effects as atmospheric refraction, and M-values are calibrated to give stellar magnitudes.

The high speed and accuracy of GALAXY make possible hitherto unmanageable programmes of astromeric and photomeric observations involving tens of thousands of stars, and is appropriate to programmes of the kind described in this thesis.